Designing an interactive hinge with shape-memory polymers and alloys

By Wessel Marcelis

Graduation Assignment

in partial fulfillment of the requirements for the degree of

Master of Science

in Mechanical Engineering

at the Department Maritime and Transport Technology of Faculty Mechanical, Maritime and Materials Engineering of Delft University of Technology

Student number: 4383214
MSc track: Multi-Machine Engineering
Report number: 2023.MME.8857.
Supervisors: Dr. J. Jovanova and Dr. S. Ghodrat
Date: September 21, 2023

Abstract

This research aims to design and simulate a hinge consisting of shape-memory alloys and polymers, which can be actuated along two axes. By using recent research as inspiration, a design was made for a hinge. The hinge consists of a shape-memory body that is actuated externally by shape-memory alloy springs. To achieve maximum deformation, two small single hinges are made, of which the body has the shape of a plate and which are actuated externally by two springs. The two hinges are then stacked, where the second hinge is twisted 90°so it can move in two directions. Tensile tests of three different types of Nitinol wire were carried out to investigate their behavior. shape-memory springs were manufactured with these Nitinol wires. Then, the springs were deformed, the temperature of the springs was increased in steps of 10 °C, and the force was measured at each temperature step. Simulations were also carried out and compared to the force tests. The best type of Nitinol was chosen for the shape of memory wires. A prototype of the hinge was built and tested. First, the small single hinges were tested, where the displacement was documented. Also, weights were attached to the single hinges. Applying a weight of 200 g to the horizontal actuated hinge did not affect the displacement. Attaching weight to the vertical actuated hinge did affect the displacement. The hinge was not deemed energy efficient. When actuating the hinge when the shape-memory polymer was at room temperature, the energy consumption was 546.4 J for the heating of the polymer, the heating of the Nitinol spring, and the shape recovery of the polymer. This cycle takes 212 seconds. When actuating the hinge multiple times without the need to heat the polymer at room temperature, the actuation cycle has an energy consumption of 248 J with a cycle time of 111 seconds. Finally, simulations were carried out for the single and stacked hinges, which had a maximum difference of 0.1 mm compared to the tests. Hereafter, the range of motion of the stacked hinge is determined. The hinge tip had a horizontal range of motion between 39 and -39 mm, while vertical actuation resulted in a range between 0.3 and -24.6 mm. Problems with the stacked hinge were the sagging of the first hinge and twisting at the tip of the hinge. This study shows potential in shape-memory hinges, which can be actuated along two axes. This paper can be a handbook for future researchers who want to design a hinge using shape-memory alloys and polymers.

Contents

1 Introduction

1.1 Problem formulation

Due to technological advancement, the use of smart systems has increased. Smart systems usually require multiple sensors and actuators—the increase in components increases weight, volume, and cost. An increase in weight and volume increases energy consumption. Therefore, systems need to be designed efficiently, not only for economic reasons but also for environmental gains. The use of smart materials can be a way to achieve these goals. Smart materials can sense and react to environmental stimuli (1). Shape-memory materials are an example of a smart material.

A shape-memory material is a smart material that can remember its original shape when deformed. When an external stimulus is applied, the material can return to its original shape. Several external stimuli can trigger the shape-memory effect, but the most common one is an increase in temperature. The shape-memory effect occurs when the temperature of the material exceeds a certain threshold. Because of this, shape-memory materials have an excellent potential to make systems smart. Because it returns to its original shape, it can be used as an actuator and as a sensor as it deforms when the temperature exceeds its threshold (2). Two essential classes of shape-memory materials can be distinguished: shape-memory alloys and shape-memory polymers. Shape-memory polymers generally exhibit a higher capacity for elastic deformation than shape-memory alloys but have, on the other hand, lower strength. The interest in shape-memory polymer has recently increased due to the development of 3D printing. Shape-memory polymer structures can now quickly and cheaply be manufactured.

Shape-memory material can be used in numerous fields of engineering. One of these fields is soft robotics. Because shape-memory polymers are flexible and lightweight, it is safe to use around humans (3). An application prospect for shape-memory material is to use it as a hinge actuator. This actuator type will set a system in motion by rotating it. A potential prospect of shape-memory hinges is that they can be used in transport engineering. Shape-memory hinges may push objects from one conveyor belt to another, lift objects, or serve as a gripper.

Much research has been conducted concerning shape-memory material hinges. Two major classes of shape-memory hinges are one-way and two-way shape-memory material hinges. One-way shape-memory hinges can return to their permanent shape from a programmed temporary shape. The shape-memory effect is not reversible, only when the hinge is programmed again. On the other hand, two-way shape-memory material hinges can alter between two or more different shapes. The most common way to achieve this is by using two shape-memory materials. One shape-memory material actuates the hinge from the starting position to the actuated position. The other shape-memory material actuates the hinge back to the start position. In most research about shape-memory hinges,

the hinge can be actuated in the 2D plane like an elbow joint. Very little research was conducted concerning hinges that work in the 3D space.

1.2 Objective and research questions

This paper investigates the possibilities for designing and modeling a hinge that works in the 3D space and consists of a combination of shape-memory alloys and polymers. This paper may serve as a manual for future researchers who want to design and simulate shape-memory hinges.

Following the objective of this research, the main research question is: *How to design an interactive hinge with shape memory alloys and polymers?* To answer the main research question, these sub-questions should be answered:

1. What is the state of the art of shape-memory hinges?
2. How much force does a shape-memory alloy deliver, and how can it be modeled?
3. What are important design parameters for designing a shape-memory hinge?
4. How can a model be built to simulate the behavior of the hinge?
5. What is the energy consumption of the hinge?
6. What is the range of motion of the shape-memory hinge?

2 Theory

In this section, the theory behind shape-memory materials is explained. As mentioned, shape-memory material can remember its original shape when deformed. The shape-memory effect is triggered when an external stimulus is applied. External stimuli that can trigger the shape-memory effect are heat, magnetism, light, moisture, and a change in pH value (4). There are two main classes of shape-memory material: shape-memory alloys and shape-memory polymers. First, the working principle of shape-memory alloys is explained, followed by the working principle of shape-memory polymers.

2.1 Shape-memory alloys

Shape-memory alloys are metallic materials that can recover to their original shape when a certain stimulus is applied. Multiple external stimuli can trigger the shape-memory effect, but the most common is the temperature increase of the material. Returning to their original shape is possible, even when it reaches inelastic deformation (5). The existence of shape-memory materials has been known since 1932 when the shape-memory effect was discovered in a gold-cadmium alloy (6). The same effect was discovered in a nickel-titanium alloy called Nitinol in 1963. Nowadays, Nitinol is the most frequently used shape-memory alloy. Nitinol can recover from strains up to 8% (7).

Phase transformation is the driving force behind the shape-memory effect of shape-memory alloys. Shape-memory alloys can have two phases: martensite and austenite. Each phase has a different crystal structure and properties. The martensite phase usually has a monoclinic (B19') crystal structure or an orthorhombic (B19) structure with the addition of copper. The martensite has a lower Young's modulus than the austenite phase. Conversely, the austenite phase has a cubic (B2) structure and a higher Young's modulus (8).

Shape-memory alloys have a permanent phase and a temporary phase. When the alloy is at the low-temperature permanent phase, it is in the martensite phase with a twinned structure. When the alloy is deformed to its temporary shape, it changes to a detwinned structure but is still in the martensite phase. When the deformed alloy is heated, it transforms into the austenite phase. When the temperature decreases, the alloy will return to the twinned martensite phase. The phase transformation results from shear lattice distortion (8). The phase transformation cycle can be seen in Figure 1.

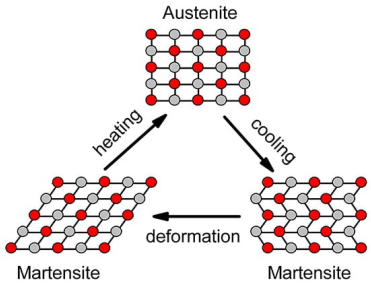

Figure 1: Phase transformation cycle of a shape-memory alloy and the different crystal structures (9)

The shape-memory effect takes place when it reaches certain characteristic temperatures. A deformed alloy starts its shape recovery when the austenite start temperature is reached. At this temperature, the austenite begins to form. When the austenite finish temperature is reached, the alloy is fully in the austenite phase. When the alloy is cooled again and reaches the martensite start temperature, the austenite transforms into martensite. The alloy is fully in the martensite phase when it drops to the martensite finish temperature. There is a hysteresis in the heating-cooling cycle. The start and finish temperatures for martensite and austenite are stress-dependent, as seen in Figure 2.

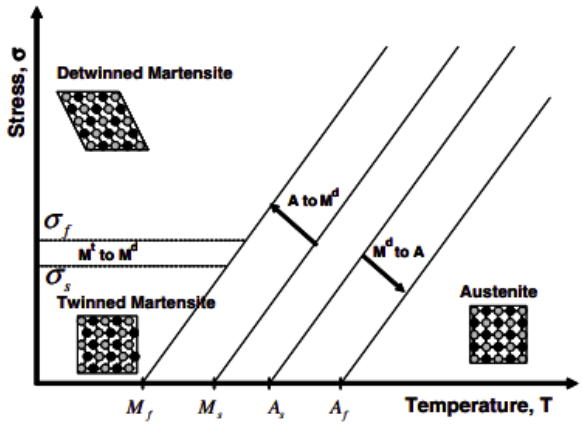

Figure 2: The stress-temperature phase diagram which shows the shape-memory effect for a NiTi shape-memory alloy (8)

Figure 3 is a stress-strain-temperature graph showing a Nitinol alloy's shape-memory effect. Starting from point A, the Nitinol is in the austenite phase. When the material cools down to martensite start temperature (M_s), martensite forms. The material is entirely martensite when the temperature cools down further to the martensite finish temperature (M_f). The martensite is now in the twinned phase (point B). When a load is applied to the material, the material behaves linearly until σ_s. When the load exceeds σ_s, the material behaves superelastic, and the strain increases

rapidly when the load increases just slightly. The material transforms from the twinned to the detwinned martensite phase until the stress level reaches σ_f. After this point, the material starts behaving linearly again (point C). When the material is unloaded, the material behaves linearly and recovers the strain partly(point D). When the material is heated again, austenite starts to form when the austenite start temperature is reached (A_s) (point E). When heated further to the austenite finish temperature, the material is entirely in the austenite phase (point F).

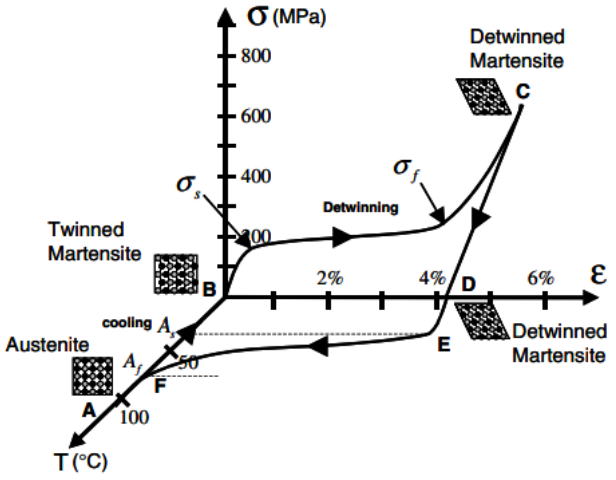

Figure 3: The stress-strain-temperature phase diagram which shows the shape-memory effect for a NiTi shape-memory alloy (8)

2.2 Shape-memory polymers

Like shape-memory alloys, shape-memory polymers can return from a temporary shape to their original shape. Polymers are a material built up of many molecular chains (10). Unlike shape-memory alloys, shape-memory polymers are lighter, are often biodegradable, and can recover larger strains but have a lower strength (11)(12). Interest in shape-memory polymers has recently increased due to the development of 3D printing, which makes it easy to manufacture complex polymeric structures. 3D printing is the process of constructing a structure by adding material layer by layer. The 3D printing of shape-memory polymer structures is called 4D printing. Not every material is suitable for 4D printing because some materials barely exhibit shape change in the presence of a stimulus (12). Research still focuses on identifying smart materials that exhibit the shape-memory effect(13)(14).

A shape-memory polymeric network consists of permanent netpoints connected by chain segments. These chain segments can form switches. Permanent netpoints are not affected by deformation, and that is why a shape-memory polymer can remember its original shape. The switches are sensitive to an external stimulus, which triggers the shape recovery effect (15)(16). Netpoints can

be of chemical or physical nature. Netpoints with a chemical nature are covalent cross-links, while netpoints with a physical nature result from inter-molecular interaction.

Shape-memory polymers have two states: a glassy and a rubbery state. When the temperature of the polymer exceeds the glass transition temperature T_g, the material will transform from the glassy state to the rubbery state. In the rubbery state, the switches are flexible, and the material is easily deformed, while in the glassy state, the switches prevent the mobility of the material.

When the material is in the permanent shape, it is in the state with the highest entropy. When the material is heated above the glass transition temperature and deformed to its temporary shape, it is in a lower entropy state. When the material is cooled, while a load lets it stay in its deformed configuration, the switches are activated again. The switches prevent the material from returning to its permanent shape. When the temperature of the polymer exceeds the glass transition temperature again, entropic elastic behavior takes place, and the shape-memory effect takes place (17).

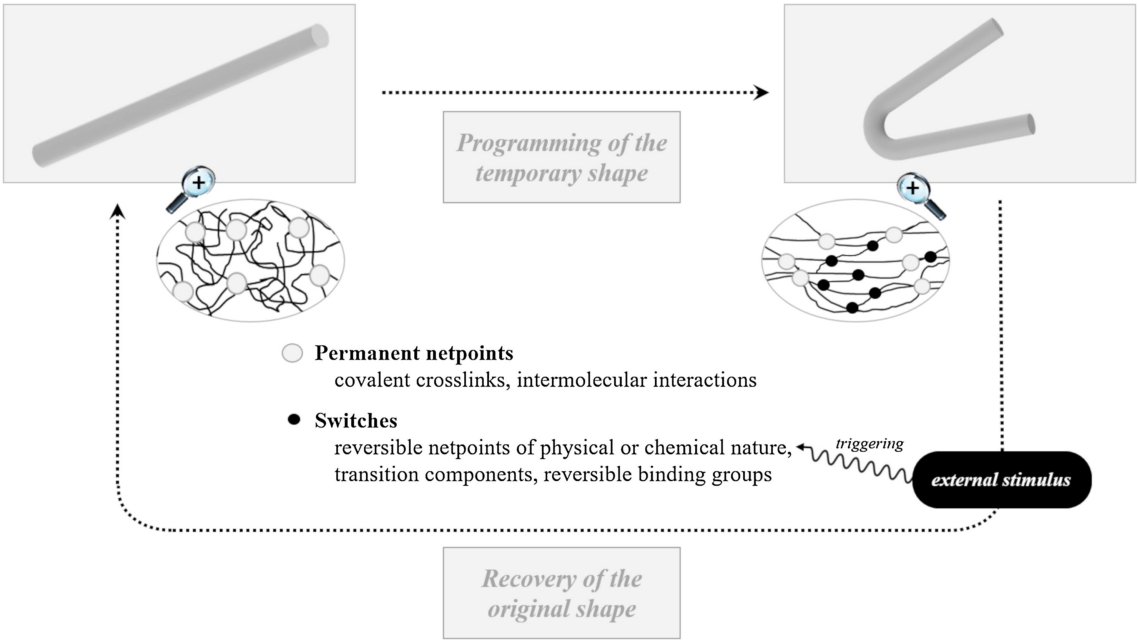

Figure 4: The working principle of the shape-memory effect in polymers (16)

When a polymer is manufactured, it is in its permanent shape. It must be programmed first to obtain the shape-memory effect in a polymer. This is done by heating the polymer above its transition temperature, applying a load to deform it to its temporary shape, decreasing the temperature, and releasing the load. The polymer will still be in its temporary shape. When the material is heated again above its transition temperature, it will return to its permanent shape. The polymer has to be reprogrammed to repeat the shape-memory effect (18).

3 State-of-the-art

In this section, recent research concerning shape-memory material hinges is discussed. Two major classes of shape-memory hinges can be distinguished: one-way and two-way hinges. There are shape-memory materials that are intrinsically two-way, both alloys (19) and polymers (20), but often, making actuators two-way is achieved by combining two or more materials. This section discusses recent research on hinges with a one-way shape-memory effect, followed by hinges with a two-way shape-memory effect. The design, fabrication process, and experiments are handled for each hinge.

3.1 One-way shape-memory hinges

3.1.1 One-way shape-memory actuated hinge used in a deployable structure

Liu et al. (21) designed a deployable structure using multiple-shape-memory polymer composite hinges. This deployable structure was designed for aerospace applications in a low-gravity environment. The hinge consists of carbon fiber reinforced shape-memory epoxy composites. The carbon fiber reinforced shape-memory composite was manufactured using vacuum-assisted transfer molding. Resistor heaters supply the heat, which triggers the shape-memory effect. The hinge consists of two symmetrical arc-shaped laminates. The arc of the laminates has an angle of 120°, which was found optimum in experiments.

Experiments were carried out to determine the temperature sensitivity, elastic modulus, and material strength. A 3-point bending and shape-memory recovery test was performed to verify the variable stiffness under different temperatures and superior shape-memory properties. The strain distribution during the bending process was obtained using the digital image correlation technique and the ABAQUS simulation software, which showed good consistency with each other.

Figure 5: Fabricated deployable structure made by Liu et al., where the shape-memory recovery process is shown (21)

Pros

- Structure can be folded in a small shape
- No assembly in the manufacturing process
- Lightweight
- Hinge maintains a shape recovery ratio of 100% after ten times fold-deploy process

Cons

- One-way shape-memory effect, which limits the potential applications
- Complex fabrication process because of relatively long product
- Relatively long recovery process of about 60 seconds

3.1.2 One-way shape-memory actuated hinge with multiple fiber layers

Liu et al. (22), the same research group as in previous research, designed another shape-memory composite hinge, as seen in Figure 6, where the same reinforced fiber and manufacturing technique were used as in previous research. This hinge is also designed for application in aerospace. The design consists of only one hinge. A heating film provides the heat, triggering the shape-memory effect. An aluminum tape was pasted between the heating film and the hinge fiber sheet for an even heat distribution. The micro buckling problem that occurs during the bending of hinges when the shape-memory effect occurs is solved by designing the bending path using a mold.

This research investigated how the properties of the hinge change when different amounts of shape-memory composite layers were used in the hinge and determined an optimum number of layers for the hinge. First, the optimum voltage used for heating is determined. Then, the recovery speed, heat distribution, and strain distribution using the digital image correlation technique were obtained. The recovery force and the deployed stiffness of the material with different fiber layers are determined. Finally, surface morphology is carried out.

Pros

- Lightweight
- Even heat distribution using an aluminum tape
- With the right surface temperature, the recovery rate reaches 100%

Cons

- One-way shape-memory effect, which limits the potential applications
- Assembly needed
- Relatively long recovery process of about 180 seconds

3.1.3 Passive 4D-printed elastomer hinge

Yamamura et al. (23) designed a hybrid hinge that can be elastically deformed when the material is below the glass transition temperature. The material used is polyurethane. Polyurethane in a glassy state at room temperature is used as a shape-memory polymer, while polyurethane in a rubbery state at room temperature is used as the elastomer. The hybrid hinge consists of an elastomer and

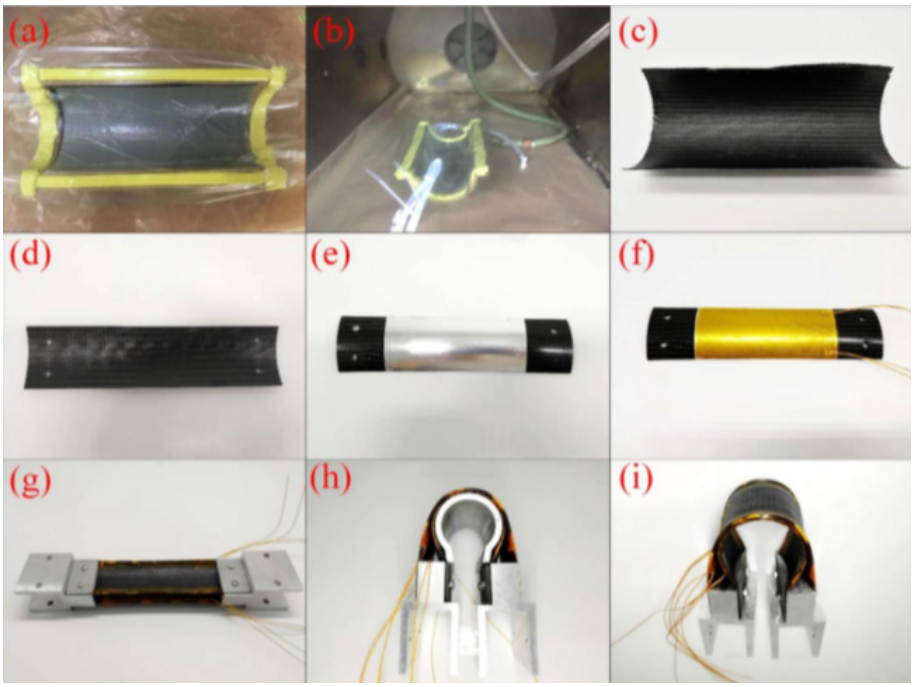

Figure 6: Fabricated process for the hinge made by Liu et al., (a) inject the shape-memory epoxy resin into the mold of the reinforced fabric, (b) cure the mold in an autoclave, (c) remove the material from the autoclave, (d) cut the material to the right dimensions, (e) paste aluminum tape that is used to get an even heat distribution, (f) paste heat films on the material, (g) assemble the hinge, (h) bend the hinge in the temperature chamber, (i) take out the finished shape-memory hinge (22)

two shape-memory polymer hinges. When the material is heated, bending deformation occurs due to the difference in expansion coefficients. This is the 4D part. When the material is cooled, it stays in its permanent shape. The elastomer part of the hinge is less rigid than the shape-memory polymer part. The deformation occurs at the elastomer part when an external force is applied after 4D printing.

The hinge is fabricated using an additive manufacturing FDM 3D printer. The manufacturing process can be seen in Figure 7. The manufacturing process is divided into three parts. First, the bottom model is made, which consists of shrinkable and non-shrinkable shape-memory polymers. Then, the middle part is manufactured, which consists of elastomer. Finally, the top part is manufactured with a non-shrinkable shape-memory polymer.

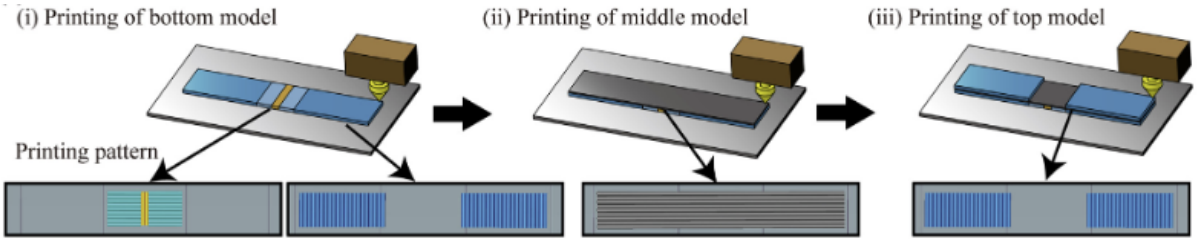

Figure 7: The fabrication process for the hybrid hinge (23)

Several experiments were carried out. The effect of the hinge length on the self-folding angle was investigated. The larger the hinge length, the larger the self-folding angle. Furthermore, the material is cyclically loaded and unloaded to determine how well the material returns to its permanent shape when the material is unloaded. After 500 loading cycles, the object returned almost to its original shape without failure. This shows that the hinge has high durability and elasticity. The experiment can be seen in Figure 8.

Pros

- Lightweight
- High recovery rate, reaching 99%, after 500 cycles
- No assembly process

Cons

- The hinge cannot be actuated
- Only tested on a sample the size of a thumb

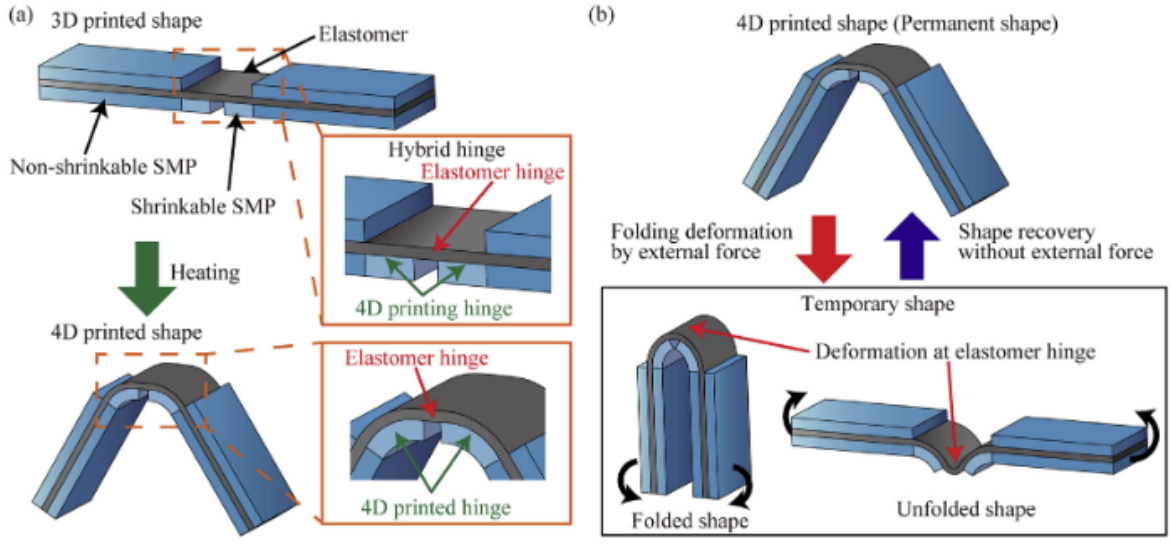

Figure 8: The experiment carried out with the hybrid hinge structure made by Yamamura et al. (23)

3.1.4 Two one-way shape-memory polymer hinge structures using active and passive hinges

Akbari et al. (24) designed two one-way shape-memory polymer hinge structures. Both structures are made using a fused deposition modeling 3D printer. The structures consist of active and passive hinges. The active shape-memory polymer hinge locks the structure in a temporary shape during the programming process, while the passive elastomer hinge increases the actuation force and load-bearing capacity. Resistant wires actuate the active hinges.

Structure 1 is a morphing wing flap, shown in Figure 9a. This structure consists of 2 active hinges and a passive hinge. Large bending deformation is exhibited in this structure. It was manufactured in a bent shape and subsequently programmed in a straight shape. Structure 2 is a deployable structure, shown in Figure 9b. This structure consists of two active hinges and two passive hinges. This structure can achieve large extensional deformation. It was initially manufactured upright and programmed in a folded shape.

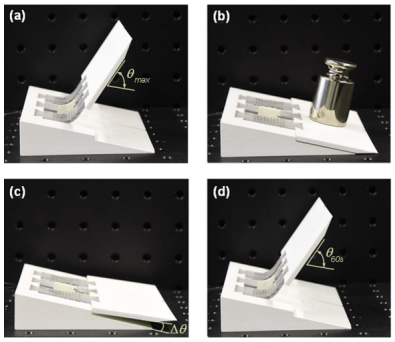

(a) Structure 1 made by Akbari et al. (24)

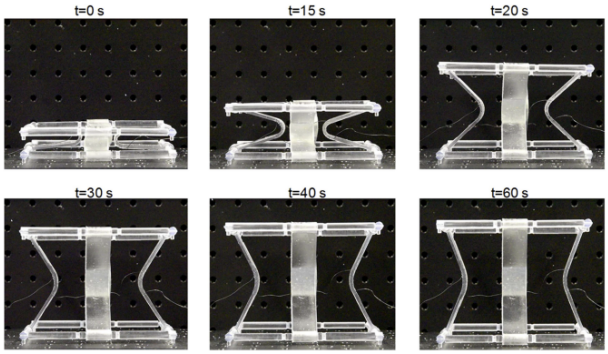

(b) Structure 2 made by Akbari et al.(24)

A broad range of mechanical properties can be achieved by using different materials for the active and passive hinges. Dynamic mechanical analysis and a uni-axial tensile test were carried out for ten different shape-memory materials.

Important design parameters like local deformation, shape fixity, and recovery ratio are obtained using finite element simulations, which can predict nonlinear deformations. The research showed that the passive hinge increased the recovery ratio. Furthermore, a coupled thermal-electrical finite element analysis was carried out to model the heat distribution during the heating process. The model predicted the heat well compared to the measured temperature data.

Pros

- When using a flexible hinge, a higher recovery ratio is achieved
- Short fabrication time compared to other manufacturing methods

Cons

- One-way shape-memory effect, which limits the potential applications
- Relatively long recovery process of about 60 seconds

3.2 Two-way shape-memory hinges

3.2.1 Two-way fiber-reinforced plastic hinge in combination with Nitinol

Ashir et al.(25) made a shape-memory hinge using fiber-reinforced plastic in combination with a nickel-titanium shape-memory alloy. The shape-memory alloy was converted into hybrid yarns using friction spinning technology. Then, the resin is infused into the hybrid yarn fabric and cured to complete the fiber-reinforced plastic. The shape-memory alloy was heated using current, which triggers the shape-memory effect. Five variations of the hinge were made in this research.

The research investigates the effect of the hinge width and the distance between different shape-memory alloy wires, as seen in Figure 10. Young's modulus decreases with an increase in the hinge width. When the hinge width is increased, the maximum deformation becomes larger. When the distance between the wires increases, the maximum deformation becomes smaller. The first heating and cooling cycles are inhomogeneous, but the deformation behavior becomes homogeneous after the first few cycles.

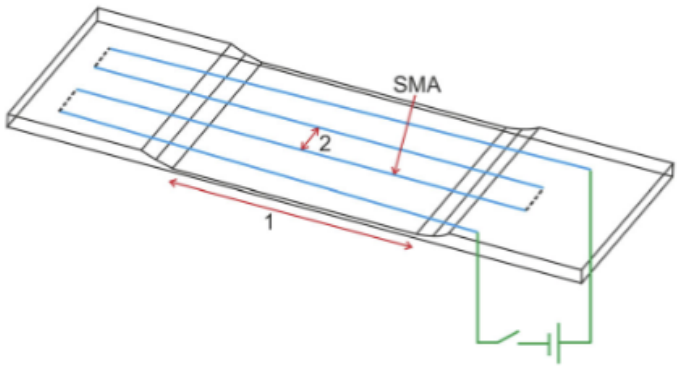

Figure 10: Fabricated hinge made by Ashir et al., where parameters 1 and 2 are changed (25)

Pros

- Two-way shape-memory effect, which enhances the number of potential applications
- Lightweight structure
- The actuation time is 40 seconds, which is relatively low compared to other hinges
- Consistent deformation curves after five deformation cycles

Cons

- Complex manufacturing technique
- Thin sample that can't bear high loads

3.2.2 Two-way fiber-reinforced shape-memory material hinge actuated by Nitinol springs

Testoni et al. (26) designed a two-way shape-memory hinge. The hinge comprises two shape-memory polymer parts and two shape-memory alloy springs. The shape-memory polymer part was fabricated using a material jetting process 3D printer. Each shape-memory polymer part has a heater connected to it. The heaters result in a decrease in bending stiffness, which allows for the bending of the hinge. Between the two shape-memory polymers, a carbon fiber reinforced polymer separates the two parts to support the shape-memory polymer parts at large deformations. The shape-memory alloy springs are used for the actuating of the hinge. A current heats them. The designed hinge can be seen in Figure 11.

The angle of the hinge can be modified by adjusting the currents through the different parts of the structure: The shape-memory polymer heater is activated, reducing the stiffness of the polymer. A current is sent through the shape-memory alloy spring, resulting in the hinge bending. The polymer heater is then turned off, increasing the polymer's stiffness due to the cooling of the material. The heating of the spring is stopped, ending the bending actuation. The spring returns to its original shape when the polymer heaters are again activated.

Some tests are carried out. One of the tests is the maximum angle test. It is found that the maximum angular position is 97°, and when the springs are deactivated, the hinge locks at an angular position of 90°. The cycle to reach the maximum angular position and return to its original shape takes about 820 seconds. The second test is the multiple actuation test. When the polymer is heated constantly, and when each spring is actuated in turn, it is found that the maximum angle reaches 100°after the second cycle, and each cycle takes about 180 seconds. The third test is the gradual increase in angular position test. The hinge increased its angular position from 0°to 90°in increments of 10°. The hinge could reorient itself with a precision of 3°. The last test is the multi-

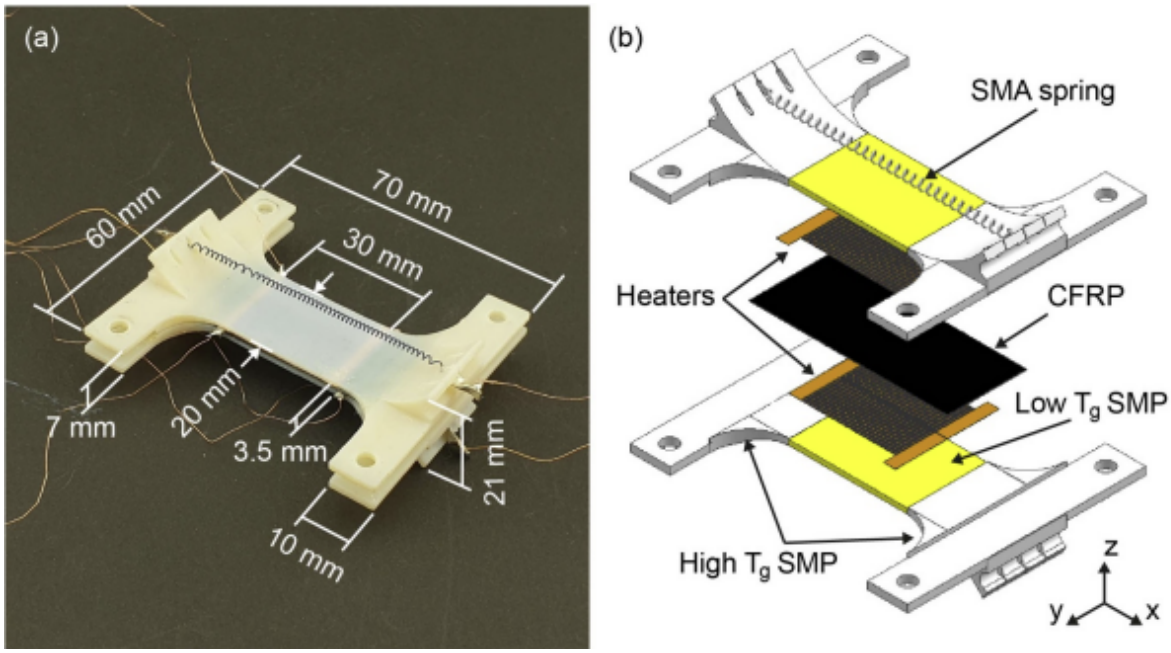

Figure 11: The two-way shape-memory hinge made by Testoni et al. (26)

step actuation test. The result shows that an angular position of 45°can be achieved in 30 seconds starting from 0°. When going from 90°to -45°, it takes about 120 seconds.

Pros

- Two-way shape-memory effect, which enhances the number of potential applications
- Hinge can orientate itself to multiple angular positions with a precision of 3°

Cons

- Assembly needed
- To reach the desired angular position, some fine-tuning is required

3.2.3 Two-way shape-memory polymer hinge embedded with shape-memory alloy wires

Akbari et al. made a reversible actuator using a multi-material inkjet 3D printer. The structure consists of shape-memory polymers, soft layers of elastomeric polymer, resistive wires, and shape-memory alloy wires. They eccentrically embedded the shape-memory alloy wires into the printed shape-memory polymer. They made two structures, as shown in Figure 12. Both structures have two hinges, which can be actuated separately. The actuators differ in the amount of printed soft material in the hinge area. This results in actuator 1 having a lower bending stiffness. Resistive wires in the hinge area heat the shape-memory polymer segments via joule heating. The temperature

of the shape-memory alloy wires can also be regulated using a current. The shape-memory alloy wires are used to restore the original shape of the structure by applying compressing force. The shape-memory alloy wires are connected to the end of the actuator using copper crimp connections.

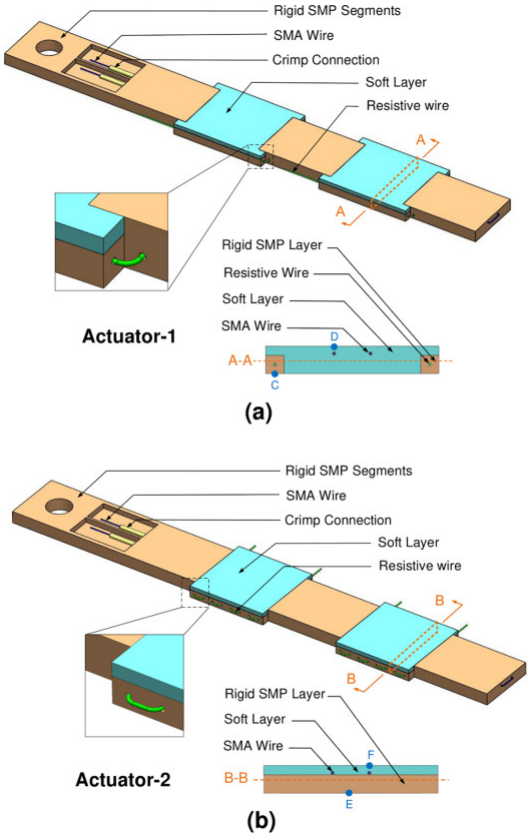

Figure 12: Design for the reversible actuator made by Akbari et al. (27)

The actuators are actuated as follows: First, a current is applied through the resistive wires to heat the shape-memory polymer, transforming it from a glassy state to a low-stiffness rubbery state. Then, the current through the resistive wires is stopped, and the current through the shape-memory alloy is activated, resulting in a bending deformation. The current through the shape-memory alloy wire is stopped when the shape-memory polymer is cooled down, and a glassy state is formed. The actuator remains in its deformed shape. When a current is applied to the resistive wires, the actuator transforms to its original state.

The actuators are implemented in a FEM tool, and by using ABAQUS, the thermomechanical behavior is simulated. It can be concluded that the finite element model could predict the effect of the shape-memory polymer thickness on the shape fixity, the recovery ratio, and the fixity ratio with reasonable accuracy. It is measured how fast the shape-memory polymer reaches 60°C under

different applied currents. Measurements were also carried out on the effect of the resistive wires on the shape-memory alloy temperature. It is found that the shape-memory alloy is not actuated as a result of the temperature increase due to the resistive wires. Actuator 2 is found to have better fixity and recovery but has a lower maximum deformation. The lower bending deformation results from a higher stiffness in the hinge area. This research group made a gripper using these reversible actuators, as shown in Figure 13.

Pros

- Two-way shape-memory effect, which enhances the number of potential applications
- Each hinge can be actuated independently

Cons

- Assembly needed
- Cannot control the angle of the hinge
- Shape recovery ratio relatively low compared to other hinges

Figure 13: Gripper made by Akbari et al (27)

3.2.4 Two-way fiber reinforced plastic shape-memory hinge embedded with a shape-memory alloy and controlled using an Arduino board

Lalegani Dezaki et al. (28) designed an actuator with a 2-way shape-memory effect. The actuator consisted of a two-way shape-memory alloy, low-temperature liquid epoxy cure composites, and fiber-reinforced plastic. The two-way shape-memory alloy wires are trained using the pre-straining method. The shape-memory alloy wires are directly inserted into the fiber-reinforced plastic strips. Copper wires are soldered to the shape-memory alloy wires for optimal electricity distribution. Threads are used for better stability of the actuator. The epoxy resin is used as an adhesive. A structure representing human fingers was 3D printed using a fused deposition modeling 3D printer, and the built actuator actuated these fingers. The gripper can be seen in Figure 14. The actuator was actuated using an electrical current and controlled using an Arduino board. A video camera recorded the action of the actuator. A bending resistive sensor is used to measure the bending angles of the actuator.

The robustness, controllability, mechanical properties, and the 500 life cycle of the actuator are tested. Results show that the actuator has a bending angle of 58°with a 30 mm deflection in 7 seconds after the actuating starts. The recovery time of the actuator is 40 seconds. The wires heat faster when using a higher current, but the fiber-reinforced plastic can be damaged with higher voltages. When airflow is used, the recovery time of the gripper reduces to 20 seconds. A tensile test is carried out, and it is found that the structure tears apart when a force of 300 N is applied. A fatigue test was performed on a single actuator when it was actuated 500 times. The gripper could lift weights to 300 g.

Pros

- Two-way shape-memory effect, which enhances the number of potential applications
- Relatively fast gripping and releasing cycle of 25 seconds
- Gripper could pick up objects of different shapes with a weight of up to 300 g

Cons

- Complex manufacturing process
- Deflection of the tip is not constant when actuated

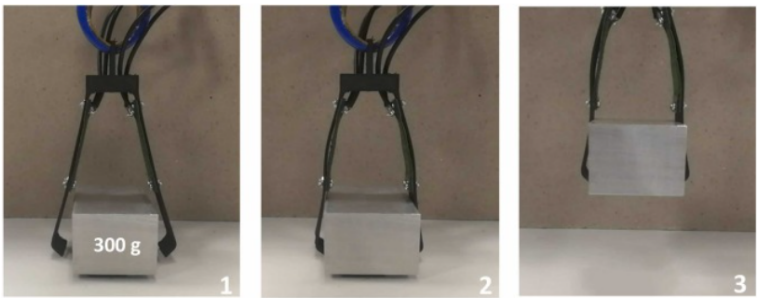

Figure 14: gripper made by Lalegani Dezaki et al. (28)

3.3 Chapter summary

When looking at the designs of the hinges in this section, there is a variety of hinges, fabrication processes, and working principles. The hinges could be divided into one-way and two-way shape-memory hinges. Unlike two-way shape-memory hinges, one-way shape-memory hinges need manual reprogramming to be actuated again. Multiple fabrication methods were used, like injection molding, friction spinning, and, most frequently, 3D printing. A way to increase the actuation force was the use of passive hinges. Some hinges were designed to be used in space to unfold solar panels, others were used to push objects in vertical directions, or they were used as grippers. The heating of the

material was caused either by the use of heating films or by supplying current to the shape-memory alloy. The working principle of the one-way shape-memory was fabricating the hinge in its original position, moving it to the temporary position, and heating the shape-memory material to return to its original position. The working principle of the two-way hinges was either using strained Nitinol wires embedded in a polymer structure or externally applied strained Nitinol springs. The heating of the Nitinol resulted in the material recovering shape, bending the structure. When removing the heat, the material either returned to its original position by internal stress or by the shape-memory effect of the polymer.

4 Conceptual design

This chapter handles the design process, which resulted in the conceptual design of the hinge. The process starts with finding the objective, followed by finding the problem. Then, the basic design cycle, described in the Delft Design Guide (29), is applied to designing the hinge. This design cycle consists of 5 stages: analyze, synthesize, simulate, evaluation, and decision. In the analyze stage, aspects related to the design problem are analyzed. In this stage, the design criteria are drawn up. In the synthesize stage, possible solutions are generated. This is done by sketching some solutions to solve the problem. In the simulate stage, the designs are simulated to determine the expected behavior. This is done by simulating the deformation of the possible solutions. In the evaluation stage, the designs are evaluated using the design criteria. Finally, in the decision stage, a decision for a concept is made. After the conceptual design, the material for the conceptual design is selected. The steps made in this chapter is visualized in the flowchart in Figure 15.

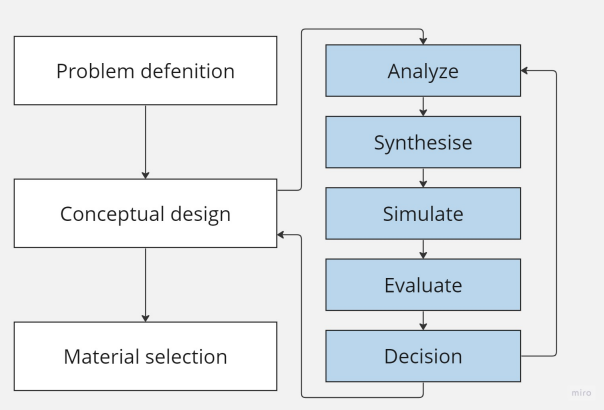

Figure 15: Flowchart conceptual design

4.1 Objective finding

As was already described in the introduction, there is an increased use of smart systems, which require sensors and actuators. The use of sensors and actuators results in an increase in weight, volume, and cost. This results in an increase in energy consumption. Shape-memory material can be a good alternative to make systems smart because the material can be used as an actuator and sensor, reducing cost and energy consumption. Due to the invention of 3D printing, complex shape-memory systems can easily be manufactured. Interactive hinges are one application for shape-memory material. An interactive hinge is a hinge that changes its shape due to interaction with its environment. Interactive hinges can be used in many domains, such as for example soft robotics, where they can be used to grab or hoist objects. This research explores the potential of interactive hinges by focusing on a combination of shape-memory polymers and alloys.

4.2 Problem finding

To contribute to exploring the potential for interactive hinges, it needs to be determined what recent research has already achieved and, by that, determine the research gap. The state-of-the-art section, seen in section 3, showed what has already been achieved. It showed that there are a variety of manufacturing techniques, working principles, sizes, and shapes. When studying recent research, most interactive hinges could only be actuated along 1 axis. For some purposes, it can be useful for a hinge to be able to actuate along more axes to increase mobility. For example, when using an interactive hinge for a soft robotic arm, multi-axe actuation allows a robot to be actuated in horizontal and vertical actuation. Most shape-memory materials are one-way shape-memory. They can recover their original shape when deformed, but they must be reprogrammed again to perform their shape-memory effect. A two-way shape-memory effect can be achieved by combining two one-way shape-memory materials. A two-way shape-memory hinge is desirable to decrease human dependence, so it must not be manually reprogrammed.

4.3 Analyze - design and performance criteria

This research aims to design a prototype of a hinge that consists of shape-memory alloys in combination with a shape-memory polymer that works in the 3D space. The last chapter discussed state-of-the-art shape-memory hinges, showing different designs and working methods for shape-memory actuators. Inspiration has been gained from these designs. Before a design is made, some design criteria are drawn up:

- The hinge consists of a combination of shape-memory alloys and polymers
- The hinge must be able to be actuated along two axes
- The hinge can actuate at least four times without reprogramming the hinge manually
- The hinge should have a considerable displacement. This is quantified by setting the displacement at the tip of the hinge when actuated from minimum to maximum of 2 cm in horizontal and vertical direction
- The angle of the hinge must be controlled

Along with these criteria, there are two wishes: the manufacturing process should be as simple as possible, and the hinge should be made of recyclable parts.

4.4 Synthesise

Some ideas are sketched to make a hinge that can actuate along two axes, as seen in Figure 16. Using the idea for Nitinol-embedded wires, two ideas were sketched. In sketch one, seen in Figure 16a, the body consists of a shape-memory polymer. Halfway through the body, the outer part

consists of soft material, while the inner part is still made of shape-memory polymer. Strained Nitinol wires are embedded at the corners through the whole body. The hinge bends when the Nitinol wires are heated, while shape recovery happens by heating the shape-memory polymer. In sketch 2, the body also consists of a shape-memory polymer, with halfway soft material and a Nitinol wire embedded. The multi-axial actuation is achieved by stacking a second hinge on top of the first hinge.

Also, some ideas are sketched for externally applied Nitinol springs. The sketches all consist of a shape-memory body, which is actuated by multiple Nitinol springs. Four designs are made. Sketches three, four, and five are very similar, but the body's shape and the number of springs differ. Sketch 6 is a hinge that consists of a plate body, but a second plate hinge is rotated 90 °and stacked on the first hinge.

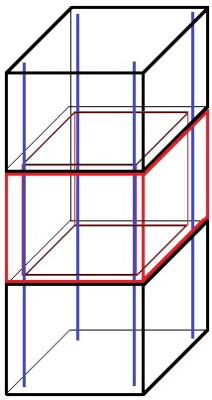

(a) Sketch 1: Square embedded hinge with the blue part the 4 wires and the red part soft material

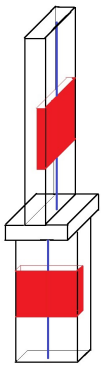

(b) Sketch 2: Stacked embedded hinge with in blue the wires and in red soft material

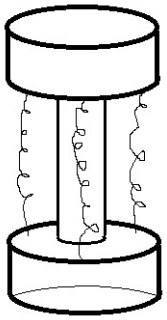

(c) Sketch 3: Round body hinge with externally applied springs

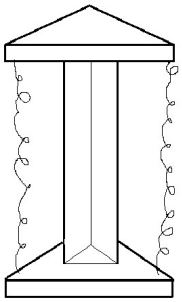

(d) Sketch 4: Triangle body hinge with externally applied springs

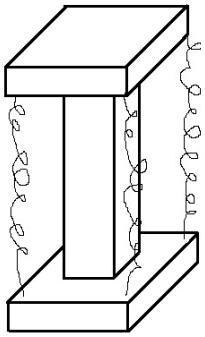

(e) Sketch 5: Square body hinge with externally applied springs

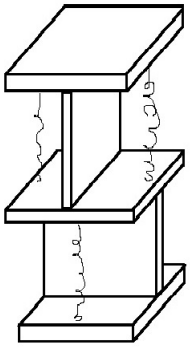

(f) Sketch 6: Stacked plate hinge with externally applied springs

Figure 16: Sketches of ideas for multi-axial actuated hinge

4.5 First evaluation

The problem with Sketch 1 is that the hinge has limited bending because when one or two wires are actuated, the other two wires will give counterforce. The problem with sketches 1 and 2 is that this hinge is hard to control. The manufacturing process is not easy because the Nitinol must be embedded. The externally applied Nitinol spring hinges can be controlled more easily. The manufacturing process is also straightforward because it just needs assembly. The working principle with the externally applied springs hinge was better than the embedded wire hinge. The working principle of the externally applied shape-memory alloy springs is chosen.

4.6 Simulate

The hinge design will consist of a shape-memory polymer body, which is actuated by shape-memory alloy springs on the outside of the body. Still, four concepts are considered. The design concepts differ in the body and the number of springs. The body's geometry is important because it determines how stiff the hinge is. A stiff hinge can be useful because it means that the hinge can withstand deformation. However, this means that the hinge has a lower range of motion. There is thus a trade-off between the range of motion of the hinge and its stiffness.

The four concepts are simulated. Each shape of the body will deform differently when a load is applied. It is investigated how different designs would displace during loading. This is done with the FEM software COMSOL. The bottom part is fixed for all the designs, while a load of 10 N is applied to a side of the top part. For the square, round, and triangle models, the inside of the body is hollow. The plates of these bodies have a thickness of 1 mm. The E-modulus of the material was set to 0.5 GPa. The drawings of these models can be seen in Appendix A.

- The simulation of the square model can be seen in Figure 17a. The displacement of the top part in the z-direction is -1.6 mm.
- The simulations of the round model can be seen in Figure 17b. The displacement of the top part in the z-direction is -2.3 mm.
- The simulations of the triangle model can be seen in Figure 17c. The displacement of the top part in the z-direction is -1.2 mm.
- The simulations of the stacked model can be seen in Figure 17d. A load of 10 N is applied on the side of the first top part and the second top part while the bottom part is fixed. The displacement of the second top part in the z-direction is -8.8 mm.

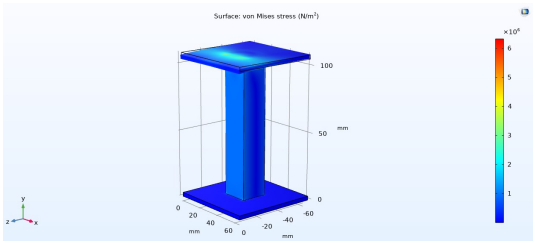

(a) The square model

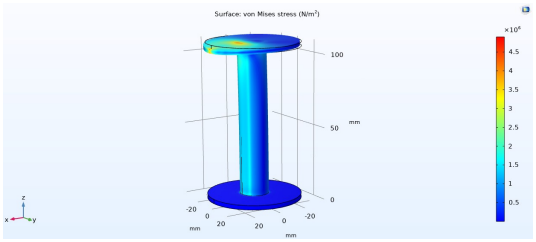

(b) The round model

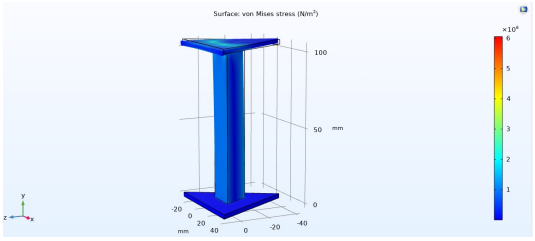

(c) The triangular model

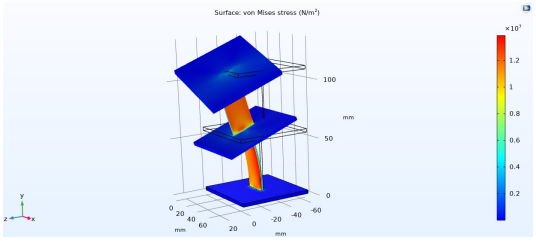

(d) The stacked plate model

Figure 17: The von Mises stress of the different designs in the deformed configuration

4.7 Second evaluation and decision

The designs of Figure 17a, Figure 17b, and Figure 17c do not deflect very much, which is caused by a large area moment of inertia, which makes the center part stiff. The dimensions of these designs can be made smaller to decrease the stiffness. However, this may complicate the structure's heating, requiring tiny heating films that were commercially unavailable. The deformation of the stacked hinge is significantly more than the previous designs. This design is chosen for further development because this concept has much larger deformation.

4.8 Material selection

Material selection is important because it is responsible for many design parameters. The material partly contributes to the stiffness of the hinge due to its E-modulus. Furthermore, the thermal properties are important for designing a shape-memory hinge. The austenite and martensite start and finish temperatures are important design parameters for shape-memory alloys because they decide at what temperatures the shape-memory effect takes place. The transition temperature is an important parameter for the shape-memory polymer, above which its shape-memory effect occurs. The E-modulus is also affected by temperature.

4.8.1 Nitinol

For the shape-memory alloy spring, Nitniol is chosen. Nitinol is a nickel-titanium alloy. Compared to other shape-memory alloys, Nitinol has a low production cost, is safer to handle, is widely available,

and has superior mechanical properties (30). Furthermore, Nitinol creates barely toxic by-products during manufacturing and has little impact on the environment (31). The material's properties will also change when the nickel or titan content changes. Other elements like copper can be added to the Nitinol alloy to change the material's properties. In section 5, three different Nitinol alloys will be investigated on their properties.

4.8.2 PLA

The shape-memory polymer Polylactic Acid (PLA) is used for the hinge's central bending part. PLA is the most widely used filament for 3D printers because it is easy to print due to its low melt temperature and biodegradable and recyclable (32). As discussed in subsection 2.2, the shape-memory effect occurs when a shape-memory polymer exceeds the glass transition temperature. It was found that the glass transition temperature for PLA is between 55 °C and 65 °C (33). The E-modulus decreases drastically when the PLA is heated to the transition temperature. This results in a softer material, making it easier to bend.

5 Nitinol springs

As mentioned before, the hinge is actuated using shape-memory springs, and the material used for the springs is Nitinol, a nickel-titanium alloy. This section investigates how different types of Nitinol behave. This is important because it influences how well the interactive hinge works. First, tensile tests are carried out to see the stress-strain curve of the different types of Nitinol. Then, it is explained how the Nitinol springs are manufactured, followed by recovery force experiments of the springs. After that, the springs are simulated and compared to the recovery force experiment results. These steps can be seen in the flowchart in Figure 18.

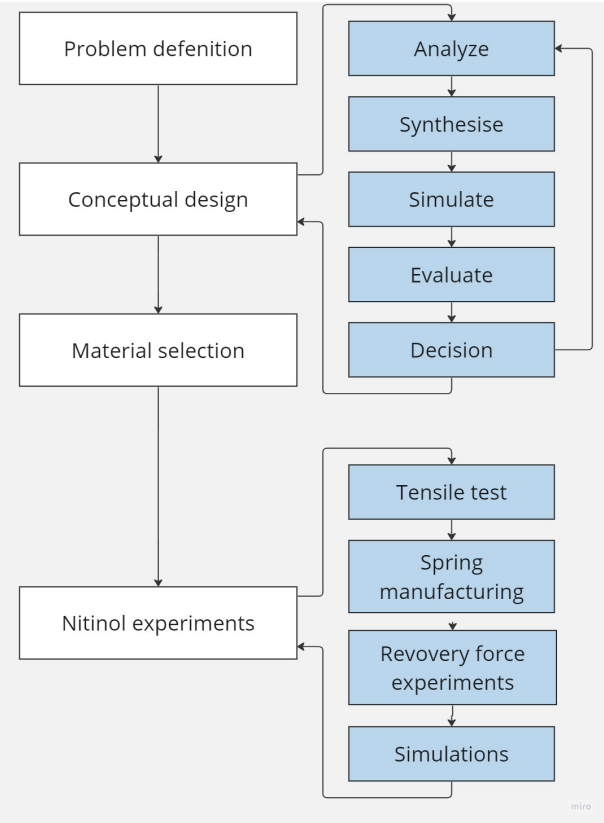

Figure 18: Updated flow chart up to and including the Nitinol experiments

5.1 Tensile tests

Three different types of Nitinol wires were bought. One wire consists of about 50% titanium and 50% nickel and has a diameter of 0.5 mm; one wire consists of about 45% titanium and 55% nickel has a diameter of 0.8 mm, and the other has a diameter of 0.81 mm and consists of about 50% titanium, 44% nickel, and 6% copper. Tensile tests were carried out with each type of wire to see the behavior of the wires. The machine used for these tests was the Zwick Z010 tensile tester. The tests were carried out at room temperature and displacement controlled with a test speed of 2 mm/min.

To mitigate the slipping effect, the wires were clamped with sandpaper between the clamp and the wire. The results of these tensile tests can be seen in Figure 19.

Four tensile tests were carried out with the 0.5 mm diameter NiTi wire, seen in Figure 19a. The samples show similar behavior but are slightly off each other, especially sample 3. Looking at the graph, a plateau can be seen when the load reaches around 100 MPa. The E-modulus was determined by determining the gradient until this point, which was 16.25 GPa. The strain increases rapidly after this point till a strain is reached of about 7.5%. This super-elastic behavior is caused by the material transforming from the twinned martensite structure to the detwinned martensite structure. The stress-strain relation is linear after this plateau until it reaches about 1100 MPa when the gradient decreases. When the stress reaches 1200 MPa, the ultimate tensile strength is reached.

Three tensile tests were carried out with the 0.8 mm diameter NiTi wire, seen in Figure 19b. Looking at the graph, the stress-strain relation is linear until the load reaches 800 MPa. The E-modulus is determined from the gradient of the linear part, which was 55 GPa. Then, there is a trough in load to 700 MPa, after which a plateau can be seen, where the load increases only slightly until the strain reaches 9%. After that, there is a trough, where the load is dropped again to 700 MPa. The stress-strain relation is linear after this plateau until it reaches about 1400 MPa when the gradient decreases. When the stress reaches 1550 MPa, the ultimate tensile strength is reached. Sample 1 differs slightly from the other samples after the plateau. The ultimate tensile stress is reached with a strain of 19%, compared with the other samples, where the ultimate tensile stress is reached with a strain of 21%.

Tensile tests were also carried out for the 0.81 mm NiTiCu wire, seen in Figure 19c. Unlike the NiTi wires, the NiTiCu wire shows no super-elastic behavior. The stress-strain relation is linear till about 900 MPa. The E-modulus was also determined using this linear part, which had a gradient of 19.5 GPa. After the linear part, the graph flattens. The ultimate tensile stress is 1100 MPa, with a strain of 33%. The tests of samples 2 and 3 were stopped after a strain of 25% because of the long testing time.

5.2 Manufacturing

The springs are manufactured according to the following steps. The Nitinol wire is made in the spring form by winding the Nitinol wire around a screw thread while clamping the ends between nuts so it stays in this shape. The springs winded around the screw thread are then put in the oven for 30 minutes at 550 °C. The heat treatment of the Nitinol wire will make the spring shape the new permanent shape. After the heat treatment in the oven, the Nitinol spring is cooled rapidly in a bucket of water. The springs are twisted off the screw thread, finishing the manufacturing process.

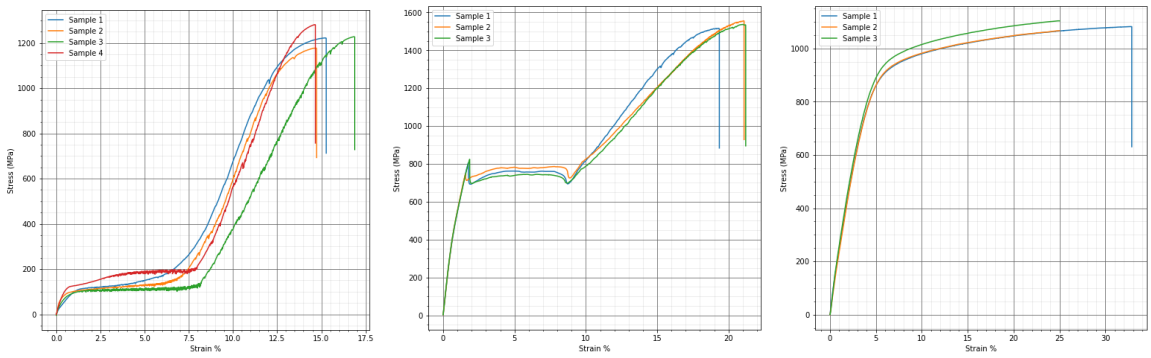

(a) Wire with 50% Nickel and 50% Titanium

(b) Wire with 55% Nickel and 45% Titanium

(c) Wire with 44% Nickel, 50% Titanium, and 6% Copper

Figure 19: The stress-strain graph for the different Nitinol wires

For each type of wire, screw threads with different diameters were used to manufacture the springs, namely M4, M5, and M6. Table 4 shows the properties of the manufactured springs.

Wire diameter	Material composition	Inner diameter spring	Spring length	Pitch	Wire length
0.5 mm	50%Ni 50%Ti	4 mm	30 mm	0.7 mm	573 mm
0.8 mm	55%Ni 45%Ti	6 mm	38 mm	1.0 mm	764 mm
0.81 mm	44%Ni 50%Ti 6%Cu	5 mm	38 mm	0.8 mm	807 mm

Table 1: Table which shows the properties of the manufactured springs

5.3 Recovery force experiment

The actuation force of the springs' recovery force must be determined. This is done by connecting one end of the spring scale and fixing the other end to a specified place, which causes the spring to deform. The force needed to deform the spring can be read on the spring scale. This is the spring force when it is not actuated. The springs are heated via joule heating by a programmable DC power supply. One end of the spring is connected to the plus side of the power supply, and the other to the minus side. The temperature of the spring is measured with a K-type thermocouple. The experiment setup can be seen in Figure 20.

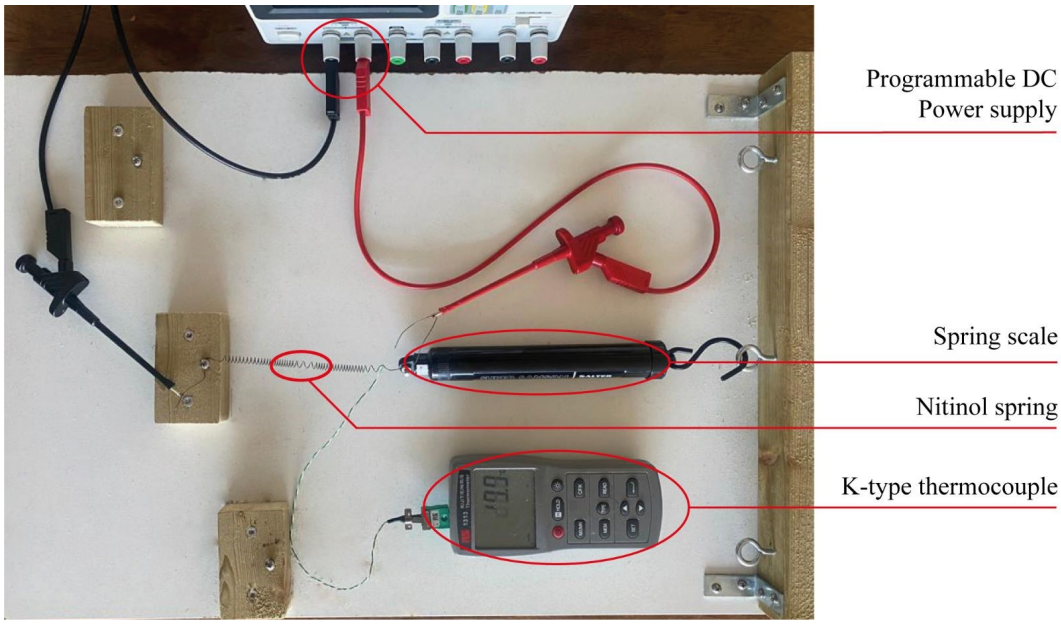

Figure 20: Setup recovery force experiments of the Nitinol spring

The different springs were tested. When deformed at 20 °C, the force for the springs was lowest for the 0.5 mm wire springs and highest for the 0.8 mm diameter springs. When the springs were heated above the austenite finish temperature, the force for the 0.8 mm wire barely increased. The force increased significantly for both the 0.5 mm and the 0.81 mm wire springs when heated above the austenite finish temperature compared to the force at 20 °C. Because of the high force when in the martensite phase and the small increase of force in the austenite phase, the 0.8 mm NiTi wire had little potential to be used as an actuator. Due to the significant increase in force when transformed from the martensite to the austenite phase, the 0.5 mm NiTi and the 0.81 mm NiTiCu springs have the most potential as actuators. That is why they are examined further.

Multiple tests were carried out with these two types of springs. For each of the two spring types, nine samples were manufactured. Three springs were deformed using our experimental setup to a state where the total spring length was 60 mm, three to a length of 100 mm, and three to a length of 140 mm. The springs are then heated using joules heating to 80 °C in steps of 10 °C.

Figure 21 shows the force-temperature graph for the NiTi and the NiTiCu springs, respectively. They all have similar behavior. At what temperature the force increases is the austenite start temperature, and at what temperature the force stops to increase is the austenite finish temperature. At what temperature the force increases and stops to increase differs for each graph. This is expected because, as seen in Figure 3, the start and finish temperatures increase with an increase in stress.

For many applications, hinges need to be actuated multiple times. It is, therefore, useful to see

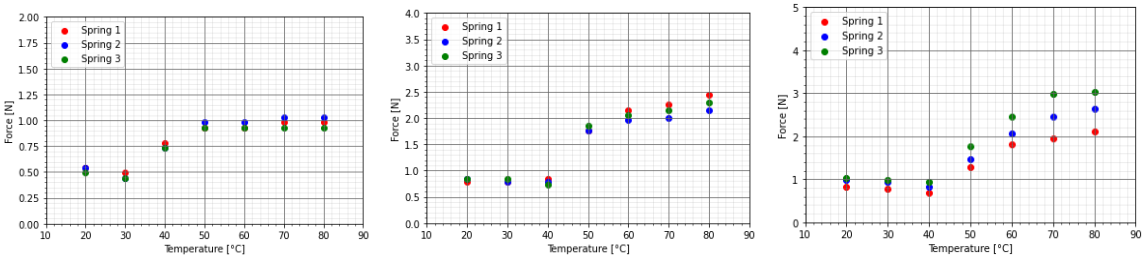

(a) Deformation NiTi spring to a length of 60 mm

(b) Deformation NiTi spring to a length of 100 mm

(c) Deformation NiTi spring to a length of 140 mm

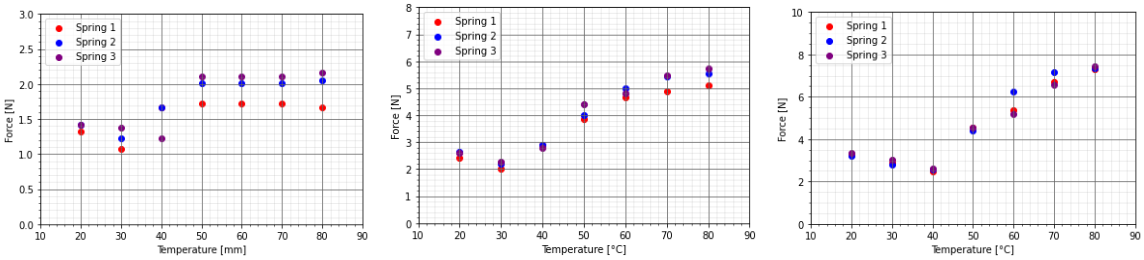

(d) Deformation NiTiCu spring to a length of 60 mm

(e) Deformation NiTiCu spring to a length of 100 mm

(f) Deformation NiTiCu spring to a length of 140 mm

Figure 21: Force-Temperature graph for the 0.5 mm diameter wire NiTi springs and 0.81 mm diameter wire NiTiCu springs deformed to 3 different lengths

what happens when springs are actuated multiple times. This can be seen in Figure 22. For both springs, when the spring is deformed to a length of 60 mm, there is a dip in reaction force after actuation number 1, but after that, the reaction force is relatively stable. When the springs are deformed to 100 mm and 140 mm, the reaction force decreases after the first few actuations. After about six actuations, the reaction force stabilizes, as it barely does not change anymore after this point.

The relation between the power input and the temperature can be seen in Figure 23. The relation can be considered linear for all deformations. It is also interesting to see the relationship between the power input and the force. This can be a guideline for how much power should be supplied to the springs to control the hinge. This can be seen in Figure 24. As can be seen, the reaction force-power input relation has a clear trend, except for Figure 24c and Figure 24d, which have a bigger spread.

Experiments are carried out to see what happens when the spring is scaled. The NiTiCu spring is made twice as small as the ones used in previous experiments. The displacement will also be twice as small. The small spring will be deformed to 70 mm, which is compared with the original spring being deformed to 140 mm. This can be seen in Figure 25. The results are quite similar.

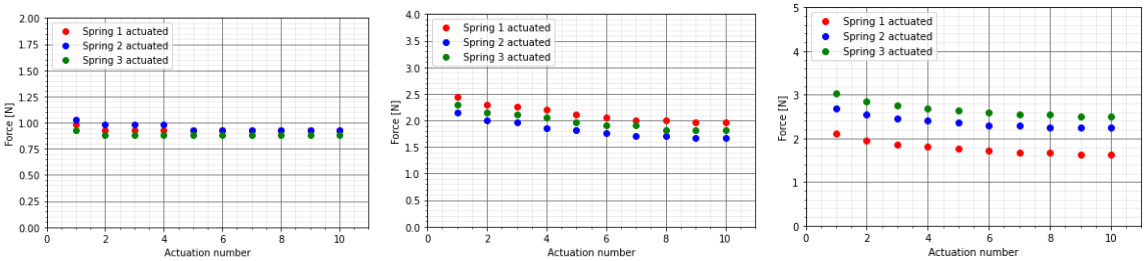

(a) Deformation NiTi spring to a length of 60 mm

(b) Deformation NiTi spring to a length of 100 mm

(c) Deformation NiTi spring to a length of 140 mm

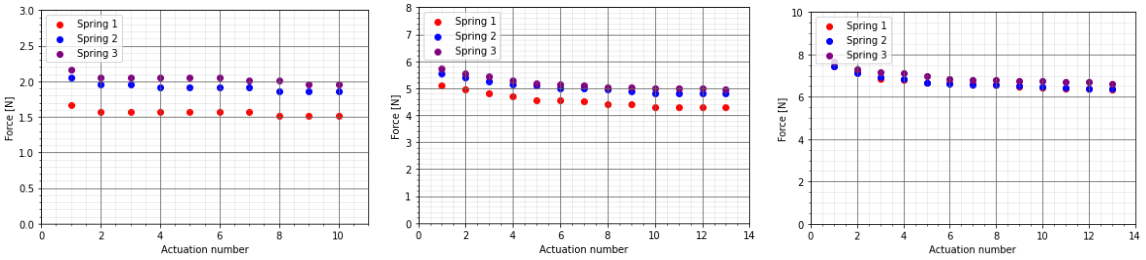

(d) Deformation NiTiCu spring to a length of 60 mm

(e) Deformation NiTiCu spring to a length of 100 mm

(f) Deformation NiTiCu spring to a length of 140 mm

Figure 22: The recovery force development when the NiTi and NiTiCu springs are actuated multiple times when deformed to 3 different lengths

The force is lower on the whole trajectory for the small springs than for the large ones. At 20 °C, the difference is small, but for higher temperatures, the difference in force increases to more than 1 N.

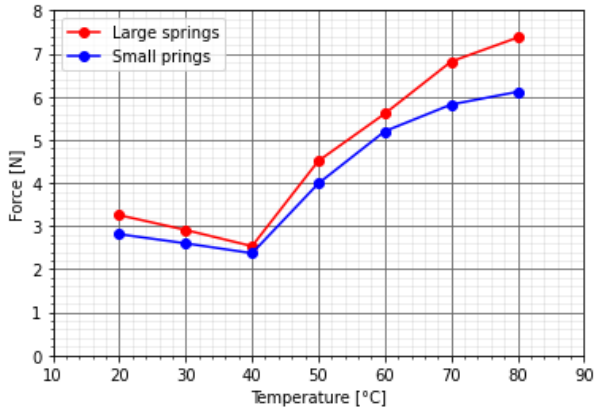

Figure 25: Force-temperature graph comparing the small NiTiCu springs to the large NiTiCu springs when the displacement and length of the small springs is a factor 2 smaller

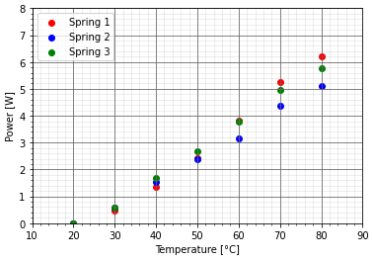

(a) Deformation NiTi spring to a length of 60 mm

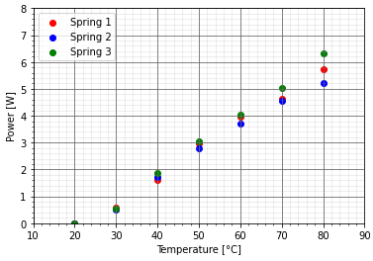

(b) Deformation NiTi spring to a length of 100 mm

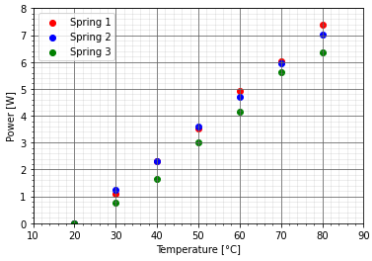

(c) Deformation NiTi spring to a length of 140 mm

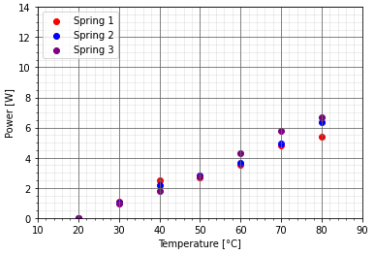

(d) Deformation NiTiCu spring to a length of 60 mm

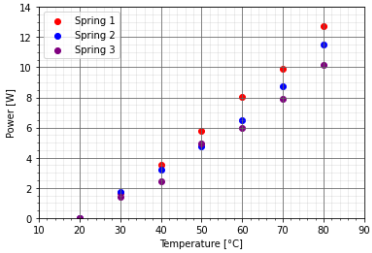

(e) Deformation NiTiCu spring to a length of 100 mm

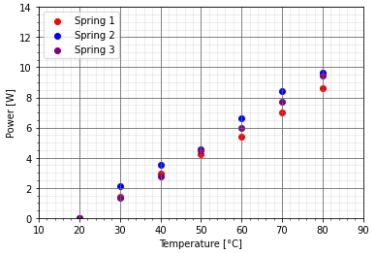

(f) Deformation NiTiCu spring to a length of 140 mm

Figure 23: The power-temperature relation for the NiTi and the NiTiCu springs when deformed to 3 different lengths

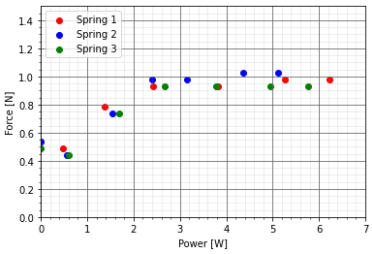

(a) Deformation NiTi spring to a length of 60 mm

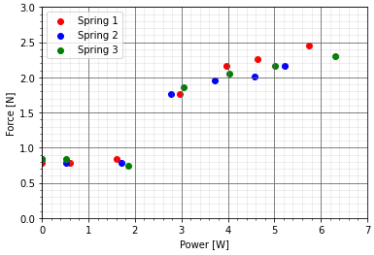

(b) Deformation NiTi spring to a length of 100 mm

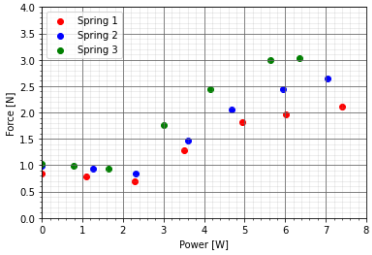

(c) Deformation NiTi spring to a length of 140 mm

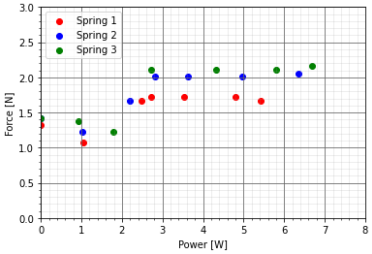

(d) Deformation NiTiCu spring to a length of 60 mm

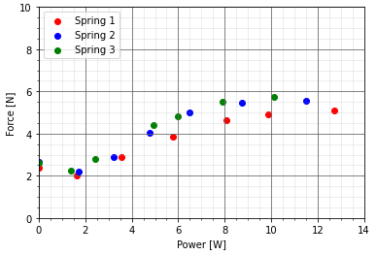

(e) Deformation NiTiCu spring to a length of 100 mm

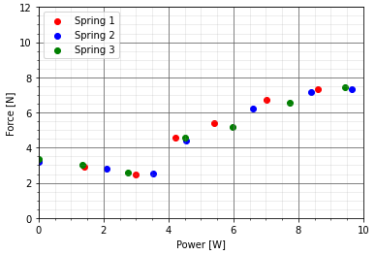

(f) Deformation NiTiCu spring to a length of 140 mm

Figure 24: The power-recovery force relation for the NiTi and the NiTiCu springs when deformed to 3 different lengths

5.4 Spring simulations

Finite element method simulations are carried out with the simulation software Comsol Multiphysics to simulate the behavior of the spring. It is determined if the recovery force of the spring in the simulations and the experiments are alike. The geometry of the spring is modeled as a helix, with the corresponding radius, thickness, axial pitch, and the number of turns. Material properties are also important parameters for performing accurate simulations. Some are found online, while others are determined based on the experiments.

The temperature when austenite starts to form and when the material is entirely austenite is determined from Figure 21. The approximate values can be seen in Table 2. As can be seen, different values are used for each spring and deformation.

	A_s	A_f
60 mm deformed NiTi	35°C	50°C
100 mm deformed NiTi	40°C	60°C
140 mm deformed NiTi	45°C	70°C
60 mm deformed NiTiCu	35°C	50°C
100 mm deformed NiTiCu	35°C	70°C
140 mm deformed NiTiCu	40°C	75°C

Table 2: Table which shows the approximate austenite start and finish temperatures

The Young's modulus in the martensite phase is determined based on Figure 19a and Figure 19c. The value of the E-modulus is the gradient of the linear part of the stress-strain graph. For the NiTi wire, this results in an E-modulus of 16.25 GPa, and for the NiTiCu wire, an E-modulus of 19.5 GPa. Since the machine for tensile testing when the wire is heated was unavailable, the austenite Young's modulus was guessed based on the recovery force measurement results. The austenite E-modulus was set as 40 GPa for the NiTi wire, while for the NiTiCu wire, it was set as 35 GPa. Solid mechanics physics is used in this simulation. One end of the helix is selected as a fixed constraint, while the other is displaced. The shape-memory alloy material model is applied. The reaction force of the helix at the end is determined when the temperature of the helix is between 20°C and 80 °C, with intervals of 10 °C.

The results can be seen in Figure 26. The simulations and experiments follow a similar trend when looking at these results. When looking at both springs, you can see that the simulations are lower for the 60 mm deformation than the experiments. Still, when the deformation becomes larger, the simulations shift more to the top until the simulations have higher values than the experiments. There is a substantial difference between experiments and simulations at some points. The largest

difference is 1.85 N, which is when the NiTiCu spring is deformed to 140 mm at 40 °C. Table 3 shows the mean absolute error of the simulations.

	Mean absolute error
60 mm deformed NiTi	0.11 N
100 mm deformed NiTi	0.18 N
140 mm deformed NiTi	0.35 N
60 mm deformed NiTiCu	0.30 N
100 mm deformed NiTiCu	0.53 N
140 mm deformed NiTiCu	0.79 N

Table 3: Table which shows the mean absolute error of the simulations when compared to the experiments

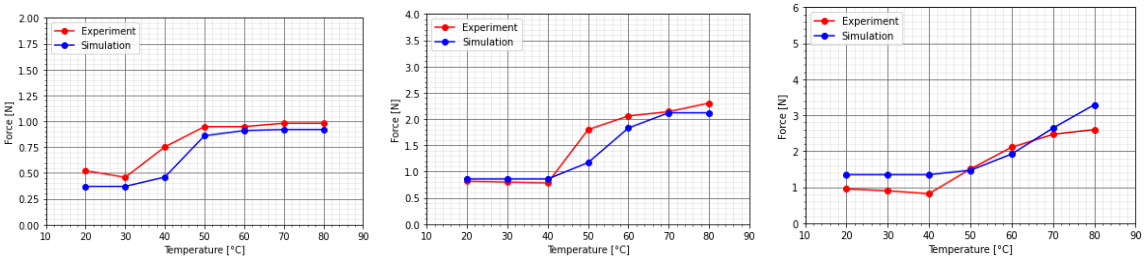

(a) Deformation NiTi spring to a length of 60 mm

(b) Deformation NiTi spring to a length of 100 mm

(c) Deformation NiTi spring to a length of 140 mm

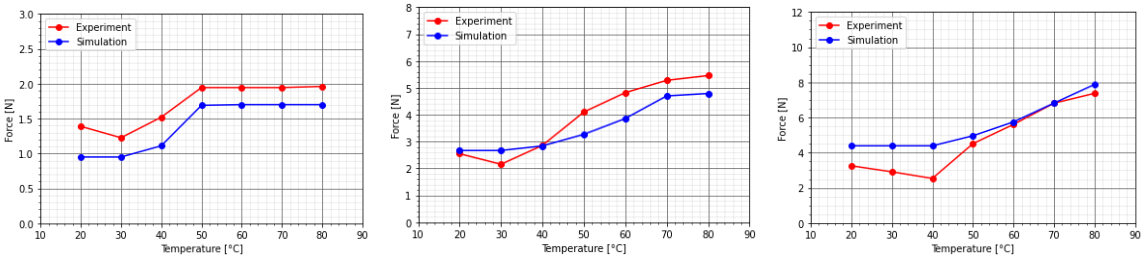

(d) Deformation NiTiCu spring to a length of 60 mm

(e) Deformation NiTiCu spring to a length of 100 mm

(f) Deformation NiTiCu spring to a length of 140 mm

Figure 26: Force-Temperature graph Comparing the simulation values to the experiments

5.5 Chapter summary

The tensile test showed that the properties of Nitinol differ a lot when the content of Nickel, Tin, and Copper changes. The wire with copper did not have the superelastic effect, while the 0.8 mm wire showed the superelastic effect at much higher stresses than the 0.5 mm wire. Furthermore, the 0.8 mm wire had a much higher E-modulus than the other wires. When the springs were

manufactured, the initial recovery force experiments showed that the 0.8 mm Nitinol was unsuitable for actuators because the force barely increased after phase transformation. The recovery force experiments showed the behavior of the springs when they were heated and the effect when springs were deformed to different lengths. Useful information could be retrieved from these experiments, like the austenite start-and-finish temperatures, but also showed how the performance degrades over multiple actuations. The power-recovery force relation is useful because it can serve as a handbook for controlling the hinge. The springs were modeled in Comsol to see if the simulations resembled reality. When looking at the results, the simulations and the experiments showed a similar trend, but the difference can sometimes be substantial.

6 Detailed design

From the conceptual design, made in section 4, a detailed design is made. The flow chart up to this point can be seen in Figure 27. The CAD model of the detailed design of a single hinge, which can actuate along one axis, can be seen in Figure 28. As can be seen, the hinge consists of multiple parts:

- The gray helix is the shape-memory alloy spring
- The white part is the shape-memory polymer body
- The black rectangle on the edges are the intermediate parts
- The parts are connected with each other with bolts and nuts

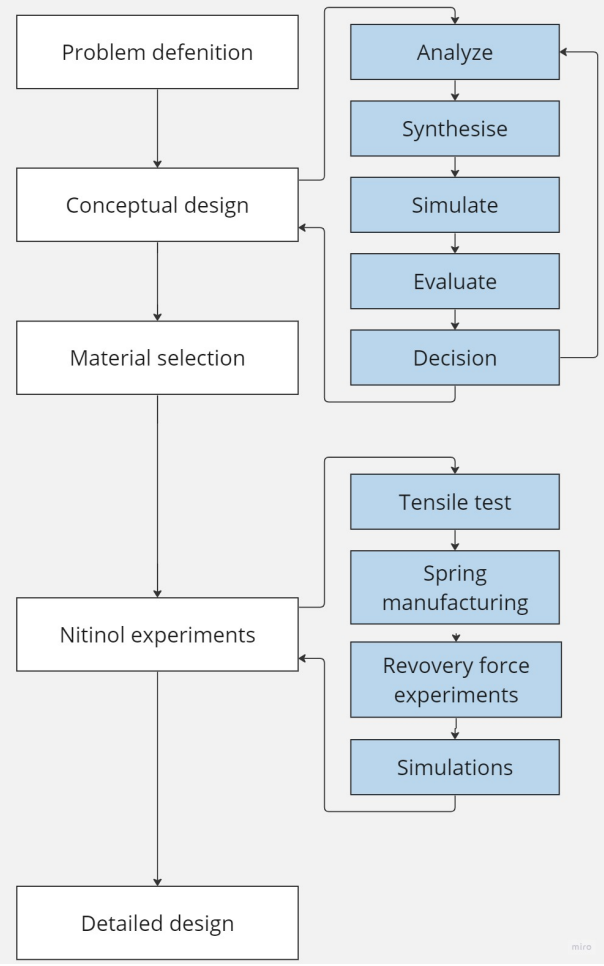

Figure 27: Updated flowchart up to and including the detailed design

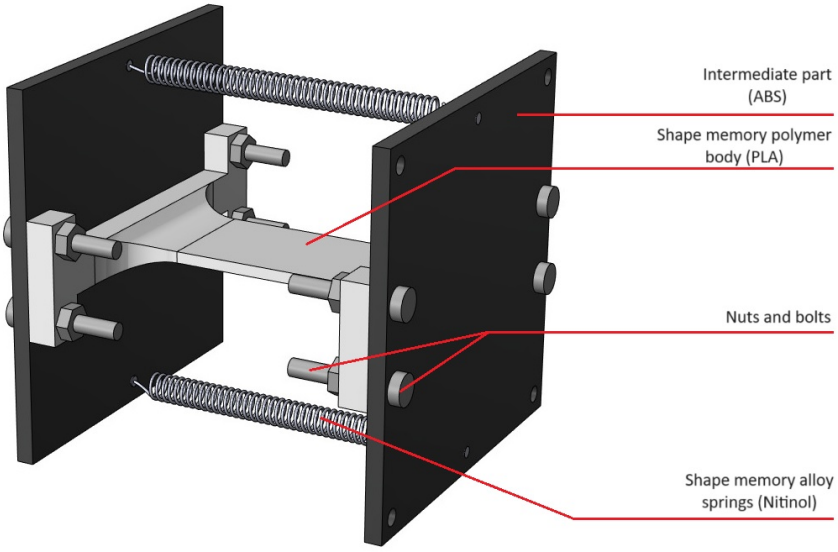

(a) Impression with a legend of the different parts

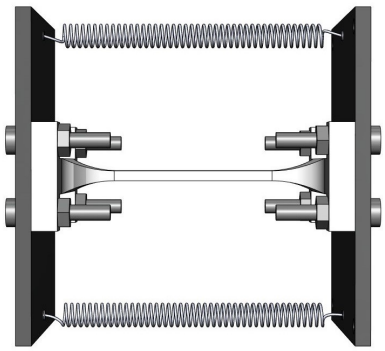

(b) Side view

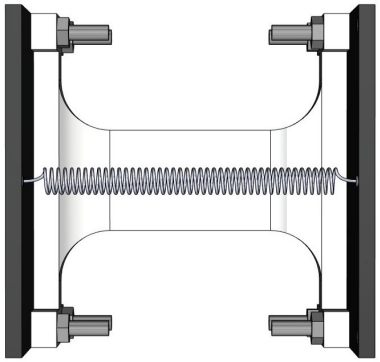

(c) Top view

Figure 28: Different views of the CAD models of the single hinge

To achieve multi-axial actuation, the single hinge is stacked on another single hinge and rotated 90 °. The single hinges are connected with each other with bolts and nuts at the corner of the ABS part. The CAD model of the stacked hinge can be seen in Figure 29.

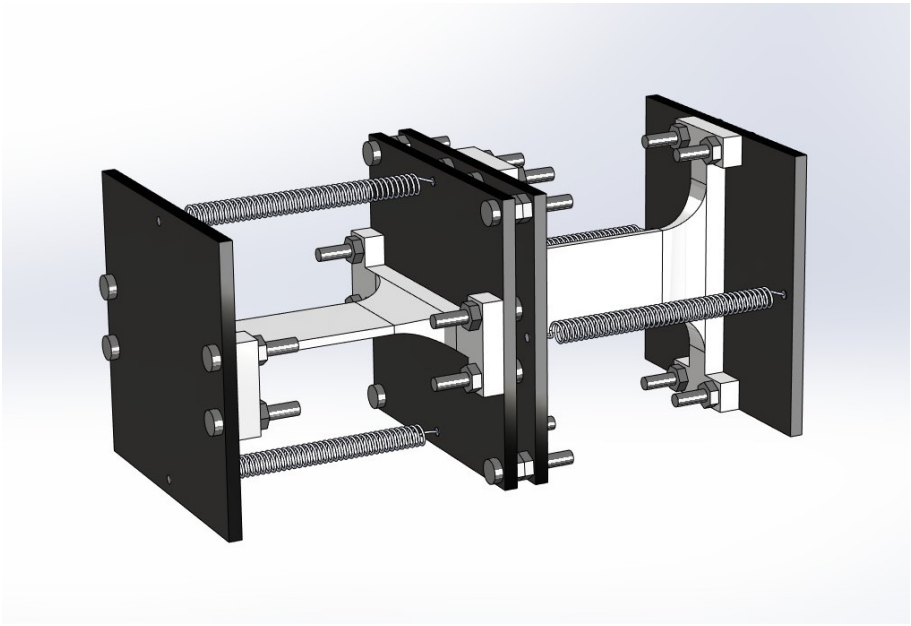

(a) Stacked hinge

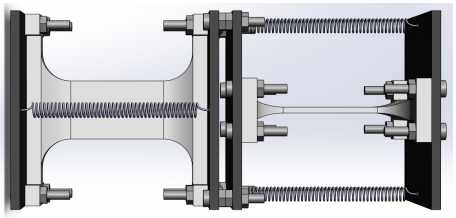

(b) Stacked hinge side view

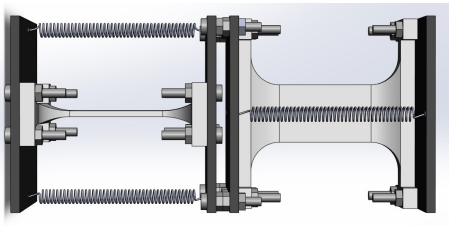

(c) Stacked hinge top view

Figure 29: Different views of the CAD models of the stacked hinge

6.1 Shape-memory alloy spring

The two spring parts are the Nitinol springs. The wire with 50% nickel and 50% titanium is chosen for the detailed design. This wire is chosen because of the superelastic effect at low stress. When the hinge is actuated by heating one spring, the other spring will not give a large counterforce. The hinge has a better shape recovery when the spring is cooled down. The wire has a diameter of 0.5 mm. The initial length of the springs is 30 mm with an inner diameter of 4 mm and has 43 revolutions. The springs are deformed to a length of 62 mm. The properties of the spring can be seen in Table 4.

6.2 Shape-memory polymer body

The white part in the middle of the figure is the PLA base. This part is manufactured using the 3D printing technique. This part is printed with an ultimaker2+ 3D printer and has 100 % PLA filament. The dimensions of the PLA body can be seen in Figure 30. The body consists of a plate in the middle with a thickness of 2 mm at the center, while the thickness increases at the outer ends. The plate has a length of 52 mm. The width is at the center 20 mm, while the width at the outer ends increases. The increase in width and thickness at the outer ends increases the stiffness, which results in the bending when actuated concentrates at the center part of the plate. On the outer ends of the PLA plate, there is an additional structure with holes with a diameter of 3 mm, designed to attach the base to the ABS parts. The PLA has to be heated to perform its shape-memory effect. That is why heating films are attached to both sides of the PLA. The heating films have a dimension of 52×20 mm, and have a power of 1 W.

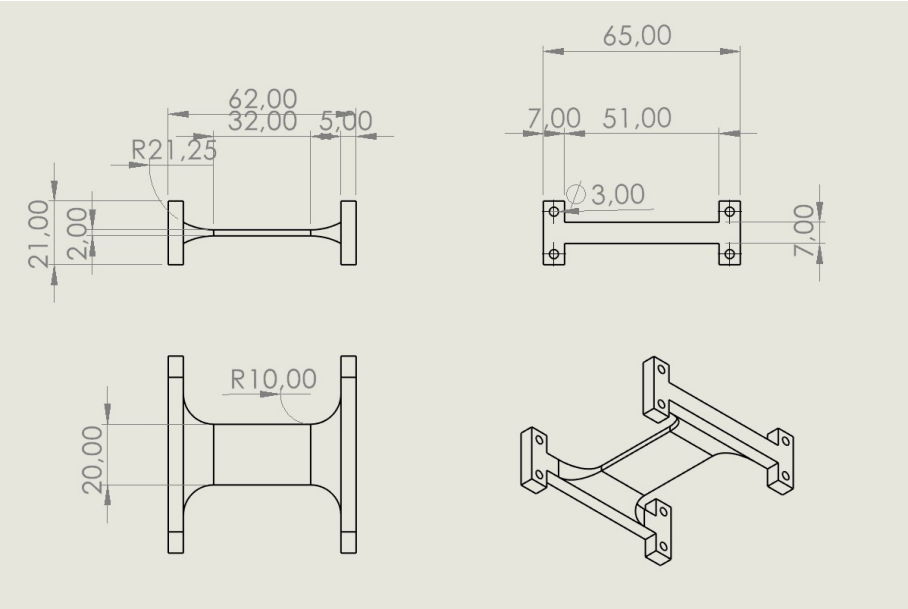

Figure 30: Drawing of the PLA part with dimensions

6.3 Intermediate part

Last section, the results show that the Nitinol spring can get to temperatures of up to 80 °C. If the PLA comes in contact with a fully actuated spring, the PLA becomes so soft that the Nitinol will cut through the material. Another material that functions as an intermediate piece to attach the spring to the body is needed to prevent this. The material used as an intermediate part is Acrylonitrile butadiene styrene (ABS). ABS is also a shape-memory polymer with a higher glass transition temperature than PLA. The shape-memory effect occurs at a temperature of about 105 °C (34). ABS will remain stiff when it comes in contact with 80 °C Nitinol spring. Furthermore, ABS can also be recycled (35). Because of these properties, ABS is a suitable material for use as

an intermediate piece.

The drawing of this part can be seen in Figure 31. They were manufactured by cutting a plate, and holes were drilled into it. They have dimensions of 65×65×3 mm. These ABS parts have 3 mm diameter holes. Some of these holes were made to attach the PLA part to the ABS part, while the holes at the corner connected two single hinges into a stacked hinge.

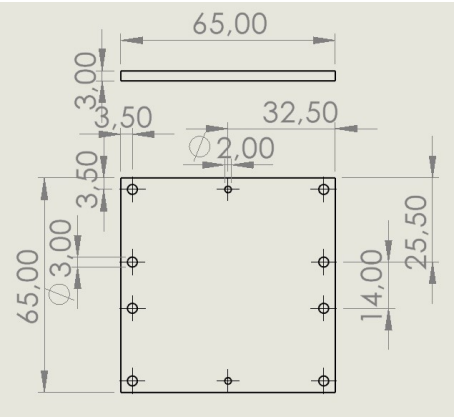

Figure 31: Drawing of the intermediate part with dimensions

6.4 Bolts and nuts

To connect the parts, bolts and nuts are used. Two different types are used for this hinge. The outer ends of the springs are connected to the ABS parts and clamped with M4×16mm bolts, M4 nuts, and M4 locking rings. In the CAD model, the clamping of the springs to the intermediate part is simplified. To connect the body to the intermediate part, and the connection between the two single hinges for the stacked hinge, M3×20 mm bolts with M3 nuts are used.

6.5 Part list

	Single hinge	Stacked hinge
Shape-memory alloy (Nitinol) springs	2	4
Shape-memory polymer body (PLA) part	1	2
Intermediate (ABS) part	2	4
M3 bolts	4	12
M3 nuts	4	16
M4 bolts	4	8
M4 nuts	4	8
M4 locking ring	4	8

Table 4: Table which shows how many parts are used for each design

7 Hinge experiments

As can be seen in Figure 29, the stacked hinge consists of two single hinges in series, but with one hinge rotated 90 °. For a better understanding of how the stacked hinge works, the single hinge is first tested when displaced in horizontal and vertical directions. In this part, experiments are carried out for the single hinge actuated horizontally, the single hinge actuated vertically, and the actuation of the stacked hinge. This section starts by explaining the method used for the displacement experiments, which were conducted to determine the working range of the hinge. This is followed by an explanation of the simulation method of the hinges. Simulations are important because the behavior of the hinge can be predicted with the simulations. Properties can be adjusted without having to build a new hinge prototype. Just like the simulations of the springs, the hinge is simulated in the finite element software program Comsol. Displacement experiments and simulations are conducted for each hinge. The actuation time and energy consumption for a single hinge are also determined. The flow chart of the whole process can be seen in Figure 32.

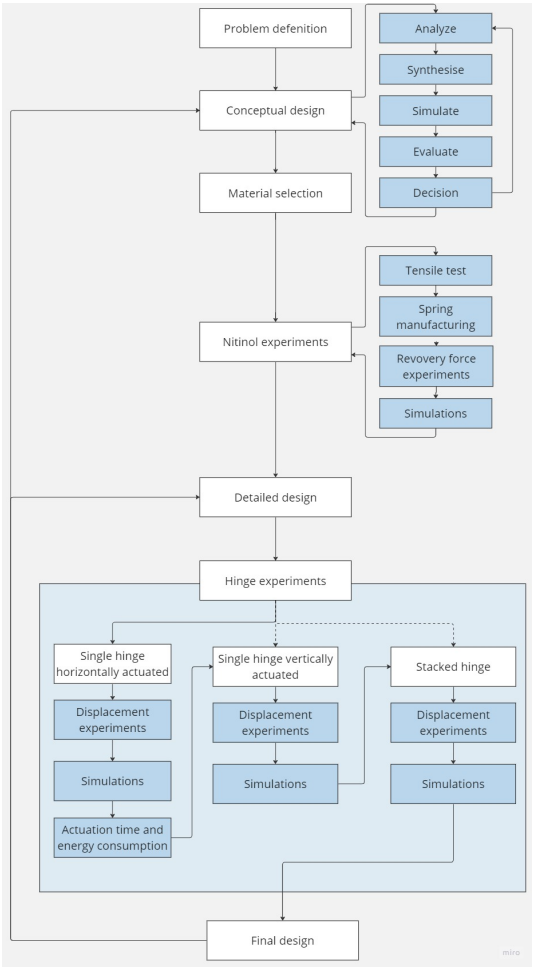

Figure 32: Flow chart

7.1 Method displacement experiments

The test setup for determining the working range of the hinges can be seen in Figure 33. As can be seen, the hinge is attached to the white T-shaped structure, so the hinge hangs in the air. This is done so that if the hinge is actuated, there is no friction from a table. The hinge in Figure 33 works in the horizontal direction, but the T-shaped structure can also be rotated 90 °so that the hinge works in the vertical direction. A DC power supply is the power source. The power to the heating films is controlled via channel 1 of the power supply, while the springs are controlled via channel 2. A k-type thermocouple is connected to the hinge to check the temperature of the PLA.

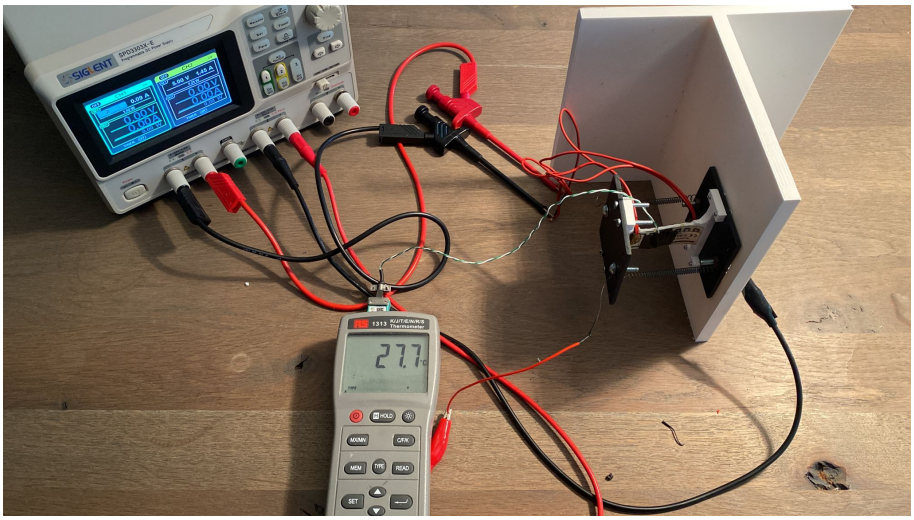

Figure 33: Test setup for determining the working range of the hinge

The hinges are actuated as follows: first, the heating films are heated till about 65 °C, so the PLA is above the transition temperature. When this temperature is reached, one of the springs is actuated by increasing power to the spring in small steps until the maximum recovery force is reached. Then, the power to the spring is stopped, and the hinge will recover its shape. For each power increment, the distance is measured from the outer end of the left ABS plate to the outer end of the other ABS plate. From what point to what point the distance is measured can be seen in Figure 34.

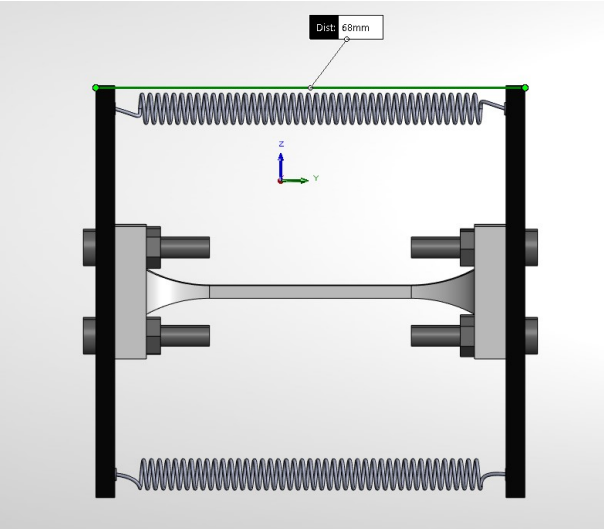

Figure 34: The measured distance for determining the working range

7.2 Simulation method

The hinges were designed in Solidworks, as seen in section 6. The geometry was imported into Comsol. The materials were created with the right material properties. The density of the materials was obtained by weighing the parts and dividing the volume of the parts by the weight. The E-modulus of the Nitinol was obtained from subsection 5.4. Two materials were created for Nitinol: one with the martensite E-modulus and one with the austenite E-modulus. The E-modulus of the ABS was found online. As mentioned before, the PLA part is 3D printed. Several printing parameters can affect the E-modulus of 3D printed PLA (36). That is why the E-modulus is obtained from the simulations.

Solid mechanics physics is used in the simulations. One outer end of the ABS part is fixed. Gravity is applied, and gravity acts accordingly depending on whether the horizontal or vertical actuation is simulated. The actuation of the springs is simplified. An initial strain is applied to the springs. The low E-modulus martensite material is applied when the spring is not actuated. When the spring is actuated, the higher E-modulus austenite material is applied. The stationary study is used for these simulations.

The unknown is the PLA E-modulus. The heating film is glued to the PLA in the experiments. This increases the E-modulus. The E-modulus of the PLA in the simulations will be the combination of the PLA itself and the heating film. To determine the E-modulus of the PLA, it is checked at what E-modulus the experiments and simulation behave the same way. This is done by evaluating a point at the ABS plate in Comsol and determining the displacement field of that point. Using

the displacement field and the initial ABS-to-ABS distance, the distance in the deformed state can be determined using Pythagoras.

7.3 Single hinge horizontal actuation

7.3.1 Displacement experiments

First, displacement experiments are carried out when the hinge is actuated horizontally, as seen in Figure 35. The tests are carried out for three hinges. Each hinge is actuated three times. The results can be seen in Figure 36. The y-axis is the ABS-to-ABS distance, and the x-axis is the power supplied to the spring. For all actuations, the distance changes significantly until a power of about 4 W is supplied. When the power is increased further, the distance almost does not increase. This behavior is expected because the same behavior occurred when experiments with the springs were carried out, as seen in Figure 24a.

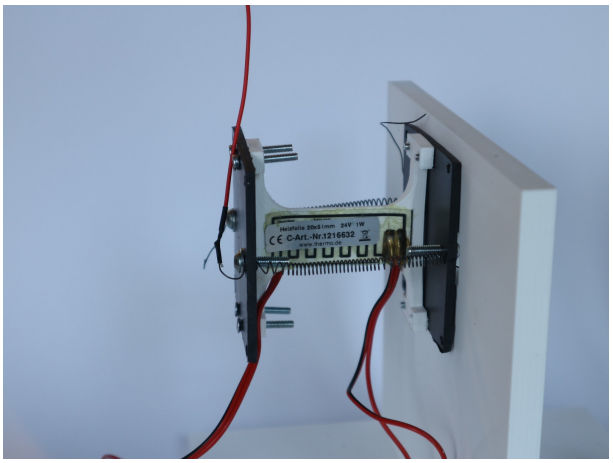

Figure 35: Side view when the hinge is actuated horizontally

When looking at the first actuation, it can be seen that each hinge has a start position of 68 mm. When the power increases, the spring shrinks, and the distance decreases to about 58 mm. There is not much difference between the hinges when they are actuated for the first time. Between the first and second actuations, the power supply to the springs is stopped, and the hinge partly recovers its original shape. Now, the other spring is actuated. The distance is now also measured from the other side. The initial distance is about 71 mm, and the displacement reaches about 58 mm, with hinge 1 having a slightly smaller distance. In the third actuation, the same spring as the first actuation is actuated again. The initial distance is now about 70 mm. The displacement of the hinges is now a bit more scattered. The mean distance is now 59 mm, with hinge 3 having a larger distance and hinge 1 having a smaller distance.

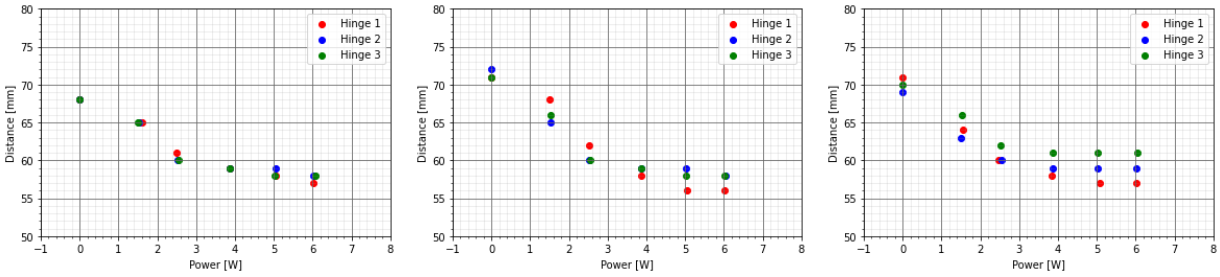

(a) First actuation **(b)** Second actuation **(c)** Third actuation

Figure 36: ABS-to-ABS distance of the horizontal actuated hinge on the y-axis and the power supplied to the spring on the x-axis

To see if there is a trend in the maximum deformation, multiple actuations are carried out. This can be seen in Figure 37. The first actuation has the smallest distance. After a few actuations, the distance stabilizes to a steady state of about 60 mm. After these actuations, a weight of 200 g was added at the end of the hinge to see if it affected the distance when actuated. It was found that the distance did not change when this weight was added.

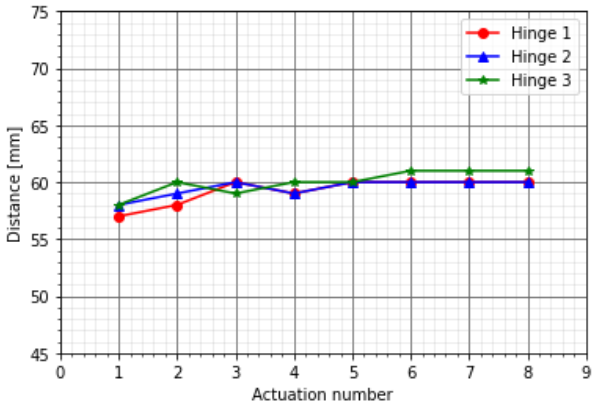

Figure 37: The ABS-to-ABS distances of the hinge when fully actuated horizontally where each spring is actuated alternately

7.3.2 Simulation

The horizontal actuated single hinge is imported into Comsol. In the displacement experiments, when one of the springs is actuated when the PLA is not heated, the ABS-to-ABS was 66 mm. It was found that when the E-modulus was set to 620 MPa, the simulations had an ABS-to-ABS distance at the end corner of about 66 mm. When the PLA is heated to 65 °C, the ABS-to-ABS distance is about 58 mm. This corresponds to an E-modulus of 28 MPa. Figure 38 shows the hinge in the FEM simulation in the fully actuated state when the ABS-to-ABS distance is 58 mm. The

hinge makes an angle of 10°.

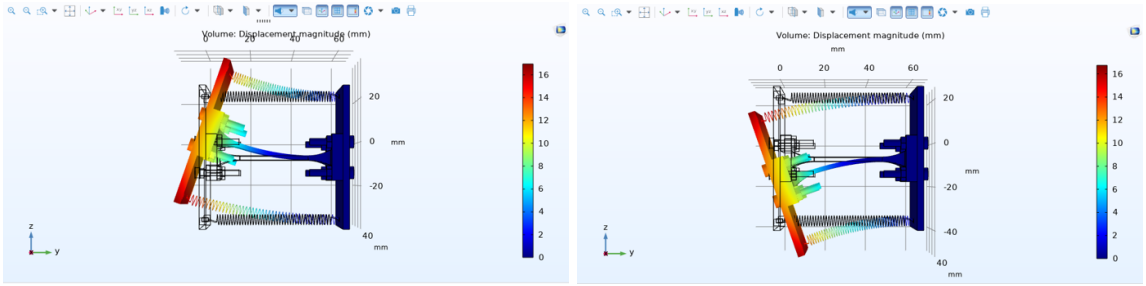

(a) Actuation spring 1 **(b)** Actuation spring 2

Figure 38: Top view horizontal simulations

7.3.3 Actuation time and energy consumption

To determine the energy efficiency of the hinge, it is determined how long it takes for the PLA body and the Nitinol springs to be heated. This is done by applying power to both heating films and measuring the temperature of the PLA with the k-type thermocouple. This is done when two different powers are supplied to the heating films. The results can be seen in Figure 39.

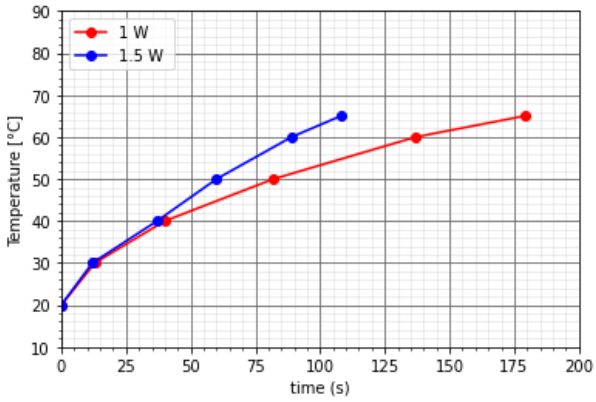

Figure 39: Time versus temperature relation of the PLA when two different powers are supplied to each heating film

It is also determined how fast a spring is heated. The austenite finish temperature is 50 °C when the spring is deformed to 60 mm. This is the temperature at which the spring needs to be heated to give the maximum force with the lowest temperature. It is checked how fast the spring heats when different powers are supplied to the spring. It is found that the spring is heated to 50 °C in 33 seconds when a power of 4 W is supplied, 10 seconds when 6 W is supplied, and 7 seconds when 8 W is supplied.

Using the formula $E = P \times t$, it is found that the heating films were the most energy efficient

when 1.5 W was supplied, while the springs were the most energy efficient when 8 W was supplied. Figure 40 shows the energy supply to the heating films and the spring. As can be seen, when the hinge is fully actuated, the film's power is dropped to 0.8 W, so the PLA stays at 65 °C, while the power to the spring is cut off. At this point, the shape recovery takes place and lasts 104 seconds. The integral of this graph has to be determined to determine the amount of energy that has to be supplied for the actuation of a single hinge. This results in an energy use of 546.4 J, when each heating film is powered with 1.5 W and the spring is powered with 8 W.

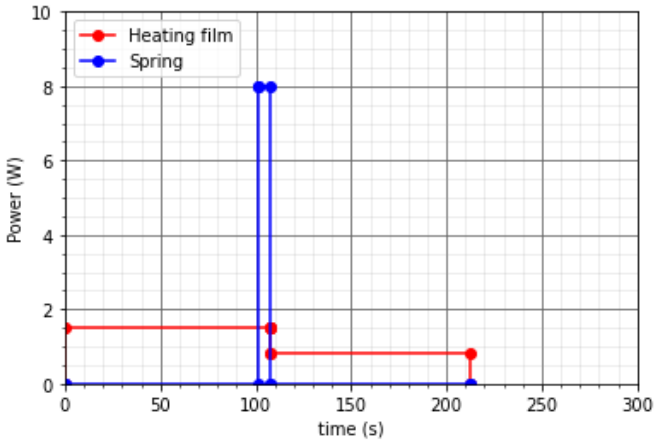

Figure 40: Power supply over time for one actuation cycle

Much energy is needed to heat the PLA when it is still at room temperature to be able to actuate it. If the hinge is already at 65 °C, the actuation cycle now only consists of heating the spring and, subsequently, shape recovery. The actuation cycle now takes 111 seconds with an energy consumption of 248 J.

7.4 Single hinge vertical actuation

7.4.1 Displacement experiments

The hinge is now actuated when rotated 90 degrees, as seen in Figure 41. Now, gravity is important because the springs must also overcome the hinge's gravity. The hinge is actuated similarly as in subsection 7.3. The results can be seen in Figure 42.

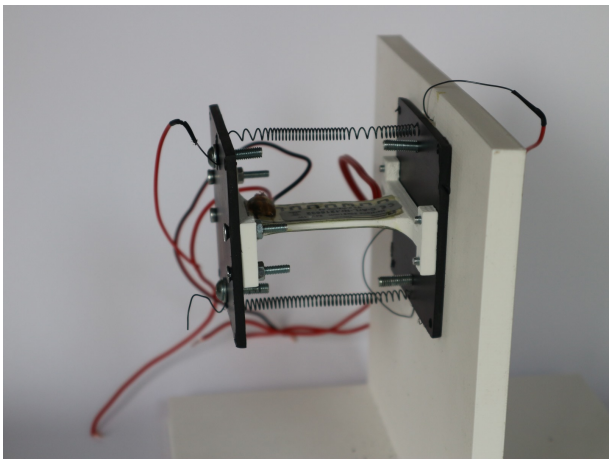

Figure 41: Side view when the hinge is actuated vertically

When looking at the first actuation, the initial distance is not 68 mm, as when the hinge is actuated horizontally, but around 72 mm. This is because the material gets softer and is pulled down by its own weight. The distance decreases to about 61 mm when the top spring is actuated. After the first actuation, the power supply to the top spring is stopped, and the material recovers its shape. The second actuation starts with an initial distance of about 65 mm, meaning the hinge is already downward. When fully actuated, the distance decreases to about 52 mm. For the third actuation, the initial distance increases to 79 mm, and when fully actuated, it reaches about 64 mm. The fourth actuation begins with a distance of around 62 mm and, when fully actuated, decreases to about 52 mm.

Comparing actuation 2 with actuation 4, there is not much difference. They have a similar start and ending position. Actuations 1 and 3 differ more, especially the start position. The top spring of hinge one has also plastically deformed due to being used multiple times, which can be seen by a lower initial distance and a higher fully actuated distance.

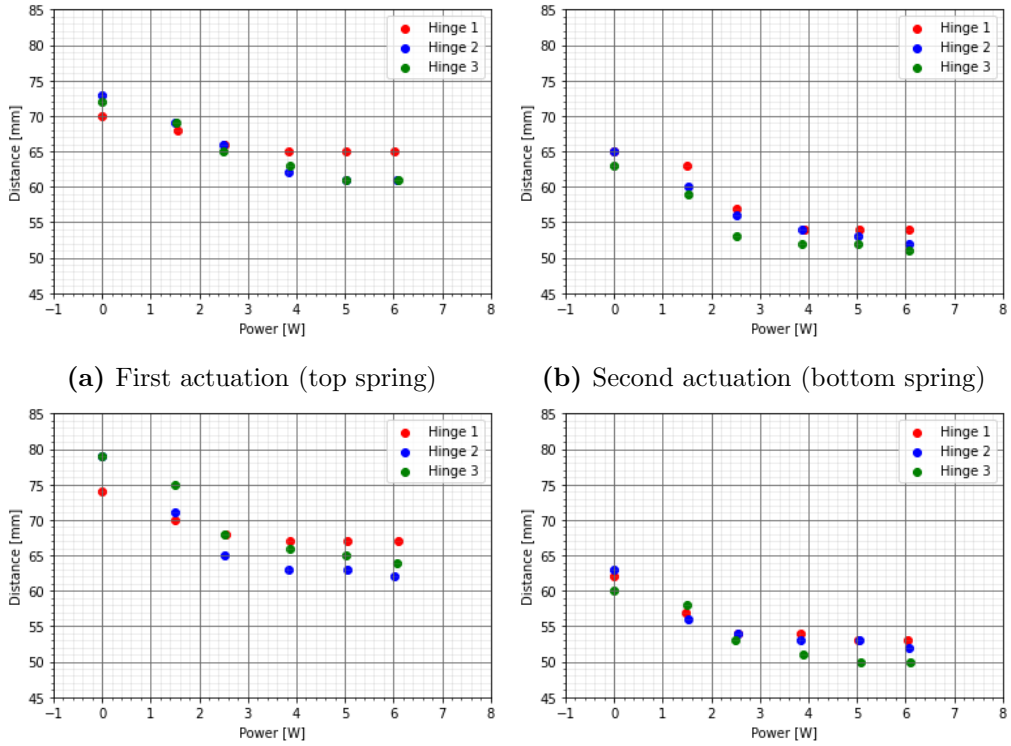

(a) First actuation (top spring)

(b) Second actuation (bottom spring)

(c) Third actuation (top spring)

(d) Third actuation (bottom spring)

Figure 42: ABS-to-ABS distance of the vertical actuated hinge on the y-axis and the power supplied to the spring on the x-axis

Due to the similarities between Figure 42b and Figure 42d, it is investigated if the actuation distance stabilizes for the top side after multiple actuations. This can be seen in Figure 43. After actuation number 3, the top distance stabilizes to a distance of 65 mm, while the bottom distance stabilizes after actuation number 6 to a distance of about 53 mm.

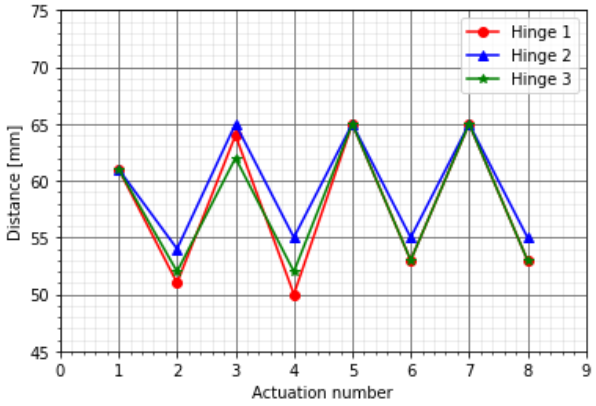

Figure 43: The ABS-to-ABS distances of the hinge when fully actuated vertically where the uneven actuation numbers are the top actuations and the even actuation numbers are the bottom actuations

A test is done if weight is applied at the end of the hinge. Three spoons with different weights were applied. The results can be seen in Figure 44. The difference in distance between the top spring actuation and bottom spring actuation is 7 mm for a weight of 65 g, compared to 8 mm for the other applied weights.

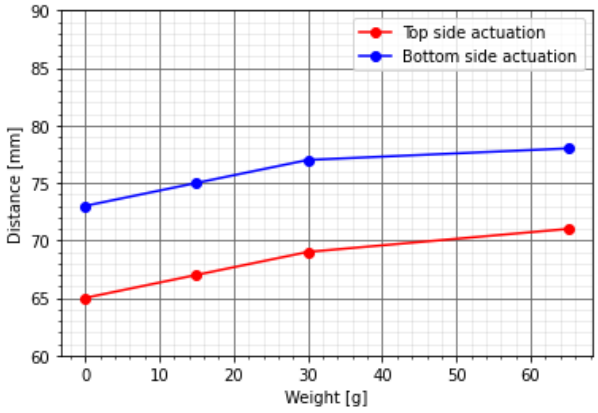

Figure 44: ABS-to-ABS distance at the top side of the hinge when different weights are applied to the hinge

7.4.2 Simulations

It is now interesting to see if we can use the E-moduli for the PLA at 65 °C, obtained from the horizontal simulation, in the vertical simulation and still have similar results. First, we look at the top spring actuation. When looking at Figure 42a, it can be seen that the distance is about 61 mm. The simulation values using an E-modulus of 28 MPa result in a distance of 60.9 mm. The hinge makes an angle of 4 °. Since the tests started with a top actuation, the bottom value could not be retrieved from Figure 42a. One test was carried out that started with a bottom actuation, which, after the first actuation, reached a distance of 55 mm. When simulated, the ABS-to-ABS distance of the spring is 55.6 mm with an angle of 16°. More tests should be conducted to prove that the simulations are accurate for the bottom actuation. The simulations can be seen in Figure 45.

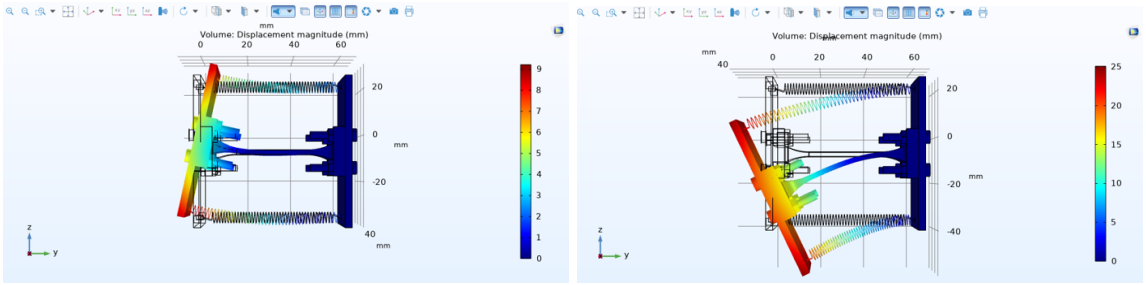

(a) Top spring Actuation **(b)** Bottom spring actuation

Figure 45: Side view vertical simulations

7.5 Stacked hinge

7.5.1 Displacement experiments

The prototype was built, as seen in Figure 46. The prototype consists of 2 single hinges in series. The first hinge connected to the T-shaped structure acts horizontally, while the second hinge is connected to the first hinge and acts vertically. The reason why the first hinge acts horizontally is that the effect of the weight of the second hinge is smaller than when the first hinge acts vertically due to the area moment of inertia. It is now mainly interesting how the first hinge behaves because the conditions of the second hinge are similar to the hinge in subsection 7.4.

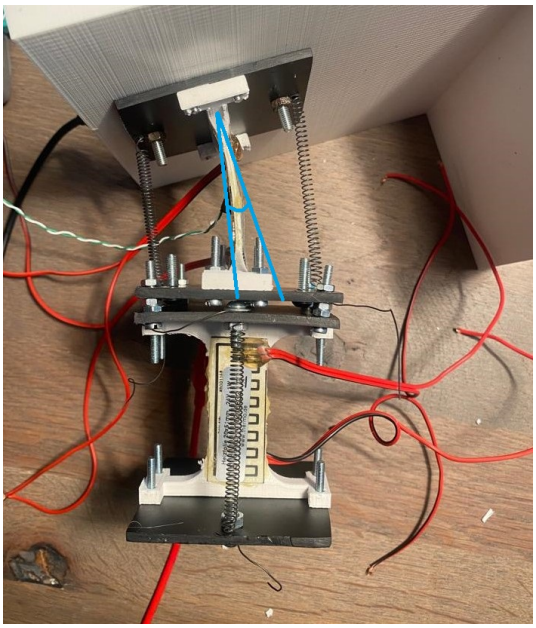

Figure 46: The stacked hinge when the first hinge is actuated with the blue lines indicating the angle that the first hinge makes

Figure 47 shows the result of the stacked hinge when the first hinge is actuated. As can be seen, when the hinge is actuated the first time, the smallest ABS-to-ABS distance is obtained. The distance for hinges 1 and 2 is largest for actuation number 2, and actuation 3 is slightly lower for both. After that point, the distance stabilizes. Hinge 3 has a different trend because the distance continues to increase after actuation number 1 until actuation number 5, stabilizing to a steady state. Some problems occurred with the stacked hinge. One problem was that when the first hinge was heated, the hinge sagged a little bit. The weight of hinge 2 caused this. Furthermore, the hinge was also twisted. The twist direction depended on which side was actuated.

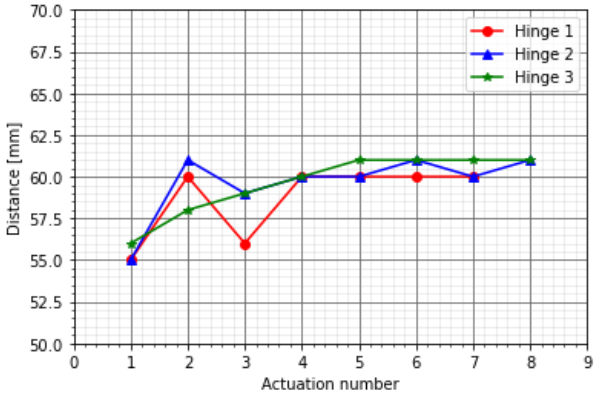

Figure 47: Multiple actuations of the stacked hinge where each spring is alternated actuated

7.5.2 Simulations

Finally, it is checked what the results would be if the stacked hinge is simulated when the E-modulus of the PLA is 28 MPa. The results can be seen in Figure 48. The ABS-to-ABS distance of the first hinge was about 56 mm in the experiments. When the hinge was simulated, the distance was 56 mm and had an angle of 10°.

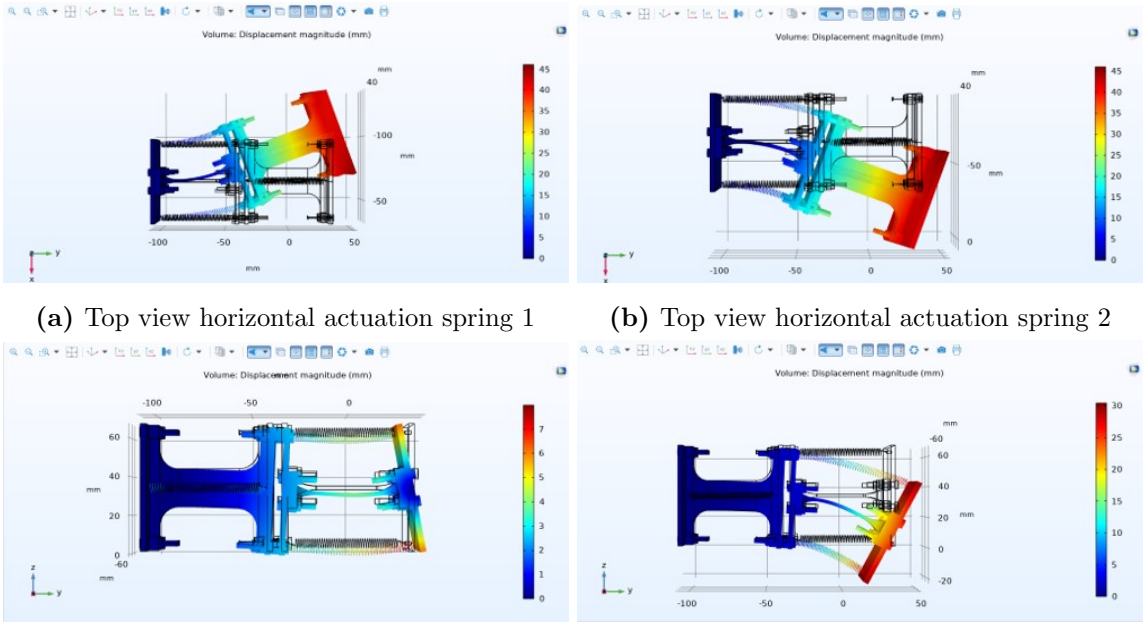

(a) Top view horizontal actuation spring 1

(b) Top view horizontal actuation spring 2

(c) Side view vertical actuation top spring

(d) Side view vertical actuation bottom spring

Figure 48: Stacked hinge simulations

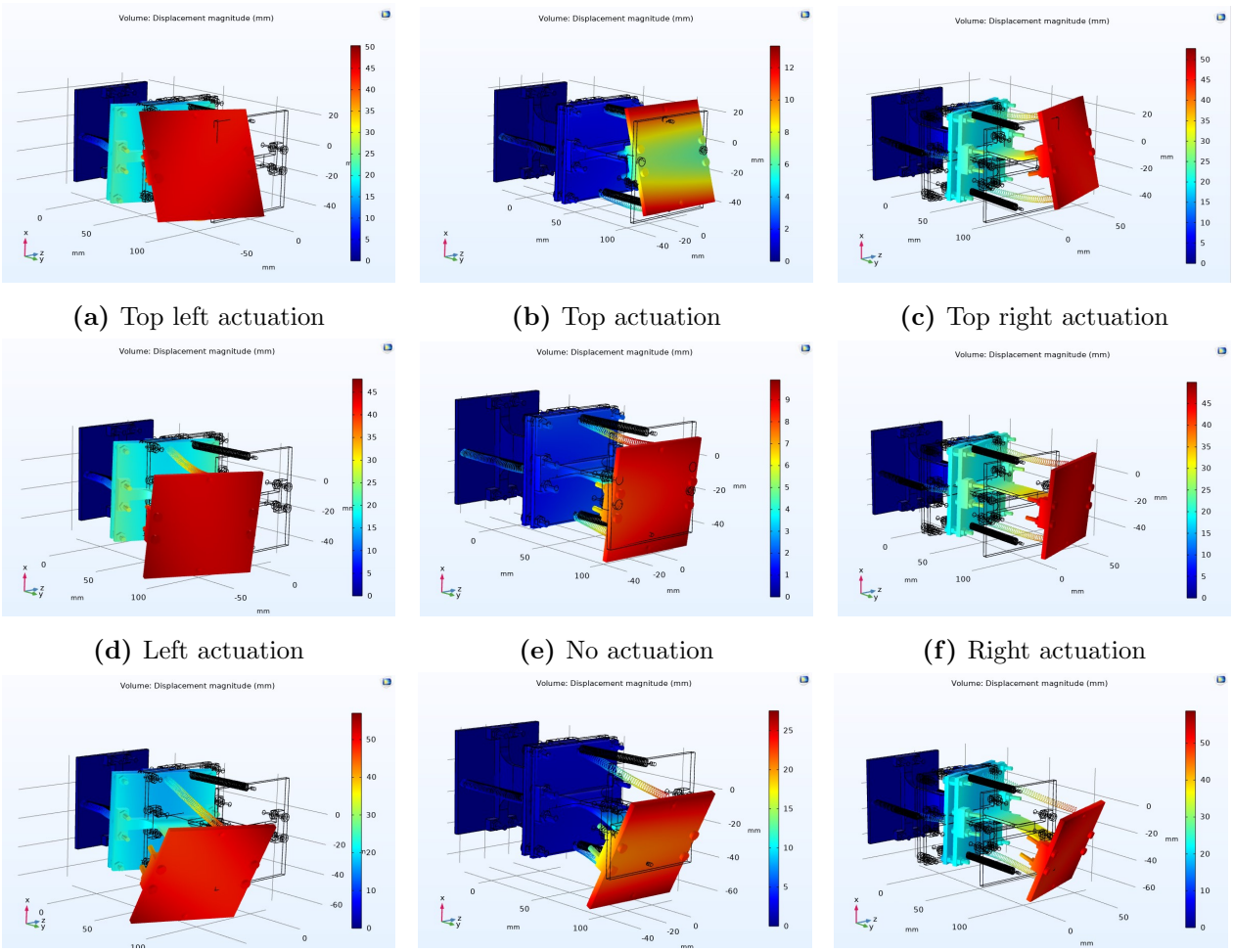

(a) Top left actuation **(b)** Top actuation **(c)** Top right actuation

(d) Left actuation **(e)** No actuation **(f)** Right actuation

(g) Bottom left actuation **(h)** Bottom actuation **(i)** Bottom right actuation

Figure 49: Hinge actuated in 9 different configurations, which were used to determine the range of motion

It is determined what the range of motion is for the stacked hinge. This is done by adding a point at the tip of the hinge in the middle of the ABS plate. The hinge is actuated to 8 different positions by actuating different springs. This can be seen in Figure 49. It is determined how the added point moves when actuated in different positions. The results can be seen in Figure 50. The stacked hinge can be moved much more in the x-direction than in the y-direction, resulting from the second hinge enlarging the deformation at the tip. It can be seen that due to gravity, the range in the positive y-direction is much lower than in the negative y-direction. A footnote: This is the range of motion when actuated from an undeformed configuration. As seen in the experiments, after a few actuations, the deformation is in a steady state. The ABS-to-ABS distance tends to be higher when actuated when it reaches the steady state, which means that the mobility of the hinge decreases. This means that the orange area in a steady state will shrink a bit.

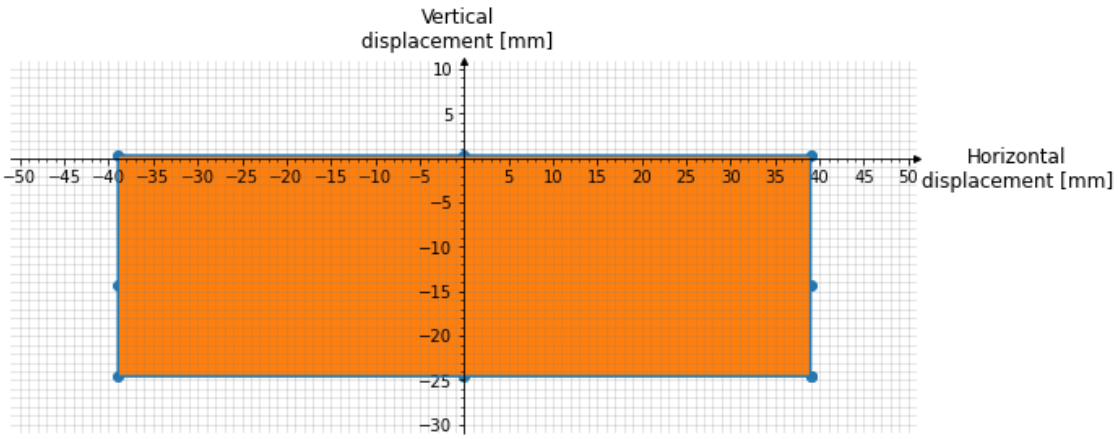

Figure 50: The range of motion at the tip of the hinge, where the coordinate (0,0) is the center of the ABS plate when no deformation occurs. The orange area is the area that the center point can cover

7.6 Chapter summary

Displacement experiments

Tests have shown how the hinge behaves when actuated. When a single hinge is actuated in the undeformed configuration in the horizontal direction, the ABS-to-ABS distance could be decreased by 10 mm to 58 mm. When actuated multiple times, the abs distance would reach a steady state of 60 mm on both sides. Adding a weight of 200 g to the hinge would not change the distance. When actuating the hinge vertically, there is a difference in distance. The distance is smaller due to gravity when the bottom spring is actuated. The distance here also reaches a steady state after a few actuations. Multiple weights were lifted by the spring. The top distance increased with an increase in weight, but even the heaviest weight could be lifted, although not to a horizontal position. For the stacked hinge, the first hinge would reach a distance of 56 mm from the undeformed configuration but finally reach a steady state, which was comparable to the horizontal actuated single hinge. Problems with the 3D-actuated hinge were the sagging of the first hinge and the tip of the hinge twisted a bit.

Simulations

A FEM model was built to compare the FEM model results with the test results. The E-modulus of the PLA part had to be determined when the temperature was 20 °C and at 65 °C. These were obtained by simulating horizontal actuation, determining the ABS-to-ABS distance, and changing the E-modulus to compare the simulations and tests. These resulted in an E modulus at 20 °C and 65 °C of 620 MPa and 28 MPa, respectively. When using these values when the hinge was vertically actuated, the difference in distance between simulations and the mean of the tests was just 0.1 mm.

These values were also used on the stacked hinge. They resulted in a difference in distance of 0.03. Due to the small difference in distance, it can be concluded that the simulation approximates the actual values well. The range of motion of the stacked hinge was also determined. The horizontal actuation at the center point of the ABS plate from the fabricated position was about 39.0 mm to both sides. The hinge could vertically be actuated 0.3 mm to the top and 24.6 mm to the bottom.

Actuation time and energy consumption

It is determined that the time for the actuation of a single hinge is 108 seconds when the films are powered by 1.5 W. The shape recovery takes 104 seconds, which results in a complete cycle of 212 seconds. Furthermore, the energy consumption of an actuation cycle is 546.4 J when the PLA is still at room temperature. When the PLA is already at 65 °C, the energy consumption of an actuation cycle is 248 J with a cycle time of 111 seconds.

8 Discussion

This research has shown that an interactive hinge with a simple design that could be actuated along two axes is relatively easy to manufacture. The hinge was able to be actuated multiple times without requiring manual reprogramming. The distance, when actuated, stabalizes after a few actuations. As was mentioned before, the first hinge of the stacked hinge sagged a bit, and the tip of the hinge twisted. These problems could be solved in numerous ways. One way to tackle this is to make the PLA part of the first hinge thicker or wider or use a shape-memory polymer with a higher E-modulus. However, this will affect the range of motion. When the vertically actuated single hinge hoists an object, the hinge cannot reach a horizontal position for larger weights. This problem can be solved in numerous ways. One way is to use a spring with a smaller end-to-end length. The spring will have a larger strain, resulting in a larger recovery force, as seen in the graphs of Figure 22. Also, a thicker wire can be used to increase the recovery force. The deformation of the hinge is measured by measuring the ABS-to-ABS distance. Using software that tracks the deformation using a camera might be a better way to see how the hinge deforms. The simulation of the hinge was carried out linearly. Since there are large displacements, non-linear simulations will probably be more accurate. When you look at the energy consumption, the amount of energy needed to hoist an applied weight of 65 g 1 cm with a single vertically actuated hinge, where the weight has a potential energy of 0.006 J, it can be concluded that the hinge is very inefficient. Furthermore, it takes some time for the PLA of the hinge to heat up for the hinge to be actuated. The energy efficiency can be improved by embedding the heating films in the PLA plate and by using heating films with more power. Embedding the heating films in the PLA will also increase the range of motion because attaching the heating films on the PLA's outer ends increases the PLA's stiffness.

9 Conclusion

Prior research has already been conducted concerning shape-memory hinges using different materials and designs, which recently received increased attention due to the development of 3D printing. However, studies mainly designed hinges that can be actuated along one axis. This study proposes a design for a hinge that works along two axes. This research tries to answer the question: *How to design an interactive hinge with shape memory alloys and polymers??* This study tries to answer this question by dividing the problem into multiple parts.

First, the theory behind shape-memory material is explained, which shows that shape-memory alloys and polymers have different working mechanisms. Research about the state-of-the-art shape-memory hinges showed different designs and working methods, which served as inspiration. Different designs were made using the basic design cycle. The chosen working principle of the design was a 3D printed shape-memory polymer body that is actuated externally by shape-memory springs. To maximize the range of motion, the body of the hinge has the shape of a plate, and to obtain motion along two axes, a second hinge is stacked at the end of the first part. The springs were made of Nitinol, and the body was made of PolyLactic Acid (PLA). An intermediate part was used, made of Acrylonitrile butadiene styrene (ABS), because the temperature of the springs was too hot so that it would melt through the PLA.

Three types of Nitinol, with different material contents, were investigated to be used as material for the springs. Tensile tests were carried out, which showed that the Nitinol with copper had no superelastic effect, in contrast to the other two types of Nitinol. The tensile tests were also used for determining the E-modulus. Springs were manufactured for each type of Nitinol, and recovery force experiments were carried out. Springs were elongated to three different lengths, and the temperature was increased in steps of 10 °C to see how the recovery force changed. The springs were also actuated multiple times to see if the recovery force changed. For each spring and deformation, the recovery force eventually stabilizes. The springs were also simulated in Comsol. When looking at the results, how well the reality and simulations resembled depended on the deformation and the spring type. The smallest mean absolute error was 0.11 N for the 60 mm deformed NiTi spring, and the largest error was 0.79 N for the 140 mm deformed NiTiCu spring. The simulation followed a similar trend when compared to the experiments for each spring and deformation. It was found that Nitinol, which consists of 45% titanium and 55% Nickel, had little recovery force and a high E-modulus, which is why it is not useful to be used as an actuator. Because the Nitinol with copper did not have the superelastic effect, this type of Nitinol was also not suitable for a two-way shape-memory hinge because when wanting the hinge to be actuated to the other side, this type of Nitinol will give a large counter force. The Nitinol used has a content of 50% Titan and 50% Nickel.

Three different tests are carried out: a single hinge actuated horizontally, a single hinge verti-

cally, and a stacked hinge. When actuated from an undeformed configuration, the horizontal hinge had an ABS-to-ABS distance of about 58 mm, the vertical actuated hinge had a distance of 61 mm, and the stacked hinge had a distance of about 56 mm. For each test, the hinge had a smaller ABS-to-ABS distance when actuated from an undeformed configuration than when actuated multiple times. For the horizontal actuated single hinge, the distance is equal for both sides after a few actuations, namely about 60 mm. The vertical actuated single hinge differed in distance when the top spring was actuated compared to the bottom spring, caused by gravity. Both for the top side and the bottom side actuation, the distance stabilized after multiple actuations, with a top side distance of 65 mm and a bottom distance of about 53 mm. The vertical actuated hinge was also used to lift small objects, which showed how the ABS-to-ABS distance changes with increasing weight. The first single hinge was actuated for the stacked hinge, and its distance was measured. After a few actuations, the distance stabilizes to 61 mm. Problems occurred with the designed hinge. One problem with the stacked hinge was that the first hinge sagged due to the weight of the second hinge. Furthermore, the end of the hinge twisted when actuated. The energy consumption of the hinge was determined. When the PLA was still at room temperature, it took 108 seconds to heat the PLA to 65 °C when the heating films were powered by 1.5 W. The heating of the springs took 7 seconds when powered by 8 W. From undeformed to actuated position took 108 seconds. Shape recovery took 104 seconds, resulting in a total actuation cycle of 212 seconds. The energy consumption of this actuation cycle was 546.4 J. If the hinge is already at 65 °C, the actuation cycle took 111 seconds with an energy consumption of 248 J.

Finally, the hinges were simulated. A CAD model was built in Solidworks and imported into Comsol. Since 3D printing influences the E-modulus of PLA, and because heating films are glued to the PLA part, the E-modulus of PLA had to be determined. This was done by simulating the horizontal actuation and adjusting the E-modulus of the PLA until simulations resembled the experiments. The E-modulus of PLA at room temperature was found to be 620 MPa, while at 65 °C, the E-modulus was 28 MPA. These values were also applied to the simulations of the vertical actuated hinge and stacked hinge tests. The maximum difference in distance between the simulations and the tests was 0.1 mm. The range of motion of the stacked hinge was determined. The tip of the hinge could be actuated 39 mm horizontally in both directions, 0.3 mm in the top direction, and 24.6 mm in the bottom direction.

Future research should focus on increasing the range of motion of the hinge, which will also increase the hoist capacity of the hinge. The hinge is not energy efficient, which can also be improved. The shape-memory effect's contribution of the PLA to shape recovery could be investigated. Also the degradation of the shape-memory effect and the fatigue behavior of the PLA is an interesting topic to investigate. Research can be conducted that scales the hinge to see how the behavior of the hinge changes and if the simulations will still be accurate in that case. Also, other physics can be

added in Comsol that simulates the heating of the hinge because heat affects material properties.

References

[1] R.E. Meirowitz. Coating processes and techniques for smart textiles. 2016.

[2] J. Kunzelman, T. Chung, P.T. Mather, and C. Weder. Shape memory polymers with built-in threshold temperature sensors. 2008.

[3] G. Scalet. Two-way and multiple-way shape memory polymers for soft robotics: An overview. 2020.

[4] J. Leng, , X. Lan, Y. Liu, and S. Du. Shape-memory polymers and their composites: Stimulus methods and applications. 2011.

[5] S. Barbarino, E.I. Saavedra Flores, R.M. Ajaj, I. Dayyani, and M.I. Friswell. A review on shape memory alloys with applications to morphing aircraft. 2014.

[6] W.M. Huang, Z. Ding, C.C. Wang, J. Wei, Y. Zhao, and H. Purnawali. Shape memory materials. 2010.

[7] F. El Feninat, G. Laroche, M. Fiset, and D. Mantovani. Shape memory materials for biomedical applications. 2002.

[8] D.C. Lagoudas. *Shape memory alloys: modeling and engineering applications*, chapter 1.3. Springer, 2008.

[9] Shape memory effect–intelligent alloys.

[10] G. Strobl. *The physics of polymers: Concepts for understanding their structures and behavior*, chapter 1.1. Springer, 2007.

[11] W. Voit, T Ware, R.R. Dasari, P. Smith, L. Danz, D. Simon, S. Barlow, S.R. Marder, and K. Gall. High-strain shape-memory polymers. 2009.

[12] M. Mehrpouya, H. Vahabi, S. Janbaz, A. Darafsheh, Mazur T.R, and S. Ramakrishna. 4d printing of shape memory polylactic acid (pla). 2021.

[13] Q. Ge, A. Hosein Sakhaei, H. Lee, C.K. Dunn, N.X. Fang, and M.L. Dunn. Multimaterial 4d printing with tailorable shape memory polymers. 2016.

[14] Y. Saad Alshebly, M. Nafea, M. Sultan Mohamed Ali, and H.A.F. Almurib. Review on recent advances in 4d printing of shape memory polymers. 2021.

[15] H. Xie, C. Cheng, X. Deng, C. Fan, L. Du, K. Yang, and Y. Wang. Creating poly(tetramethylene oxide) glycol-based networks with tunable two-way shape memory effects via temperature-switched netpoints. 2017.

[16] A. Melocchi, M. Uboldi, M. Cerea, A. Foppoli, A. Maroni, L. Palugan S. Moutaharrik, L. Zema, and A. Gazzaniga. Shape memory materials and 4d printing in pharmaceutics. 2021.

[17] M. Behl and A. Lendlein. Shape-memory polymers. 2007.

[18] A. Lendlein and S. Kelch. Shape-memory polymers. 2002.

[19] C. Hayrettin, O. Karakoc, I. Karaman, J.H. Mabe, R. Santamarta, and J. Pons. Two way shape memory effect in nitihf high temperature shape memory alloy tubes. 2019.

[20] M. Zare, M.P. Prabhakaran, N. Parvin, and S. Ramakrishna. Thermally-induced two-way shape memory polymers: Mechanisms, structures, and applications. 2019.

[21] T Liu, L. Liu, Q. Li, C. Zeng, X. Lan, and J. Leng. Integrative hinge based on shape memory polymer composites: Material, design, properties and application. 2019.

[22] Z. Liu, X. Lan, L. Liu, Q. Li, Y. Liu, and J. Leng. Design, material properties and performances of a smart hinge based on shape memory polymer composites. 2020.

[23] S. Yamamura and E. Iwase. Hybrid hinge structure with elastic hinge on self-folding of 4d printing using a fused deposition modeling 3d printer. 2021.

[24] S. Akbari, A. Sakhaei, B. Yang, A. Serjouei, Z. Yuanfang, and Q Ge. Enhanced multimaterial 4d printing with active hinges. 2018.

[25] M. Ashir, A. Nocke, and C. Cherif. Adaptive hinged fiber reinforced plastics with tailored shape memory alloy hybrid yarn. 2019.

[26] O. Testoni, T. Lumpe, J. Huang, M. Wagner, S. Bodkhe, R. Spolenak, J. Paik, P. Ermanni, L. Muñoz, and K. Shea. A 4d printed active compliant hinge for potential space applications using shape memory alloys and polymers. 2021.

[27] S. Akbari, A. Sakhaei, B. Yang, A. Serjouei, Z. Yuanfang, and Q Ge. Shape-reversible 4d printing aided by shape memory alloys. 2022.

[28] M. Lalegani Dezaki, M. Bodaghi, A. Serjouei, S. Afazov, and A. Zolfagharian. Adaptive reversible composite-based shape memory alloy soft actuators. 2022.

[29] A. van Boeijen, J. Daalhuizen, J. Zijlstra, and R. van der Schoor. *Delft Design Guide*, chapter 2. BIS, 2013.

[30] R. Chaudhari, J.J. Vora, and D.M. Parikh. A review on applications of nitinol shape memory alloy. 2021.

[31] M. Miller. Wired on nitinol: A truly green energy source.

[32] BCN3D. The most popular 3d printing materials in fdm and their properties. 2022.

[33] J.S. Bergstrom and D. Hayman. An overview of mechanical properties and material modeling of polylactide (pla) for medical applications. 2016.

[34] M. Rahman, N.R. Schott, and L. K. Sadhu. Glass transition of abs in 3d printing. 2016.

[35] R. Kumar, R. Singh, and I. Farina. On the 3d printing of recycled abs, pla and hips thermoplastics for structural applications. 2018.

[36] T.J. Suteja and A. Soesanti. Mechanical properties of 3d printed polylactic acid product for various infill design parameters: A review. 2020.

A Drawings conceptual models

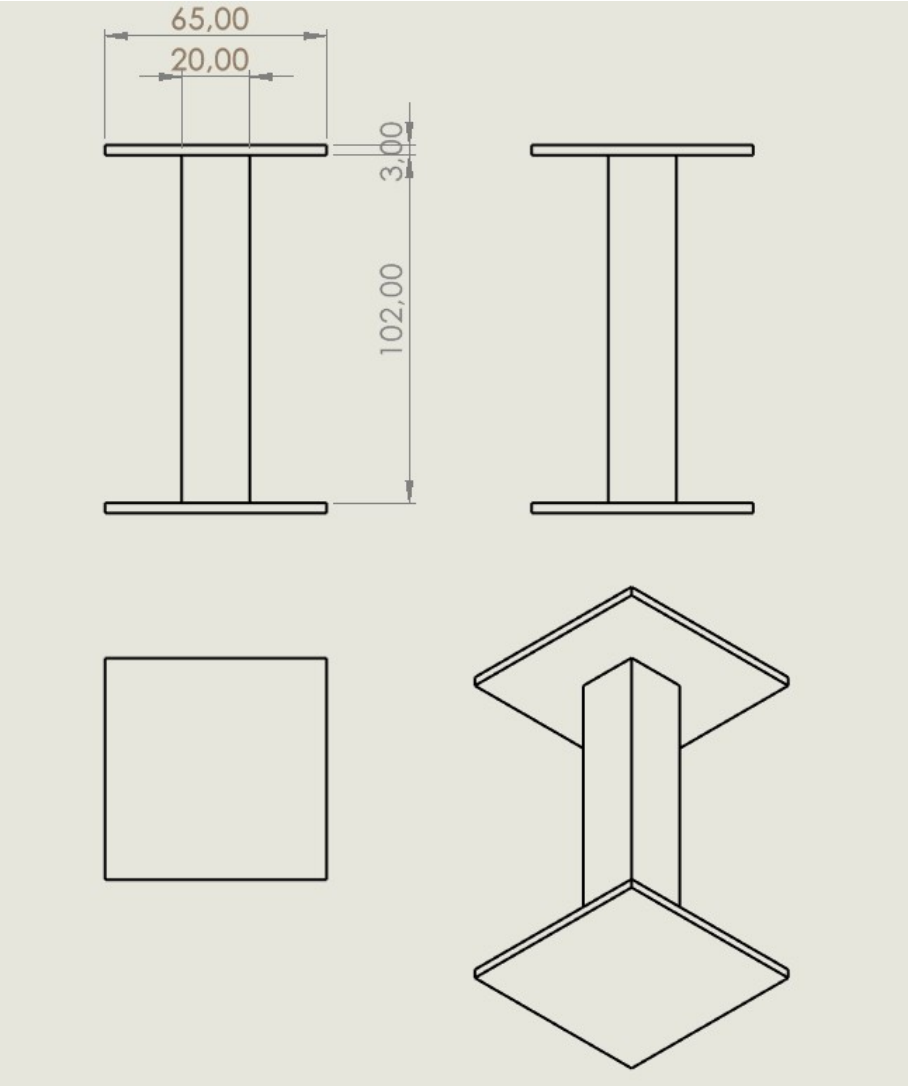

Figure 51: Drawing of the square conceptual model

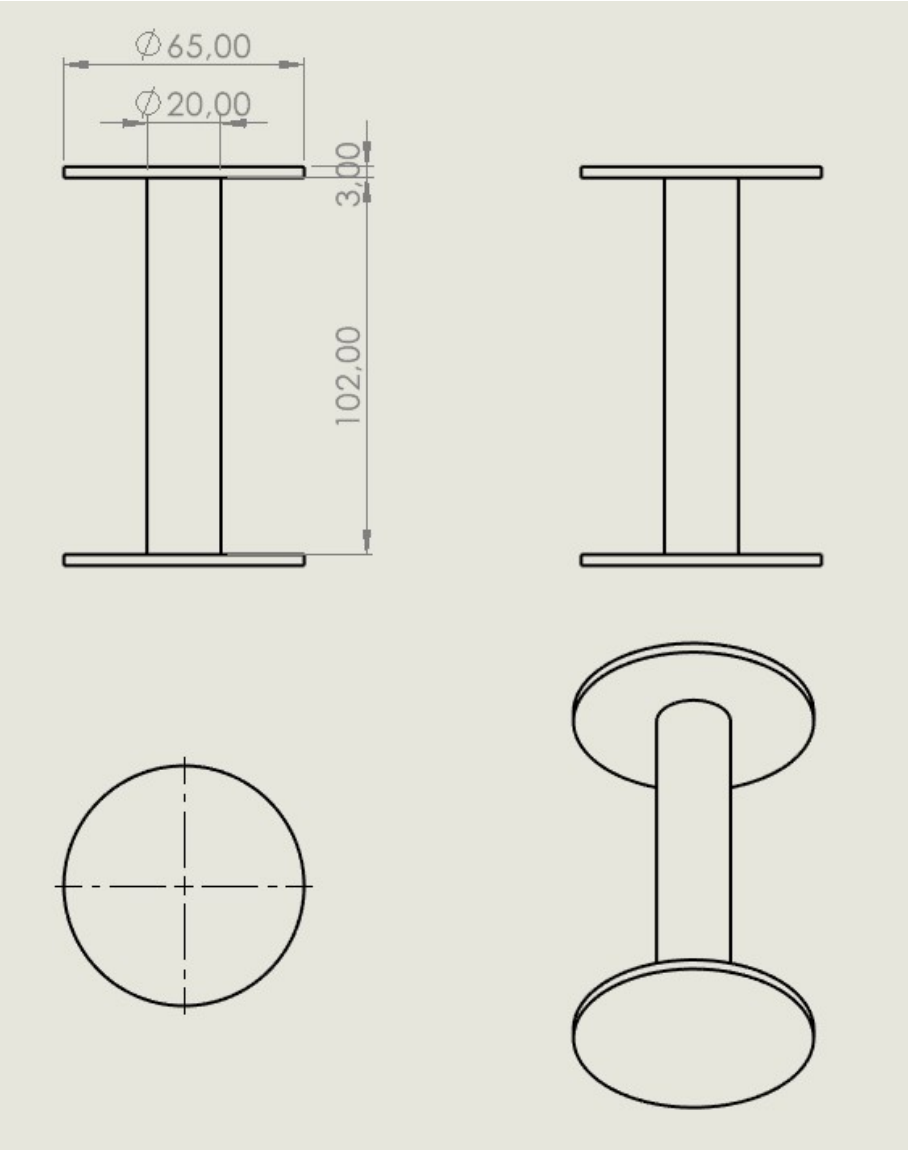

Figure 52: Drawing of the round conceptual model

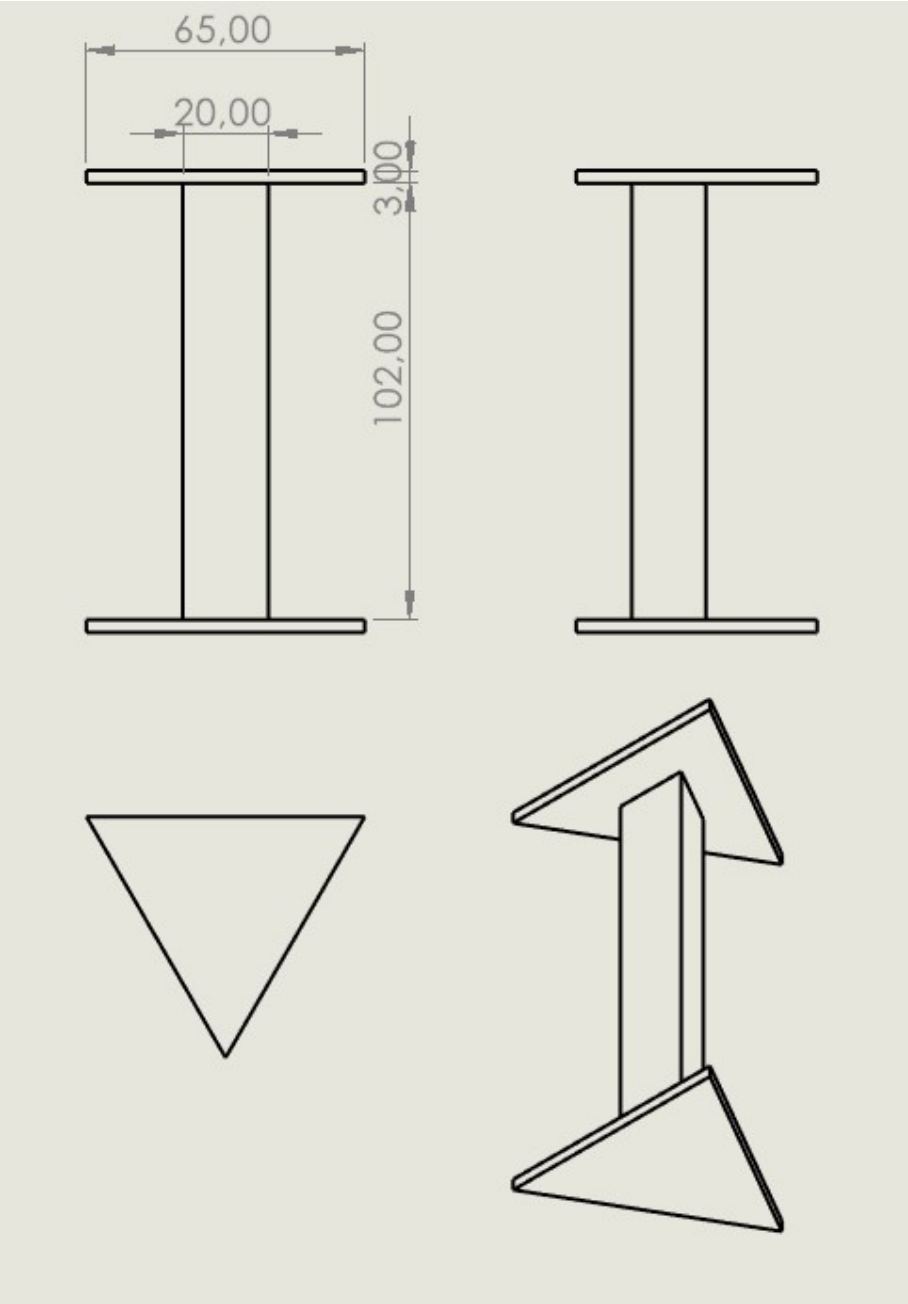

Figure 53: Drawing of the triangle conceptual model

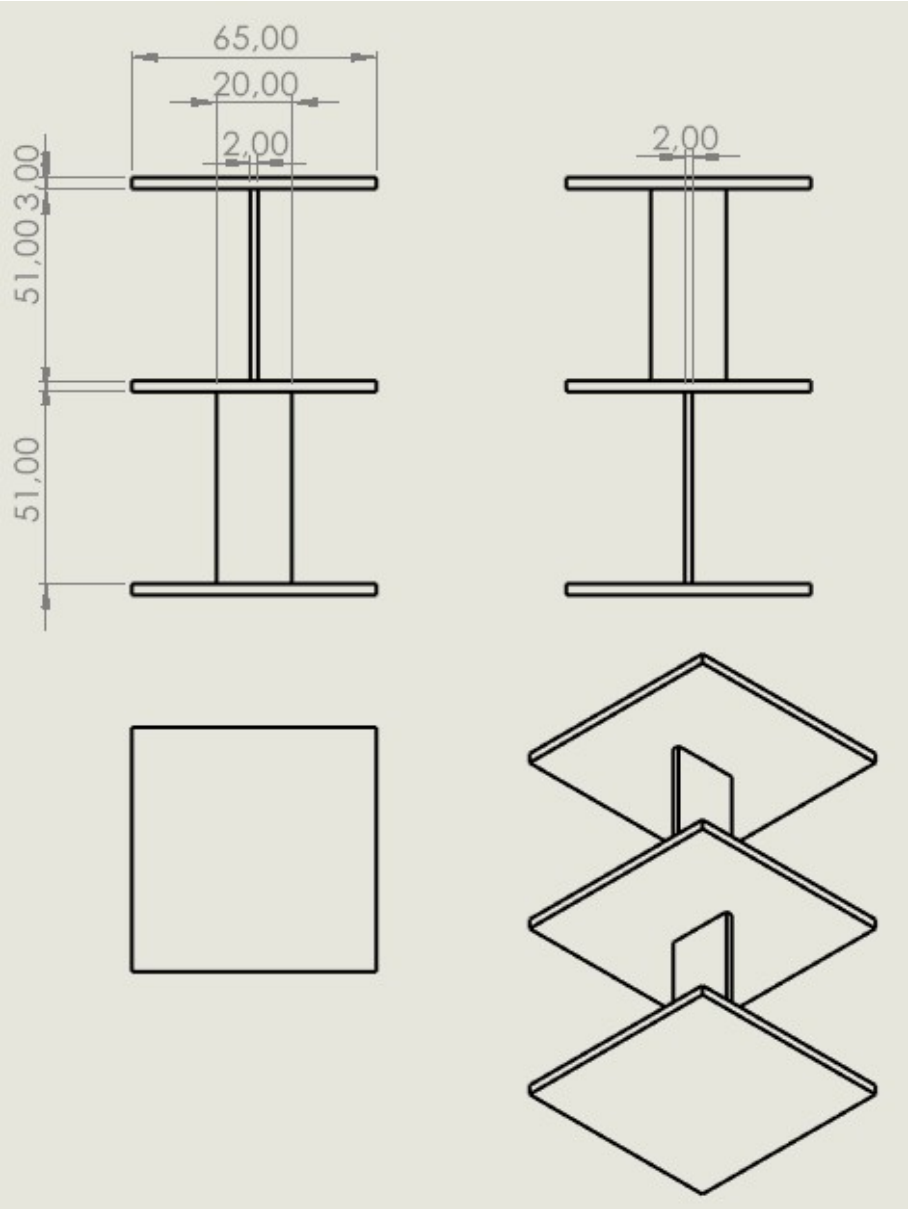

Figure 54: Drawing of the stacked conceptual model

B Drawings detailed model

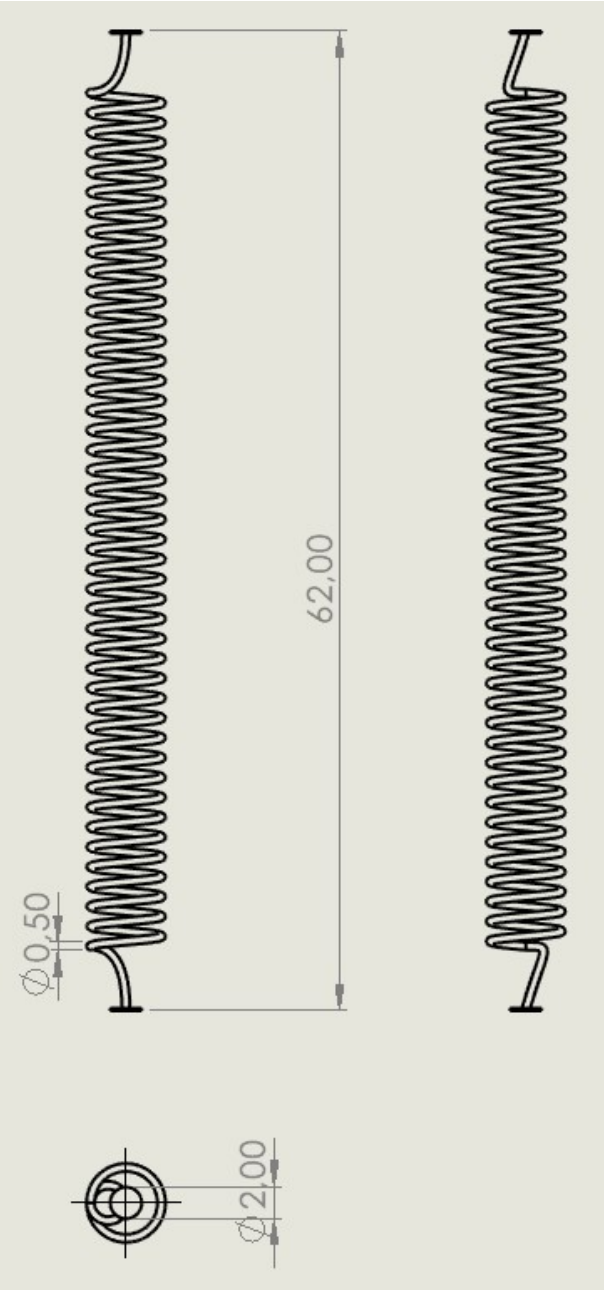

Figure 55: Drawing of the spring used in the detailed model

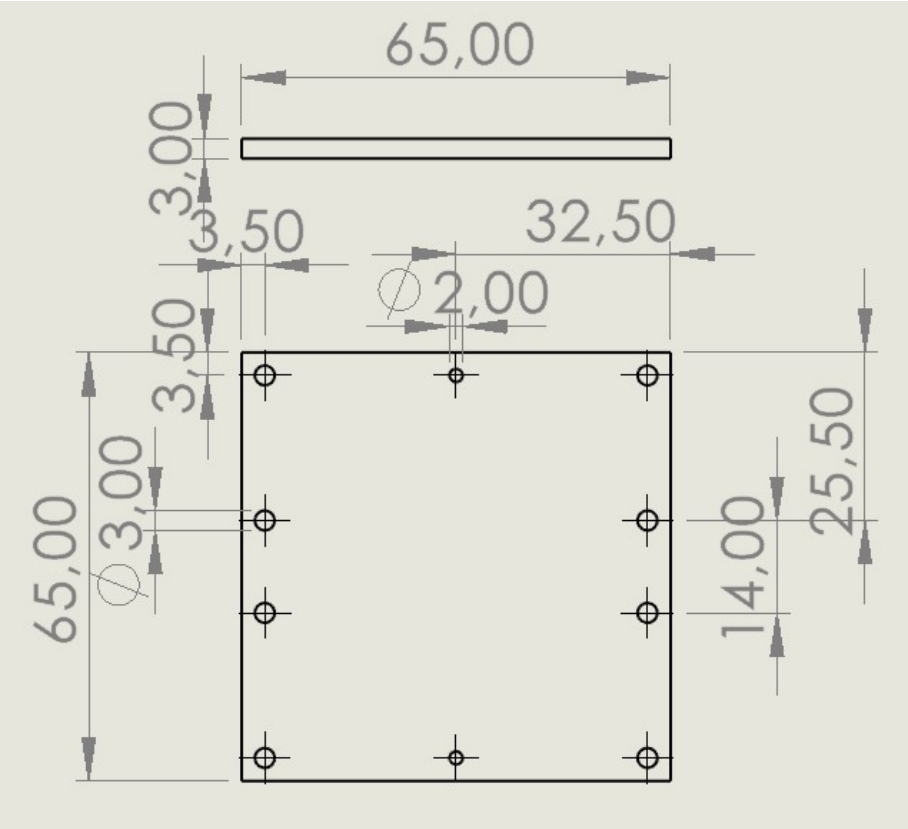

Figure 56: Drawing of the ABS plate used in the detailed model

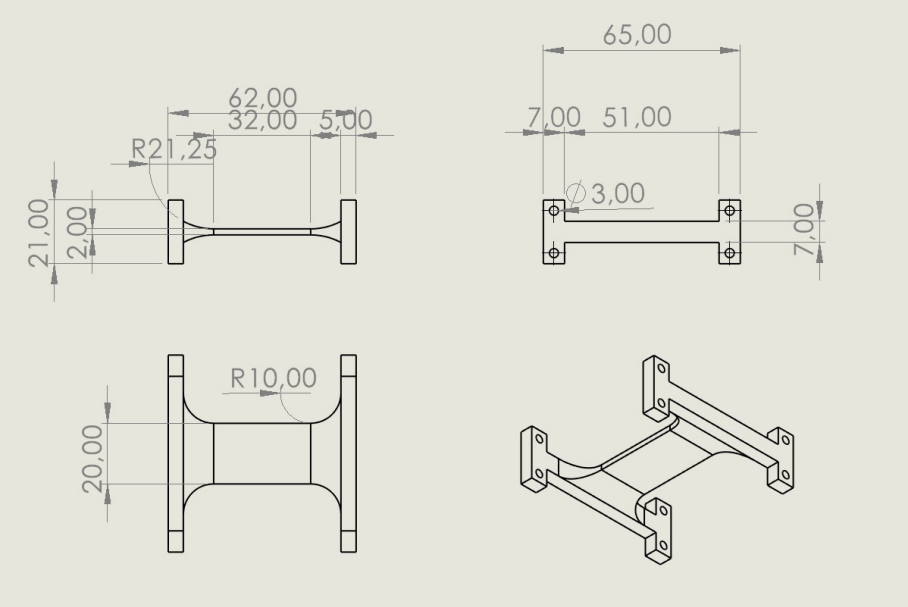

Figure 57: Drawing of the PLA body used in the detailed model

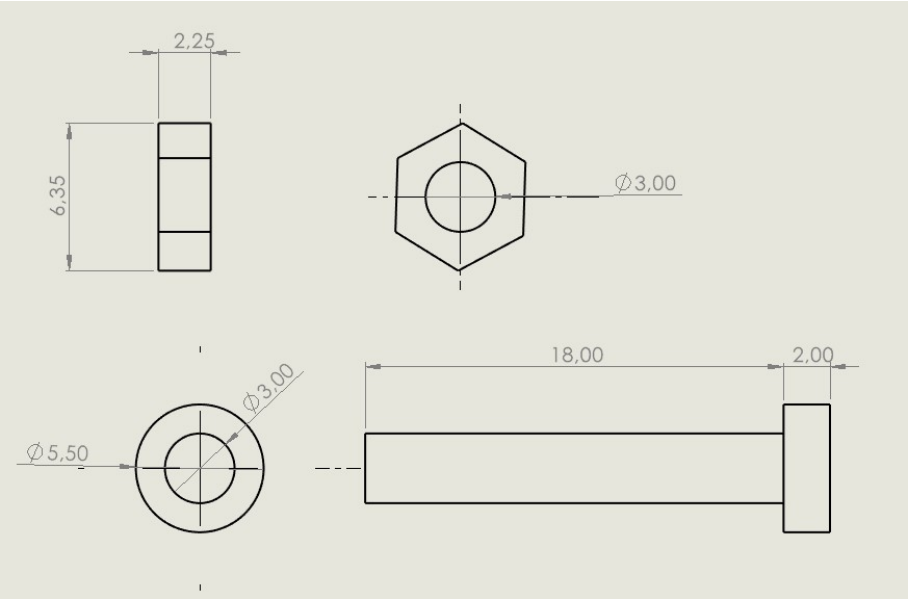

Figure 58: Drawing of the Nuts and the bolts used in the detailed model

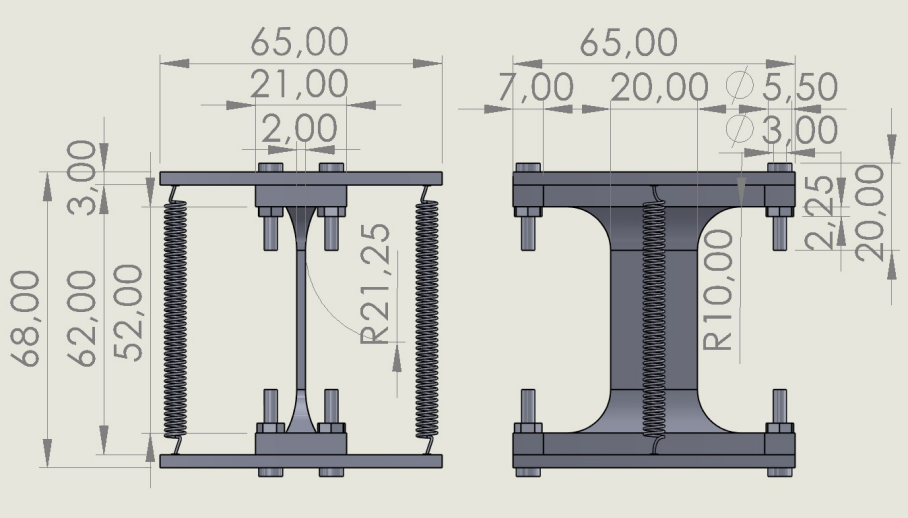

Figure 59: Drawing of the single hinge

Literature assignment

By Wessel Marcelis

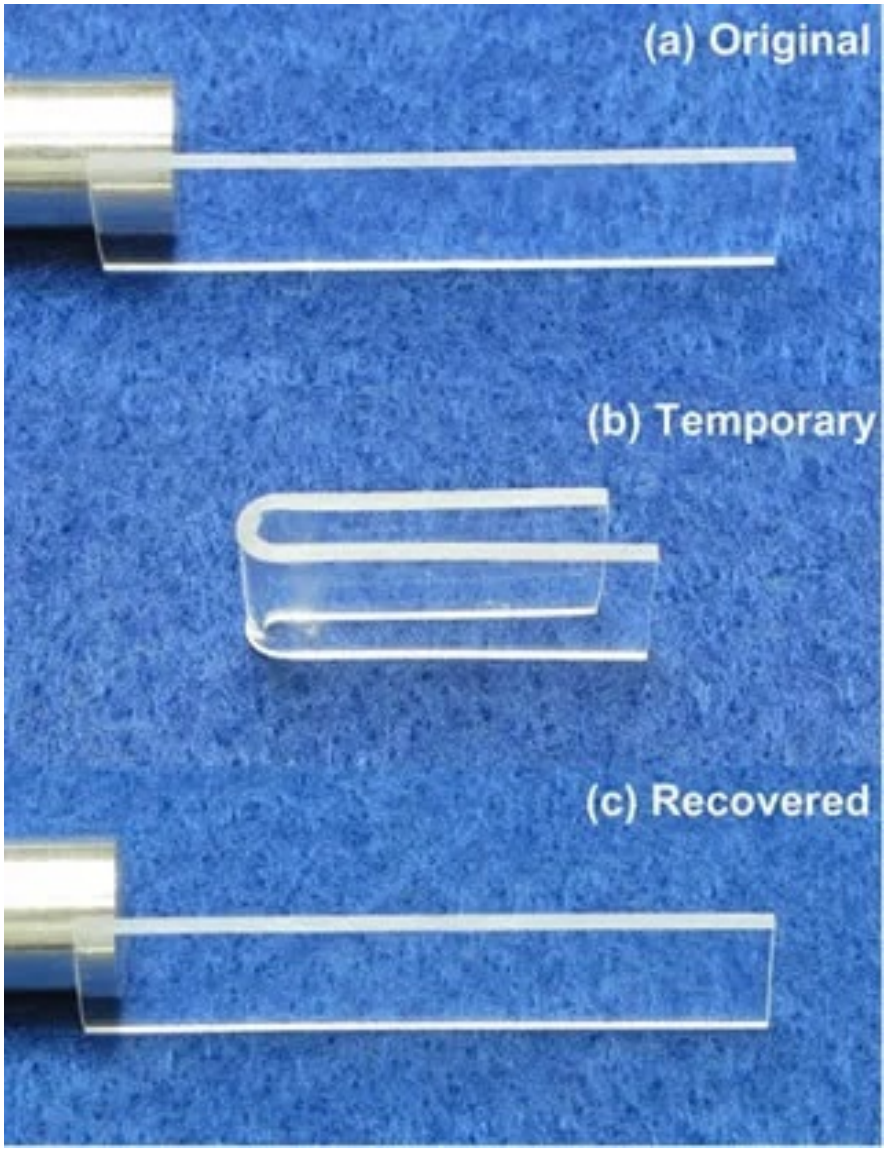

Interactive hinge – Bio-inpired design of smart programmable morphing structure

By Wessel Marcelis

Literature Assignment

in partial fulfilment of the requirements for the degree of

Master of Science

in Mechanical Engineering

at the Department Maritime and Transport Technology of Faculty Mechanical, Maritime and Materials Engineering of Delft University of Technology

Student number: 4383214
MSc track: Multi-Machine Engineering
Report number: 2022.MME.8711
Supervisors: Dr. J. Jovanova and Dr. Sepideh Ghodrat
Date: September 27, 2022

Abstract

A shape memory material is a material that can remember its original shape when it is deformed. Shape memory materials are a promising type of smart materials, which might be a cheap and sustainable alternative to make systems smart in the future. This literature survey aims to present an overview of shape memory material hinges. This review will give insight into the state of the art for shape memory material hinges and try to find research gaps on this topic. This survey starts by explaining what smart materials are. Next, it is explained what shape memory materials are. Also, the most common types of shape materials and their working principles are illustrated. After that, different shape memory effects are discussed. Frequently used modeling methods and the most used fabrication processes for shape memory hinges are explained. Recent research about shape memory material hinges is discussed next. For each research, the design, the fabrication process, and the experiments that were carried out were discussed. It is concluded that relatively little research was conducted about two-way shape memory material hinges. The research's two-way shape memory material hinges found in literature worked in the 2D plane like a knee joint. Hinges that work in the 3D space, like a shoulder joint, could be investigated in future research.

Contents

1 Introduction

1.1 Problem formulation

Due to technological advancement, there are more smart systems. Smart systems usually require increased use of sensors and actuators. More components result in an increase in the weight, volume, and cost of the system. The increase in weight and volume increases energy consumption. Shape memory materials might be an excellent alternative to make systems smart.

A shape memory material is a type of smart material that can remember its original shape when deformed. An external stimulus triggers the shape memory effect. The existence of shape memory materials has been known since 1932, when the shape memory effect was discovered in an AuCd alloy (2). In 1963, the same effect was discovered in a nickel-titanium alloy called Nitinol. Nowadays, Nitinol is the most widespread shape memory alloy. Polymers may also have the shape memory effect. In recent years, shape-memory materials received much attention due to recent advancements in 3D printing technology. The printing of shape memory materials using a 3D printer is called 4D printing, where the fourth dimension is time. The increasing interest is mainly fueled by the progression of multi-material printing (3). Because of the shape memory effect, shape-memory materials have broad application prospects (4). One of the applications is using the shape memory material as an actuator. However, using shape memory materials as actuators is not widespread due to several limitations, like low actuation frequency, low controllability, and low accuracy (5).

This paper presents the state of the art of shape memory hinge actuators. Section 2 shortly explains what smart materials are, Section 3 explains different types of shape memory polymers and the theory behind them, Section 4 talks about different shape memory effects, Section 5 shows how the shape memory effect of hinge actuators is modeled, Section 6 talks about frequently used fabrication techniques, Section 7 shows how researchers have designed and manufactured shape memory hinge actuators and finally, the literature review is concluded in Section 8 by answering the research questions, followed by discussing the research gaps and giving future research recommendations in Section 9.

1.2 Literature questions

The following research questions have been formulated that drive this literature review:

- What is the current state of the art of interactive hinges for shape memory materials?
  - What are shape memory materials?
  - What types of shape memory materials are there, and how do they work?
  - What types of shape memory effects are there?
  - How is the shape memory effect modeled?
  - What are the (recent) researches about shape memory hinge actuators, and how are they manufactured?

2 Smart materials

A smart material is a material that can change its properties due to environmental change. Smart materials can react to different kinds of environmental change, also called external stimuli. Examples of external stimuli are temperature, electric current, or magnetic field. These external stimuli can lead to a change in, for example, shape, color, or voltage. These effects make smart material useful to be applied in actuators and sensors (6). Smart materials are used in numerous fields, for example, in aerospace (7), civil engineering (8), and in the medical world (9). This paper will mainly focus on smart materials that exhibit shape memory behavior.

3 Shape memory materials

As was explained in the last chapter, a shape memory material is a type of smart material. Shape memory materials are featured by the ability to recover their original shape from a significant and seemingly plastic deformation when a particular stimulus is applied (2). This effect is called the shape memory effect. The most common stimulus that triggers the shape memory effect is an increase in temperature. This literature review will focus on the heat-induced shape memory effect. Shape memory materials can be divided into different classes. This section will feature the three most common classes of shape memory materials: Shape memory alloys, shape memory polymers, and shape memory composites.

3.1 Shape memory alloys

Shape memory alloys are metallic materials that can recover to their original shape at certain characteristic temperatures. The return of the material to its original shape is possible, even when it reaches large inelastic deformations (10). There are numerous shape memory alloys like copper-based and iron-based alloys, but the best known is Nitinol, a nickel-titanium alloy. Compared to

other shape memory alloys, Nitinol has a low production cost, is safer to handle, and has superior mechanical properties (11).

The shape memory effect of alloys results from a solid-state phase transformation. A shape memory alloy has two phases, where each phase has a different crystal structure and properties. The starting phase, called the austenite phase, generally has a cubic structure. In contrast, the final phase, called the martensite phase, generally has a tetragonal, orthorhombic, or monoclinic crystal structure. The austenite phase is the high-temperature phase and has a higher Young's modulus, while the martensite phase is the low-temperature phase with a lower stiffness (12). The phase transformation is known as the martensitic thermo-plastic transformation. The phase transformation is not the result of atomic diffusion but shear lattice distortion. The transformation to the martensite phase is obtained by applying stress or decreasing the material's temperature (10), as seen in Figure 1. Furthermore, the martensite phase can have two crystal structures: a twinned structure and a detwinned structure. When stress is applied to a material with a twinned martensite structure, the martensite structure may be detwinned, as seen in Figure 1.

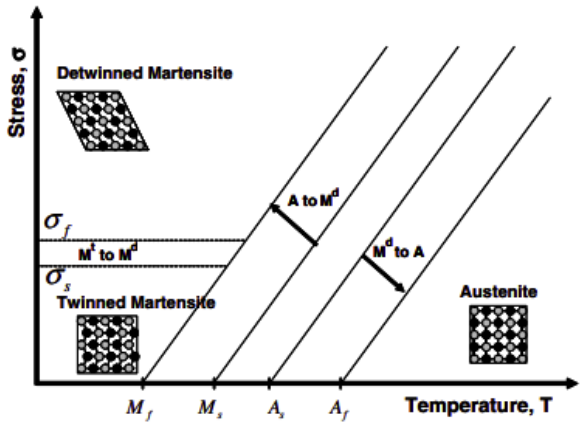

Figure 1: The stress-temperature phase diagram for a shape memory alloy (12)

The shape memory effect of a NiTi alloy will be explained with a stress-strain-temperature diagram, which can be seen in Figure 2. The starting point A is the austenite phase. When the material is cooled below the transformation temperature, the material will have a twinned martensite structure (point B). When stress is applied to the material, the structure will be detwinned, where it reaches its maximum strain (point C). The detwinned phase remains when the material is elastically unloaded (point D). When the material is heated to A_s, the material begins transforming to austenite (point E). When the material is further heated to A_f, the material is in the austenite phase and has retained its original shape (Point F) (12).

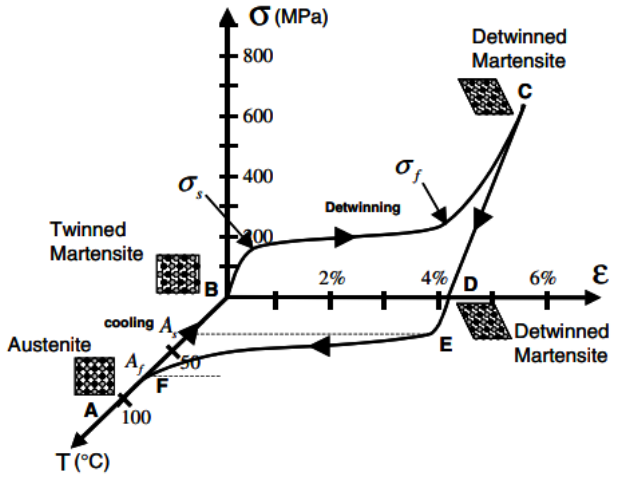

Figure 2: The stress-strain-temperature phase diagram which shows the shape memory effect for a NiTi shape memory alloy (12)

3.2 Shape memory polymers

Polymers are a material that is built up of a large number of molecular units (13). Similar to shape memory alloys, shape memory polymers can revert to their original shape when an external stimulus is applied. The advantage of polymers concerning shape memory alloys is that they are lightweight and allow more significant deformations (14). The shape memory effect has been found in different kinds of polymers, like amorphous polymers, semi-crystalline polymers, and liquid crystalline elastomers (4).

A shape memory polymeric network consists of permanent netpoints connected by chain segments. The chain segment can form switches. The netpoints are permanent because they are not affected by deformation and are the reason for the memory of the original shape. The switches are responsible for shape recovery (15). The switches are sensitive to an external stimulus, which trigger the shape recovery effect (16).

The netpoints are usually of a chemical or physical nature. The netpoints with a chemical nature are covalent cross-links, while netpoints with a physical nature result from intermolecular interaction. Chemical cross-links can be created during the synthesis of the polymer or by post-processing methods. Physical interactions are usually polymers with two segregated domains and an amorphous phase. The domain with the highest transition temperature is the hard domain, while the domains with a lower transition temperature are called the soft domain. The hard domain has a higher transition temperature than the use temperature, so they act as physical netpoints. The chain segment with a lower thermal transition temperature is the switching domains (15).

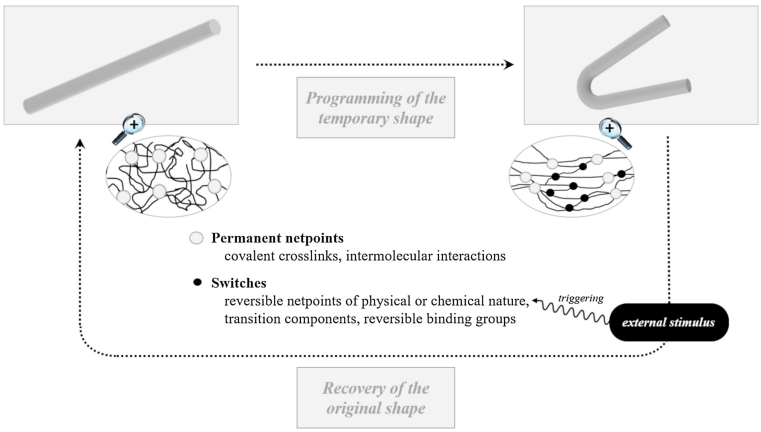

Figure 3: The working principle of the shape memory effect in polymers (16)

"The shape memory effect of polymers can be explained using the thermo-viscoelastic theory and the phase transition theory. The thermo-viscoelastic theory model is used to explain the thermodynamic behavior in SMPs. The molecular chain can be considered a small spring. These springs are tiny in diameter and large in length, and they entangle each other when mixed. In the SMPs, the polymer has higher entropy because of the random arrangement of the springs at room temperature. The molecular mobility will increase when the temperature rises, and the polymer produces thermo-viscoelasticity. At this time, the springs can be stretched and oriented by an external force, and the alignment can cause decreased entropy of the polymer. If the temperature decreases without changing the external force, the polymer loses thermo-viscoelasticity, the molecular motion is weakened, and the springs cannot return to their original form. The stress is stored in the springs as elastic potential energy during this process. When the temperature rises again, the springs gain thermo-viscoelasticity, and the stored elastic potential energy is released" (4).

"The phase transition theory is more suitable for explaining the shape transition behavior of SMPs from the thermomechanical perspective. The phase composition of SMPs can be divided into two parts (i.e., the frozen and the active phases). The frozen phase (hard phase) occurs when the enthalpy energy changes inside the material, and the molecular chain is stretched or rotated to ensure that the internal structure does not change. Any further conformational motion of the content is impossible in the frozen phase. By contrast, the active phase (soft phase) consists of dynamic bonds. In the active phase, deformation is possible, and the molecules can rotate, elongate, and compress. The frozen phase is the primary phase in the glass state. As the polymer transforms from the glass state to the rubbery state, parts of the frozen phase transform into the active phase and the ratio of the frozen phase to the active phase changes. The conformational movements are stored in the active phase during the programming process. As the temperature decreases, the

active phase transforms into frozen, with the stress localized. Stress at this time is not enough to generate adequate enthalpy to drive the shape recovery process. When the temperature rises, the frozen phase becomes active, and the stored stress is released. The transformations of the frozen and active phases embody the glass transition behavior in the thermodynamic cycle and explain the storage and release process of stress in the shape memory process."

3.3 Shape memory composites

A composite material is a material that consists of multiple materials. Shape memory composites are material that combines multiple shape memory materials. Composites can be made from multiple polymers, multiple alloys, or a combination of polymers and alloys. Shape memory polymers usually have more significant strains than shape memory alloys but are usually less strong. By combining shape memory alloys and polymers, a material with improved properties can be made (17).

4 Shape memory effect

There are several different shape memory effects. In this section, some of them will be handled.

4.1 Dual-shape memory effect

A dual-shape memory effect has two shapes: the permanent shape and the temporary shape. When the correct stimulus is applied, the material returns from the temporary shape to the permanent shape. The stimulus is usually a temperature above the transition temperature, but it could also be another stimulus, like light or a magnetic field. The shape memory effect has a programming step and a recovery step. The material is first processed in its permanent shape. The programming step for a thermally responsive shape memory effect goes as follows: The material is heated, deformed to the intended temporary shape, and then cooled. The material remains in the temporary shape after cooling. The recovery step is triggered when the material in the temporary shape is heated above the transition temperature (T_{trans}). The material will restore to its permanent shape (18). Figure 4 shows the dual-shape memory effect.

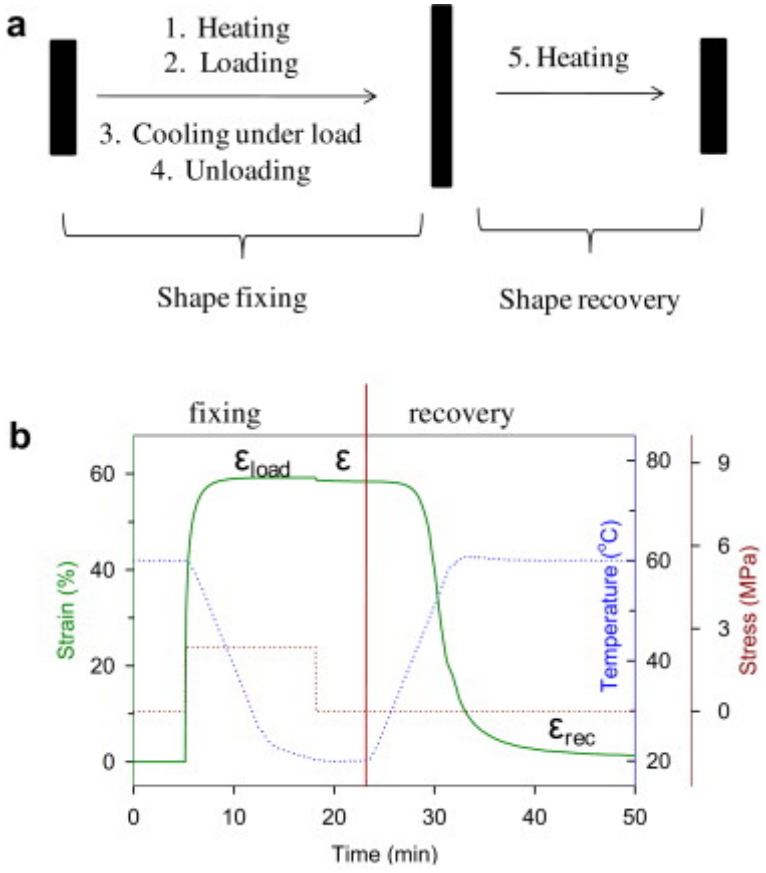

Figure 4: (a) The shape fixing and shape recovery process of a dual-shape effect, (b) Stress-strain-temperature-time graph for the fixing and recovery process (12)

Some standard parameters are used for the shape-memory effect. The strain fixity rate (R_f) describes how well the material strain is fixed after removing the load. The strain recovery rate (R_r) describes how well the material can recover to its original shape when heated above T_{trans}. Furthermore, the strain recovery rate describes how fast the material recovers to its permanent shape.

$$R_{\mathrm{f}} = 100\% \times \varepsilon / \varepsilon_{\mathrm{load}}$$
$$R_{\mathrm{r}} = 100\% \times \left(\varepsilon - \varepsilon_{\mathrm{rec}}\right) / \varepsilon$$
$$V_{\mathrm{r}} = \frac{\partial \varepsilon}{\partial t} \cdot 100\%$$

4.2 Two-way shape memory effect

The shape memory effect described in the last subsection is a one-way shape memory effect. The shape memory effect is not reversible except when the material is again programmed. There is also a two-way shape memory effect, where the shape-shifting is reversible. Four methods achieve a two-way shape memory effect: liquid crystalline elastomers, semi-crystalline networks, composites, and interpenetrating polymer networks (19).

4.2.1 Liquid crystalline elastomers

A liquid crystal elastomer (LCE) is a material that combines the entropy elasticity of a polymeric elastomer with the self-organization of a liquid crystal (20). An LCE consists of mesogenic groups. These mesogens can be aligned in a particular direction called the mono-domain. This is the anisotropic phase. When an external stimulus is applied, the mesogens are disorderly oriented. This is called the poly-domain and is the isotropic phase. When the material switches from the anisotropic phase to the isotropic phase, the material contracts (21). When the external stimulus is removed, the material will return to the anisotropic phase and expand.

4.2.2 Semi-crystalline networks

'Semi-crystalline polymers are a mixture of crystalline and amorphous structures' (22). When under constant tension, the crystalline domains orient in the direction of the tension when the semi-crystalline material is cooled. When the material is heated above the transition temperature, it contracts. It is concluded that the two-way shape memory effect of semi-crystalline networks is based on crystallization-induced elongation and melting-induced contraction (19).

4.2.3 Composites

A two-way shape memory effect using composites usually requires two layers of polymeric networks. These polymeric networks consist of two layers of one-way shape memory polymers, or with a layer of a one-way shape memory polymer and another layer of an elastomeric polymer layer (19). It is also

possible to create a shape memory composite by adding a shape memory alloy in combination with a shape memory polymer. The composite fabrication consists of a 1-way shape memory polymer and an elastomer: the shape memory polymer is heated above the transition temperature, is fully bent, and cooled. An elastomeric layer is then laminated to the shape memory polymer. When heated, the shape memory polymer recovers to its permanent shape by applying tension to the laminate. When cooled, the shape memory polymer loses its recovery tension, while the elastomeric layer expands due to the acquired stress during the heating process, resulting in reversible bending. A disadvantage of shape memory composites is that they can only bend.

4.2.4 Interpenetrating polymer networks

Two-way shape memory using an interpenetrating polymer network (IPN) usually consists of two or more polymer networks. Molecular interlacing exists in the matrix of the material, but there is no covalent bonding between the different polymer networks. A material with an IPN has a switch-spring structure with elastomeric and crystalline components. The cross-linked crystalline system is the switch phase, while the elastomer network is a built-in force for recovery (23). This can be seen in Fig 5.

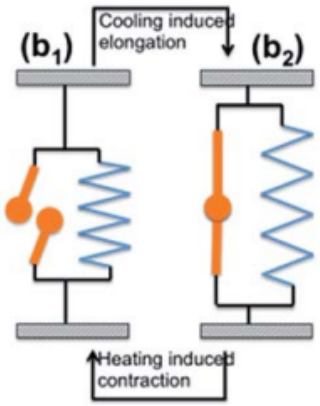

Figure 5: (b1) The material is heated above the transition temperature of the crystalline component. The switch opens, and the crystalline polymer shrinks while the elastomer polymer is compressed. (b2) The material is cooled, the crystalline polymer crystallizes, and the elastomer polymer recovers elastically (23)

4.3 Multiple shape memory effect

In the first part of this chapter, shape-memory materials with only one temporary and one permanent shape were discussed. However, there are shape memory polymers that can memorize more

than one temporary shape (24). This is called the multiple shape memory effect.

Figure 6 shows the cycle for a triple-shape memory effect for a material. Step I is applying the first temporary shape for the material at T_H. Step II is cooling down the material to T_{C_1} while keeping the material deformed. Step III applies the second temporary shape at T_{C_1}. Step IV is cooling down the material to T_{C_2} while keeping it deformed. Step V is unloading the material at T_{C_2}. Then, the material is heated to T_{C_1}, where the material recovers to its first temporary shape. Finally, the material is heated to T_H, where the material recovers to its permanent shape.

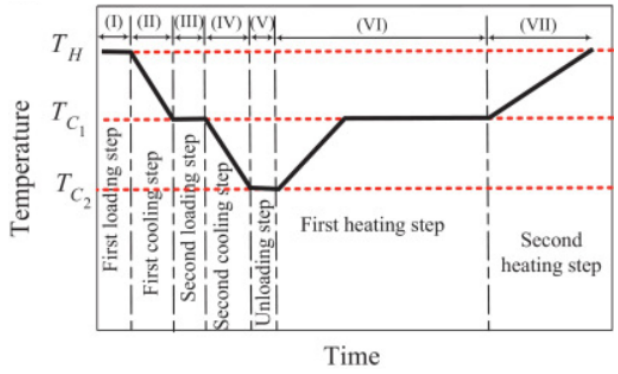

Figure 6: The cycle of a triple-shape memory effect (24)

5 Modelling

In this section, the bending of a hinge is modeled. First, a mathematical model of a two-layered composite is shown. Then, a short description of a Finite Element Method (FEM) model is given.

5.1 Two-layered composite

When the hinge is a two-layered composite consisting of an alloy layer and a polymer layer, the equation of the internal forces of the polymer layer and the alloy layer is as follows (17):

$$F_{\mathrm{a}} + F_{\mathrm{p}} = 0 \tag{1}$$

The axial strain of each layer of the hinge is:

$$\varepsilon = \varepsilon_{\mathrm{F}} + \varepsilon_{\mathrm{bending}} + \varepsilon_{\mathrm{thermal}} + \varepsilon_{\mathrm{transform}} \tag{2}$$

Where ε_{F} is strain due to the internal force, $\varepsilon_{\mathrm{bending}}$ the strain due to the bending of the hinge, $\varepsilon_{\mathrm{thermal}}$ the strain due to the thermal expansion of the beam and $\varepsilon_{\mathrm{transform}}$ the transformation strain which acts in the shape memory alloy layer.

The strain due to the internal force can be seen in Equation 3, where F is the force, b is the layer's width, h is the layer's height, and E is the Young's-modulus.

$$\varepsilon_{\mathrm{F}} = \frac{F}{bhE} \tag{3}$$

The bending strain due to the bending of the layers can be seen in Equation 4, where κ_0 is the initial curvature of the layer, κ_{final} is the final curvature of the layer, and where ρ and ρ_{final} are the radii of the curvature. The radius of the curvature is the inverse of the curvature.

$$\varepsilon_{\mathrm{bending}} = \Delta\kappa z = (\kappa_0 - \kappa_{\mathrm{beam}})\, z = \left(\frac{1}{\rho_0} - \frac{1}{\rho_{\mathrm{beam}}}\right) z \tag{4}$$

The strain resulting from thermal expansion can be seen in Equation 5, where α is the thermal expansion coefficient, and ΔT is the temperature difference.

$$\varepsilon_{\mathrm{thermal}} = \alpha\Delta T \tag{5}$$

The transformation stress in the alloy layer can be defined as can be seen in Equation 6, where ξ is the volume fraction of the martensite phase and $\varepsilon_{\mathrm{t}}^{\max}$ the maximum transformation strain of the shape memory alloy.

$$\varepsilon_{\mathrm{transform}} = \xi\varepsilon_{\mathrm{t}}^{\max} \tag{6}$$

The volume fraction of the martensite phase can be determined in Equations 7 and 8. It depends on whether the material transforms from an austenite to a martensite phase or the other way around because of the hysteresis.

$$
\begin{aligned}
&\xi = 1 - \exp\left[a^{\mathrm{M}}\left(T_{\mathrm{Ms}} - T\right) + b^{\mathrm{M}}\sigma_{\mathrm{f}}\right] \\
&\text{where } a^{\mathrm{M}} = \frac{\ln(0.01)}{T_{\mathrm{Ms}} - T_{\mathrm{Mf}}}, \\
&b^{\mathrm{M}} = \frac{a^{\mathrm{M}}}{C_{\mathrm{M}}} \text{ for the Austenite} \rightarrow \text{Martensite transformation}
\end{aligned} \tag{7}
$$

$$
\begin{aligned}
&\xi = \exp\left[a^{\mathrm{A}}\left(T_{\mathrm{As}} - T\right) + b^{\mathrm{A}}\sigma_{\mathrm{f}}\right] \\
&\text{where } a^{\mathrm{A}} = \frac{\ln(0.01)}{T_{\mathrm{As}} - T_{\mathrm{AMf}}}, \\
&b^{\mathrm{A}} = \frac{a^{\mathrm{A}}}{C_{\mathrm{A}}} \text{ for the Martensite} \rightarrow \text{Austenite transformation}
\end{aligned} \tag{8}
$$

Where C_M and C_A are the slopes of the stress-temperature phase diagram, like in Figure 1. Where σ_f is:

$$
\sigma_f = \frac{F_a}{bh_{comp}} \tag{9}
$$

As explained earlier, the E-modulus of both shape memory polymers and shape memory alloys depends on the temperature. Equation 10 shows the dependence of the E-modulus on the temperature for a shape memory polymer.

$$
\begin{aligned}
E_{\mathrm{SMP}} &= E_{\mathrm{L}}^{\mathrm{SMP}} \quad \text{at } T_{\mathrm{g}}/T \leq 0.955 \\
E_{\mathrm{SMP}} &= E_{\mathrm{g}}^{\mathrm{SMP}} \exp\left(a\left(\frac{T_{\mathrm{g}}}{T}\right) - 1\right) \\
&\quad \text{at } 0.95 < T_{\mathrm{g}}/T < 1.05 \\
E_{\mathrm{SMP}} &= E_{\mathrm{H}}^{\mathrm{SMP}} \quad \text{at } T_{\mathrm{g}}/T \geq 1.048
\end{aligned} \tag{10}
$$

Equation 11 shows the dependence of the E-modulus on the temperature for a shape memory alloy.

$$
\begin{aligned}
E_{SMA} &= E_{\mathrm{M}} \quad \text{for } \xi = 1 \\
E_{\mathrm{SMA}} &= \xi E_{\mathrm{M}} + (1 - A \quad \text{for } 0 < \xi < 1 \\
E_{\mathrm{SMA}} &= E_{\mathrm{A}} \quad \text{for } \xi = 0
\end{aligned} \tag{11}
$$

The thermal expansion coefficient is also dependent on the temperature. The thermal expansion coefficient that is used for the shape memory polymer intends whether the temperature is below or above the glass transition temperature, as can be seen in Equation 12

$$
\begin{aligned}
\alpha_{\mathrm{SMP}} &= \alpha_{\mathrm{H}}^{\mathrm{SMP}} \quad \text{at } T \leq T_{\mathrm{g}} \\
\alpha_{\mathrm{SMP}} &= \alpha_{\mathrm{L}}^{\mathrm{SMP}} \quad \text{at } T > T_{\mathrm{g}}
\end{aligned} \tag{12}
$$

The thermal expansion coefficient for a shape memory alloy depends on the fraction of the martensite and austenite phase, as can be seen in Equation 13

$$
\begin{aligned}
\alpha_{\mathrm{SMA}} &= \alpha_{\mathrm{M}}^{\mathrm{SMA}} \quad \text{for } \xi = 1 \\
\alpha_{\mathrm{SMA}} &= \xi\alpha_{\mathrm{M}}^{\mathrm{SMA}} + (1 - \xi)\alpha_{\mathrm{A}}^{\mathrm{SMA}} \quad \text{for } 0 < \xi < 1 \\
\alpha_{\mathrm{SMA}} &= \alpha_{\mathrm{M}}^{\mathrm{SMA}} \quad \text{for } \xi = 0
\end{aligned} \tag{13}
$$

5.2 Finite element model

The finite element method is a numerical method to obtain approximate solutions to various engineering problems. In the finite element method, complex differential equations are solved. In a finite element model, a structure is divided into multiple small parts called finite elements. Each element has a stiffness matrix when a structural analysis is carried out. A large stiffness matrix is made for the entire structure using the stiffness matrix for each element. Sufficient constraints are needed to solve the governing equations. The finite element method calculates the stress of each element. ABAQUS is a Finite element method program. There exist an ABAQUS User MATerial that can simulate the shape memory effect of the material. ABAQUS can also perform a heat transfer analysis. In section 7, researchers use the ABAQUS software to simulate the material's behavior.

6 Fabrication

In this section, the most common fabrication processes used for manufacturing shape memory material hinges found in recent literature are shortly explained.

6.1 Fused deposition modeling

Fused deposition modeling, also called fused filament fabrication, is a popular 3D manufacturing technique. The process manufactures structures layer by layer to create a 3D structure (25). Extrusion is used to print the structure, where the feedstock material is pushed through the extruder. The material is added to a platform. Either the platform or the extruder can move to create the desired geometry of the structure.

6.2 Material jetting

Material jetting is a 3D print technique. The process is as follows: the material is stored in air-excluding tanks. The material is heated in the transmission line when it is transmitted from tank to nozzle. Droplets of the material are then applied to the build platform to make the structure. Ultraviolet light is then emitted onto the molten material to cure it. The structure is made by applying the material layer by layer, where the build platform is lowered after each layer. Either the build platform or the nozzle can move to create the desired geometry of the structure (26).

6.3 Vacuum assisted resin transfer molding

Vacuum-assisted transfer molding is a composite manufacturing process where multiple layers of fibers are laid up in a one-sided mold. This mold is covered with a vacuum bag. The fibers are then impregnated with a shape memory resin using vacuum pressure. Finally, the resin is cured at room temperature, and the composite part is de-molded (27).

7 Recent research

In this section, recent research concerning shape memory material hinges is discussed. This section starts with hinges with a one-way shape memory effect, followed by hinges with a two-way shape memory effect. The design, fabrication process, and experiments are handled for each hinge.

7.1 One-way shape memory actuated hinge used in a deployable structure

Liu et al. (28) designed a deployable structure using multiple shape memory polymer composite hinges. This deployable structure was designed for aerospace applications in a low-gravity environment. The hinge consists of carbon fiber reinforced shape memory epoxy composites. The carbon fiber reinforced shape memory composite was manufactured using vacuum-assisted transfer molding. Resistor heaters supply the heat, which triggers the shape memory effect. The hinge consists of two symmetrical arc shape laminates. The arc of the laminates has an angle of 120°, which was found optimum in experiments.

Experiments were carried out to determine the temperature sensitivity, elastic modulus, and material strength. A 3-point bending and shape memory recovery test was performed to verify the variable stiffness under different temperatures and superior shape memory properties. The strain distribution during the bending process was obtained using the digital image correlation technique and the ABAQUS simulation software, which showed good consistency with each other. The motivation for researching this paper was to investigate the effect of carbon fiber on shape memory materials and how multiple hinges in series are fabricated and actuated.

Figure 7: Fabricated deployable structure made by Liu et al., where the shape memory recovery process is shown (28)

Pros

- Structure can be folded in a small shape
- No assembly in the manufacturing process
- Lightweight
- Hinge maintains a shape recovery ratio of 100% after ten times fold-deploy process

Cons

- One-way shape memory effect, which limits the potential applications
- Complex fabrication process because of relatively long product
- Relatively long recovery process of about 60 seconds

7.2 One-way shape memory actuated hinge with multiple fiber layers

Liu et al. (29), the same research group as in previous research, designed another shape memory composite hinge, as seen in Figure 8, where the same reinforced fiber and the same manufacturing technique were used as in previous research. This hinge is also designed for application in aerospace. The design consists of only one hinge. A heating film provides the heat triggering the shape memory effect. An aluminum tape was pasted between the heating film and the hinge fiber sheet for an even heat distribution. The micro buckling problem that occurs during the bending of hinges when the shape memory effect takes place is solved by designing the bending path using a mold.

This research investigated how the properties of the hinge change when different amounts of shape memory composite layers were used in the hinge and determined an optimum number of layers for the hinge. First, the optimum voltage used for heating is determined. Then, the recovery speed, heat distribution, and strain distribution using the digital image correlation technique were obtained. The recovery force and the deployed stiffness of the material with different fiber layers are determined. Finally, surface morphology is carried out. The motivation for researching this paper was to see the effect of multiple fiber layers on shape memory materials.

Pros

- Lightweight
- Even heat distribution using an aluminum tape
- With the right surface temperature, the recovery rate reaches 100%

Cons

- One-way shape memory effect, which limits the potential applications
- Assembly needed
- Relatively long recovery process of about 180 seconds

7.3 Passive 4D-printed elastomer hinge

Yamamura et al. (30) designed a hybrid hinge that can be elastically deformed when the material is below the glass transition temperature. The material used is polyurethane. Polyurethane in a glassy state at room temperature is used as a shape memory polymer, while polyurethane in a rubbery

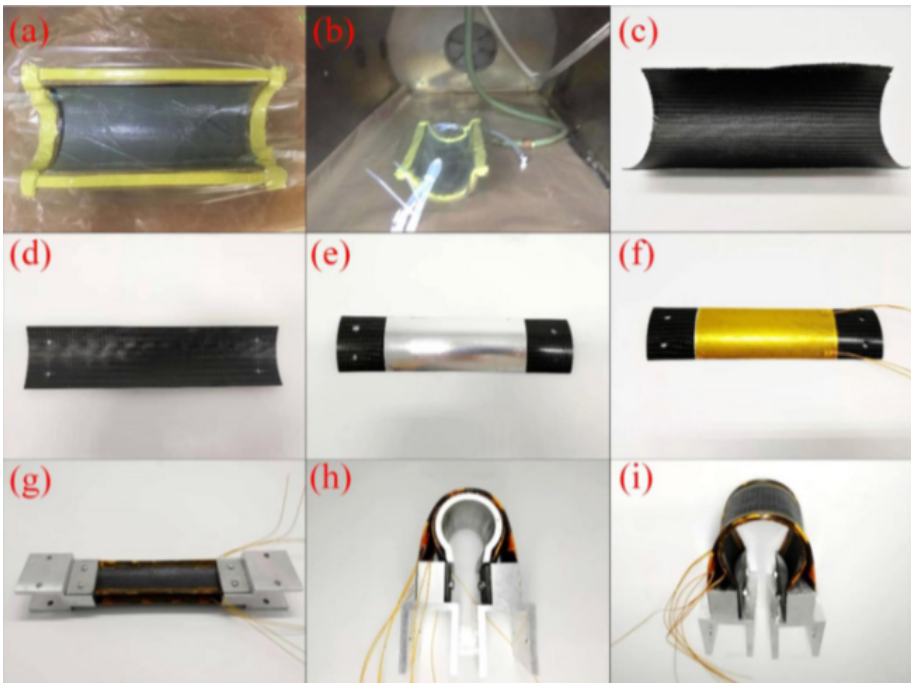

Figure 8: Fabricated process for the hinge made by Liu et al., (a) inject the shape memory epoxy resin into the mold of the reinforced fabric, (b) cure the mold in an autoclave, (c) remove the material from the autoclave, (d) cut the material to the right dimensions, (e) paste aluminum tape that is used to get an even heat distribution, (f) paste heat films on the material, (g) assemble the hinge, (h) bend the hinge in the temperature chamber, (i) take out the finished shape memory hinge (29)

state at room temperature is used as the elastomer. The hybrid hinge consists of an elastomer and two shape memory polymer hinges. When the material is heated, bending deformation occurs due to the difference in expansion coefficients. This is the 4D part. When the material is cooled, it stays in its permanent shape. The elastomer part of the hinge is less rigid than the shape memory polymer part. The deformation occurs at the elastomer part when an external force is applied after 4D printing.

The hinge is fabricated using an additive manufacturing FDM 3D printer. The manufacturing process can be seen in Figure 9. The manufacturing process is divided into three parts. First, the bottom model is made, which consists of shrinkable and non-shrinkable shape memory polymers. Then the middle part is manufactured, which consists of elastomer. Finally, the top part is manufactured with a non-shrinkable shape memory polymer.

Several experiments were carried out. The effect of the hinge length on the self-folding angle

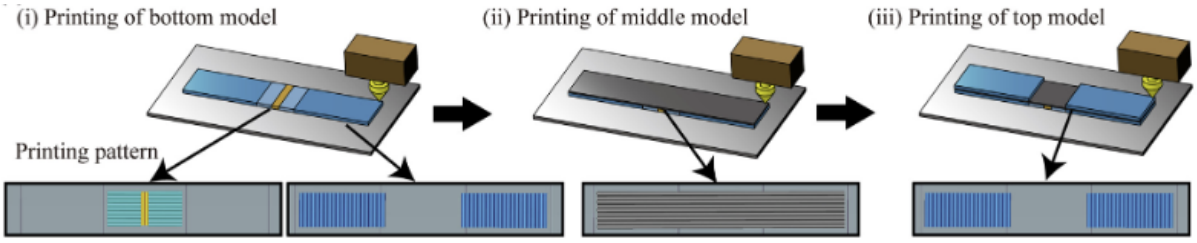

Figure 9: The fabrication process for the hybrid hinge (30)

was investigated. The larger the hinge length, the larger the self-folding angle. Furthermore, the material is cyclically loaded and unloaded to determine how well the material returns to its permanent shape when the material is unloaded. After 500 loading cycles, the object returned almost to its original shape without failure. This shows that the hinge has high durability and elasticity. The experiment can be seen in Figure 10. The motivation for researching this paper was to investigate how passive hinges work and to consider if they could be useful in further research.

Pros

- Lightweight
- High recovery rate, reaching 99%, after 500 cycles
- No assembly process

Cons

- The hinge cannot be actuated
- Only tested on a sample the size of a thumb

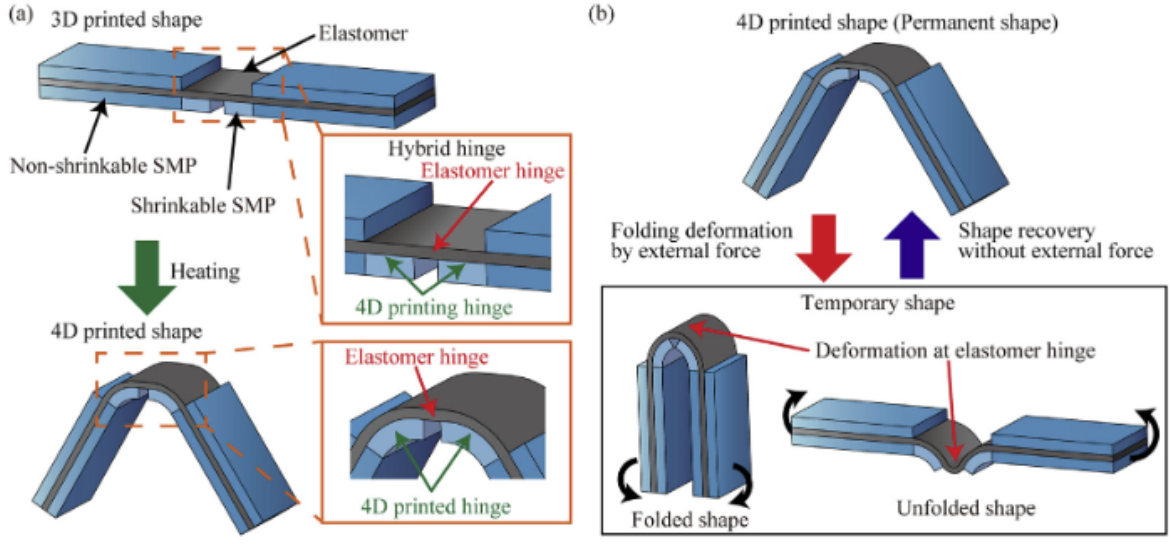

Figure 10: The experiment carried out with the hybrid hinge structure made by Yamamura et al. (30)

7.4 Two one-way shape memory polymer hinge structures using active and passive hinges

Akbari et al. (31) designed two one-way shape memory polymer hinge structures. Both structures are made using a fused deposition modeling 3D printer. The structures consist of active and passive hinges. The active shape memory polymer hinge locks the structure in a temporary shape during the programming process, while the passive elastomer hinge increases the actuation force and load-bearing capacity. Resistant wires actuate the active hinges.

Structure 1 is a morphing wing flap, shown in Figure 11. This structure consists of 2 active hinges and a passive hinge. Large bending deformation is exhibited in this structure. It was manufactured in a bent shape and subsequently programmed in a straight shape.

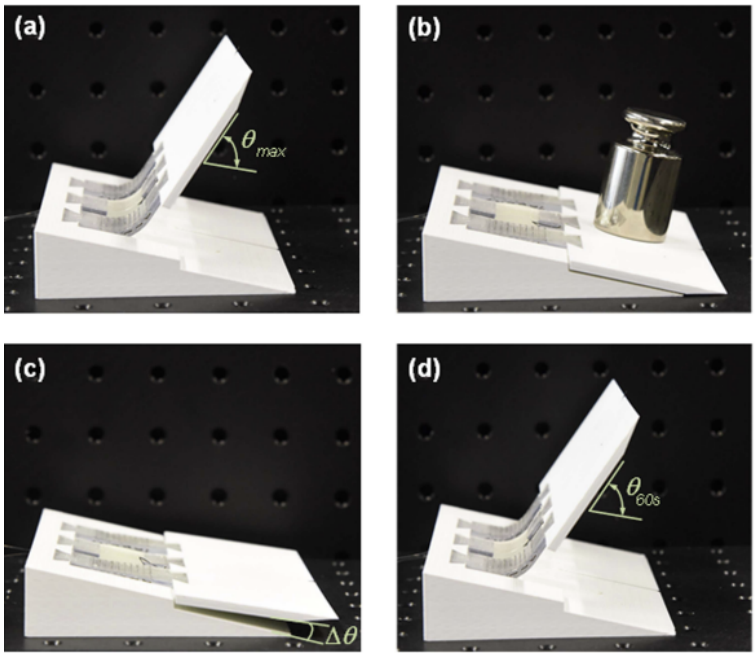

Figure 11: Structure 1 made by Akbari et al. (31)

Structure 2 is a deployable structure, shown in Figure 12. This structure consists of two active hinges and two passive hinges. This structure can achieve large extensional deformation. It was initially manufactured upright and programmed in a folded shape.

A broad range of mechanical properties can be achieved by using different materials for the active and passive hinges. Dynamic mechanical analysis and a uni-axial tensile test were carried out for ten different shape-memory materials.

Important design parameters like local deformation, shape fixity and recovery ratio are obtained by

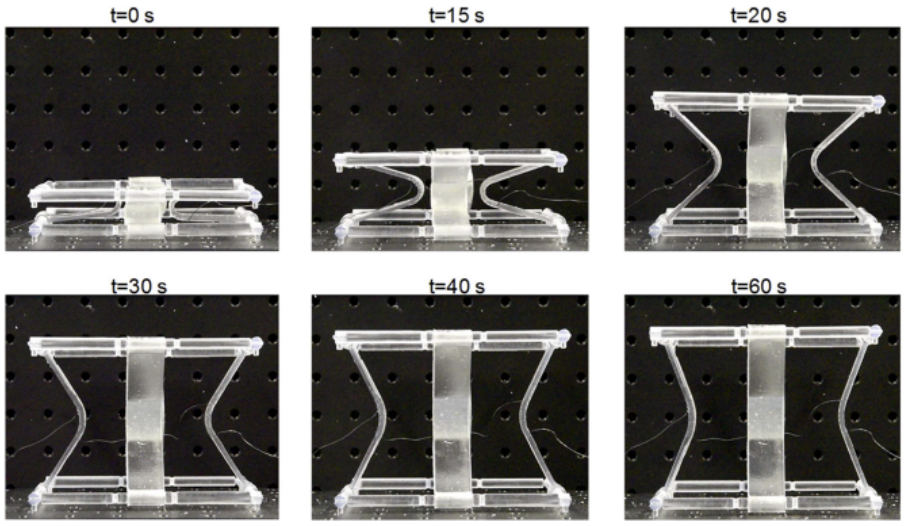

Figure 12: Structure 2 made by Akbari et al.(31)

using finite element simulations, which can predict nonlinear deformations. The research showed that the passive hinge increased the recovery ratio. Furthermore, a coupled thermal-electrical finite element analysis was carried out to model the heat distribution during the heating process. The model predicted the heat well compared to measured temperature data. The motivation for researching this paper was to see the effect of passive hinges in combination with active hinges in a structure.

Pros

- When using a flexible hinge, a higher recovery ratio is achieved
- Short fabrication time compared to other manufacturing methods

Cons

- One-way shape memory effect, which limits the potential applications
- Relatively long recovery process of about 60 seconds

7.5 Two-way fiber-reinforced plastic hinge in combination with Nitinol

Ashir et al.(32) made a shape memory hinge using fiber-reinforced plastic in combination with a nickel-titanium shape memory alloy. The shape memory alloy was converted into hybrid yarns using friction spinning technology. Then, the resin is infused into the hybrid yarn fabric and cured to complete the fiber-reinforced plastic. The shape memory alloy was heated using current, which triggers the shape memory effect. Five variations of the hinge were made in this research.

The research investigates what the effect is of the hinge width and the distance between different shape memory alloy wires, as can be seen in Figure 13. Young's modulus decreases with an increase in the hinge width. When the hinge width is increased, the maximum deformation becomes larger. When the distance between the wires increases, the maximum deformation becomes smaller.

The first heating and cooling cycles are inhomogeneous, but the deformation behavior becomes homogeneous after the first few cycles. The motivation for researching this paper was to see the effect of fiber-reinforced plastic in combination with shape memory alloys and the effect of different parameters of shape memory alloy wires on the shape memory effect.

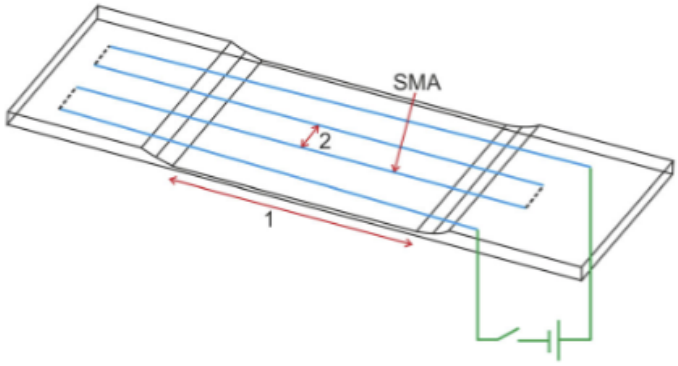

Figure 13: Fabricated hinge made by Ashir et al., where parameters 1 and 2 are changed (32)

Pros

- Two-way shape memory effect, which enhances the number of potential applications
- Lightweight structure
- The actuation time is 40 seconds, which is relatively low compared to other hinges
- Consistent deformation curves after five deformation cycles

Cons

- Complex manufacturing technique
- Thin sample which can't bear high loads

7.6 Two-way fiber-reinforced shape memory material hinge actuated by Nitinol springs

Testoni et al. (33) designed a two-way shape memory hinge. The hinge consists of two shape memory polymer parts and two shape memory alloy springs. The shape memory polymer part was fabricated using a material jetting process 3D printer. Each shape memory polymer part has a heater connected to it. The heaters result in a decrease in bending stiffness, which allows for the

bending of the hinge. Between the two shape memory polymers, a carbon fiber reinforced polymer separates the two parts to support the shape memory polymer parts at large deformations. The shape memory alloy springs are used for the actuating of the hinge. A current heats them. The designed hinge can be seen in Figure 14.

The angle of the hinge can be modified by adjusting the currents through the different parts of the structure: The shape memory polymer heater is activated, reducing the stiffness of the polymer. A current is sent through the shape memory alloy spring, resulting in the hinge bending. The polymer heater is then turned off, resulting in an increase in the stiffness of the polymer due to the cooling of the material. The heating of the spring is stopped, ending the bending actuation. The spring returns to its original shape when the polymer heaters are again activated.

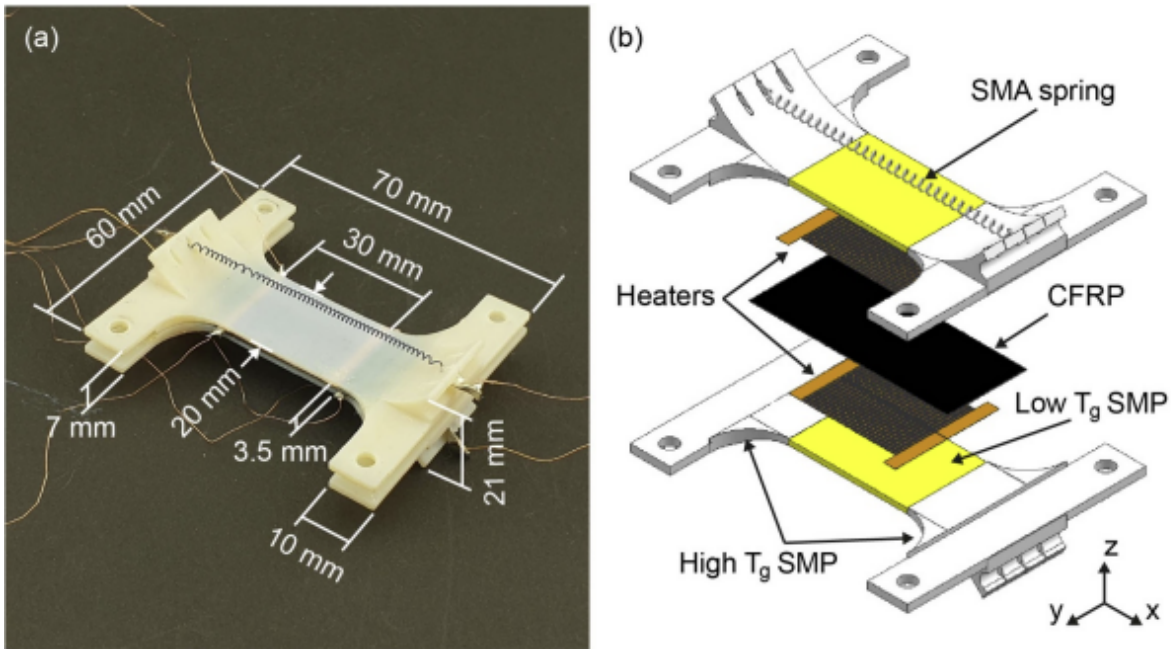

Figure 14: The two-way shape memory hinge made by Testoni et al. (33)

Some tests are carried out. One of the tests is the maximum angle test. It is found that the maximum angular position is 97°, and when the springs are deactivated, the hinge locks at an angular position of 90°. The cycle to reach the maximum angular position and return to its original shape takes about 820 seconds.

The second test is the multiple actuation test. When the polymer is heated constantly, and when each spring is actuated in turn, it is found that the maximum angle reaches 100°after the second cycle, and each cycle takes about 180 seconds.

The third test is the gradual increase in angular position test. The hinge increased its angular position from 0°to 90°in increments of 10°. The hinge could reorient itself with a precision of 3°.

The last test is the multi-step actuation test. The result shows that an angular position of 45°can be achieved in 30 seconds starting from 0°. When going from 90°to -45°, it takes about 120 seconds. The motivation for researching this paper was to see the effect of using an external shape memory alloy spring in combination with a shape memory polymer structure.

Pros

- Two-way shape memory effect, which enhances the number of potential applications
- Hinge can orientate itself to multiple angular positions with a precision of 3°

Cons

- Assembly needed
- To reach the desired angular position, some fine tuning is required

7.7 Two-way shape memory polymer hinge embedded with shape memory alloy wires

Akbari et al. made a reversible actuator using a multi-material inkjet 3D printer. The structure consists of shape memory polymers, soft layers of elastomeric polymer, resistive wires, and shape memory alloy wires. They eccentrically embedded the shape memory alloy wires into the printed shape memory polymer. They made two structures, as shown in Figure 15. Both structures have two hinges, which can be actuated separately. The difference between the two actuators is the amount of printed soft material in the hinge area. This results in actuator 1 having a lower bending stiffness. There are resistive wires in the hinge area to heat the shape memory polymer segments via joule heating. The temperature of the shape memory alloy wires can also be regulated using a current. The shape memory alloy wires are used to restore the original shape of the structure by applying compressing force. The shape memory alloy wires are connected to the end of the actuator using copper crimp connections.

The actuators are actuated as follows: First, a current is applied through the resistive wires to heat the shape memory polymer, which will transform from a glassy state to a low-stiffness rubbery state. Then, the current through the resistive wires is stopped, and the current through the shape memory alloy is activated, resulting in a bending deformation. The current through the shape memory alloy wire is stopped when the shape memory polymer is cooled down, and a glassy state is formed. The actuator remains in its deformed shape. When a current is applied to the resistive wires, the actuator transforms to its original state.

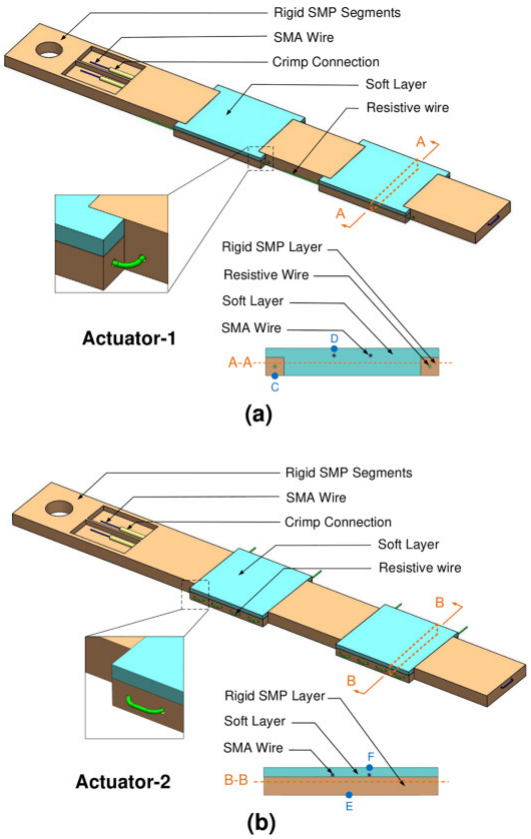

Figure 15: Design for the reversible actuator made by Akbari et al. (34)

The actuators are implemented in a FEM tool, and by using ABAQUS, the thermomechanical behavior is simulated. It can be concluded that the finite element model could predict the effect of the shape memory polymer thickness on the shape fixity, the recovery ratio, and the fixity ratio with reasonable accuracy. It is measured how fast the shape memory polymer reaches 60°C under different applied currents. Measurements were also carried out on the effect of the resistive wires on the shape memory alloy temperature. It is found that the shape memory alloy is not actuated as a result of the temperature increase due to the resistive wires. Actuator 2 is found to have a better fixity and recovery but has a lower maximum deformation. The lower bending deformation results from a higher stiffness in the hinge area. This research group made a gripper using these reversible actuators, which can be seen in Figure 16. The motivation for researching this paper was the use of multiple hinges in the design, which resembled fingers, and the combination of shape memory alloy embedded in a shape memory polymer structure.

Pros

- Two-way shape memory effect, which enhances the number of potential applications
- Each hinge can be actuated independently

Cons

- Assembly needed
- Cannot control the angle of the hinge
- Shape recovery ratio relatively low compared to other hinges

Figure 16: Gripper made by Akbari et al (35)

7.8 Two-way fiber reinforced plastic shape memory hinge embedded with a shape memory alloy and controlled using an Arduino board

Lalegani Dezaki et al. (36) designed an actuator with a 2-way shape memory effect. The actuator consisted of a two-way shape memory alloy, low-temperature liquid epoxy cure composites, and fiber-reinforced plastic. The two-way shape memory alloy wires are trained using the pre-straining method. The shape memory alloy wires are directly inserted into the fiber-reinforced plastic strips. Copper wires are soldered to the shape memory alloy wires for optimal electricity distribution. Threads are used for better stability of the actuator. The epoxy resin is used as an adhesive. A structure representing human fingers was 3D printed using a fused deposition modeling 3D printer, and the built actuator actuated these fingers. The gripper can be seen in Figure 17. The actuator was actuated using an electrical current and controlled using an Arduino board. A video camera recorded the action of the actuator. A bending resistive sensor is used to measure the bending angles of the actuator.

The robustness, controllability, mechanical properties, and the 500 life cycle of the actuator are tested. Results show that the actuator has a bending angle of 58°with a 30 mm deflection in 7 s after the actuating starts. The recovery time of the actuator is 40 seconds. The wires heat faster when using a higher current, but the fiber-reinforced plastic can be damaged with higher voltages. When airflow is used, the recovery time of the gripper reduces to 20 seconds. A tensile test is carried out, and it is found that the structure tears apart when a force of 300 N is applied. A fatigue test

was performed on a single actuator when it was actuated 500 times. The gripper could lift weights to 300 g. The motivation for researching this paper was to see how a gripper can be controlled using an Arduino board.

Pros

- Two-way shape memory effect, which enhances the number of potential applications
- Relatively fast gripping and releasing cycle of 25 seconds
- Gripper could pick up objects of different shapes with a weight of up to 300 g

Cons

- Complex manufacturing process
- Deflection of the tip is not constant when actuated

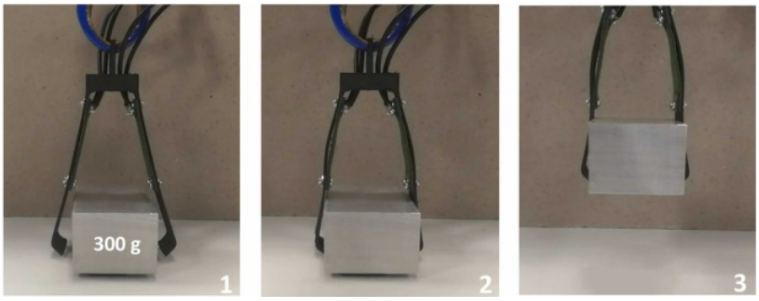

Figure 17: gripper made by Lalegani Dezaki et al. (36)

8 Conclusion

The conclusion will summarize the literature review by answering the research questions. The overall research question is: What is the current state of the art of interactive hinges for shape memory materials? The overall research question will be answered by answering the sub-research questions.

8.1 What are shape memory materials?

Shape memory materials are smart materials that can remember their original shape when plastic deformation occurs. The return from plastic deformation to its original shape is called the shape memory effect. An external stimulus triggers the shape memory effect. There are many external stimuli, but the heat-induced shape memory effect is the most frequent.

8.2 What types of shape memory materials are there, and how do they work?

The three most common shape memory materials are shape memory alloys, shape memory polymers, and shape memory composites.

8.2.1 Shape memory alloys

The shape memory effect of alloys is the result of solid-state phase transformation. Each phase has a different crystal structure and properties. The austenite phase is the high-temperature phase with a high Young's modulus, while the martensite phase is the low-temperature phase with lower stiffness. Shear lattice distortion is the cause of the shape transformation. The transformation from the austenite to the martensite phase is obtained by applying stress or decreasing the temperature.

8.2.2 Shape memory polymers

The shape memory effect of polymers results from permanent netpoints and switches. The permanent netpoints are not affected by deformation and are the reason for the memory of the original shape. The switches are sensitive to external stimuli, which trigger the shape memory effect.

8.2.3 Shape memory composites

A composite is a material that consists of multiple materials, which can be either multiple alloys, multiple polymers, or a mixture of a polymer and an alloy. The shape memory effect of composites often results from a difference in expansion coefficients of the different materials in the composite. When the material is heated, one of the materials of the composite expands less than the other. This results in the bending of the material.

8.3 What types of shape memory effects are there?

There are several shape memory effects. The most straightforward shape memory effect is the dual-shape memory effect. This shape memory effect has two shapes: the temporary and the permanent shape. This effect is not reversible. After each shape memory effect, the material must be programmed again. There also exists a two-way shape memory effect, where shape-shifting is reversible. There are several methods to achieve this, but the most commonly found in papers is the two-way shape memory effect using composites. It is also possible for a material to remember more temporary shapes, which is called the multiple shape memory effect.

8.4 How is the shape memory effect modeled?

A mathematical model is presented in Section 5 on calculating the forces in each layer of a two-layered composite consisting of an alloy and a polymer. It is, however, possible to simulate the shape memory effect in a Finite Element Method program called ABAQUS. This program can also carry out a heat transfer analysis, which can help model the external stimulus in the material.

8.5 What are the (recent) researches about shape memory hinge actuators and how are they manufactured?

When looking for papers about shape memory material hinges, hinges with various shapes, sizes, and used materials were found. Most papers were about one-way shape memory material hinges. In some fields, one-way shape memory polymers can be helpful. For example, some researchers designed one-way shape memory material hinges for deployable structures used in satellites. Few researchers focus on two-way shape memory material hinges, even though the potential for two-way shape memory material hinges is greater than one-way shape memory material hinges. In the future, two-way shape memory material hinges may, for example, be applied in robotics.

Most shape memory material hinges in recent research are fabricated either by a 3D printer or vacuum-assisted resin transfer molding. Fused deposition modeling and material jetting techniques are the 3D printing techniques used most.

9 Research gap and future research

The main challenges researchers face and try to tackle improving the recovery forces, controllability, repeatability, and cycle time of the hinges. Presently, the application of shape memory materials in engineering is limited because of the low stiffness or tensile strength of current shape memory materials. Shape memory material hinge actuators also show inaccuracy when actuated multiple times, not returning to the same shape as in previous actuation cycles. Furthermore, the cycle time from permanent to temporary shape and back should be reduced. For most actuators found in literature, the cycle time is too long to be used commercially. Different designs for hinge actuators could overcome these challenges. The shape memory material hinge actuators found in literature worked in a 2D plane like an elbow joint. Future research could investigate the possibility of a shoulder joint-like hinge actuator that worked in a 3D space.

References

[1] Shape memory polymers (smps) – current research and future applications.

[2] W.M. Huang, Z. Ding, C.C. Wang, J. Wei, Y. Zhao, and H. Purnawali. Shape memory materials. 2010.

[3] A.Y. Lee, J. An, and C.K. Chua. Two-way 4d printing: A review on the reversibility of 3d-printed shape memory materials. 2017.

[4] Y. Xia, Y. He, F. Zhang, Y. Liu, and J. Leng. A review of shape memory polymers and composites: Mechanisms, materials, and applications. 2021.

[5] J.M. Jania, M. Leary, A.Subic, and M.A. Gibson. A review of shape memory alloy research, applications and opportunities. 2014.

[6] I.N. QADER, M. KÖK, F. DAGDELEN, and Y. AYDOGDU. A review of smart materials: Researches and applications. 2019.

[7] A.A. Basheer. Advances in the smart materials applications in the aerospace industries. 2020.

[8] A. Mukherjee, Deepmala, P Srivastava, and J Kaur Sundhu. Application of smart materials in civil engineering: A review. 2021.

[9] T. Duerig, D. Stoeckel, and D. Johnson. Sma - smart materials for medical applications. 2003.

[10] S. Barbarino, E.I. Saavedra Flores, R.M. Ajaj, I. Dayyani, and M.I. Friswell. A review on shape memory alloys with applications to morphing aircraft. 2014.

[11] R. Chaudhari, J.J. Vora, and D.M. Parikh. A review on applications of nitinol shape memory alloy. 2021.

[12] D.C. Lagoudas. *Shape memory alloys: modeling and engineering applications*, chapter 1.3. Springer, 2008.

[13] G. Strobl. *The physics of polymers: Concepts for understanding their structures and behavior*, chapter 1.1. Springer, 2007.

[14] A. Melocchi, M. Cerea, A. Foppoli, S.Moutaharrik, L. Palugan, L. Zema, and A. Gazzaniga. Shape memory materials and 4d printing in pharmaceutics. 2021.

[15] H. Xie, C. Cheng, X. Deng, C. Fan, L. Du, K. Yang, and Y. Wang. Creating poly(tetramethylene oxide) glycol-based networks with tunable two-way shape memory effects via temperature-switched netpoints. 2017.

[16] A. Melocchi, M. Uboldi, M. Cerea, A. Foppoli, A. Maroni, L. Palugan S. Moutaharrik, L. Zema, and A. Gazzaniga. Shape memory materials and 4d printing in pharmaceutics. 2021.

[17] M. Taya, Y. Liang, H. Tamagawa, and T. Howi. Design of two-way reversible bending actuator based on a shape memory alloy/shape memory polymer composite. 2013.

[18] A. Lendlein and S. Kelch. Shape-memory polymers. 2002.

[19] M. Zareab, M.P. Prabhakarana, and S. Ramakrishna. Thermally-induced two-way shape memory polymers: Mechanisms, structures, and applications. 2019.

[20] C. Ohm, M. Brehmer, and R. Zentel. Liquid crystalline elastomers as actuators and sensors. 2010.

[21] A. Marotta, G. Cesare Lama, V. Ambrogi, P. Cerruti, M. Giamberini, and G. Gentile. Shape memory behavior of liquid-crystalline elastomer/graphene oxide nanocomposites. 2018.

[22] V. Goodship. Injection molding of thermoplastics. 2016.

[23] Y. Wu, J. Hu, J. Han, Y. Zhu, H. Huang, J. Li, and B. Tang. Two-way shape memory polymer with "switch–spring" composition by interpenetrating polymer network. 2014.

[24] A. Bakhtiyari, M. Baniasadi, and M. Baghani. Development of a large strain formulation for multiple shape-memory-effect of polymers under bending. 2021.

[25] O.A. Mohamed, S.H. Masood, and J.L. Bhowmik. Optimization of fused deposition modeling process parameters: a review of current research and future prospects. 2015.

[26] O. Gülcan, K. Günaydın, and A. Tamer. The state of the art of material jetting—a critical review. 2021.

[27] D. Bender, J. Schuster, and D. Heider. Flow rate control during vacuum-assisted resin transfer molding (vartm) processing. 2006.

[28] T Liu, L. Liu, Q. Li, C. Zeng, X. Lan, and J. Leng. Integrative hinge based on shape memory polymer composites: Material, design, properties and application. 2019.

[29] Z. Liu, X. Lan, L. Liu, Q. Li, Y. Liu, and J. Leng. Design, material properties and performances of a smart hinge based on shape memory polymer composites. 2020.

[30] S. Yamamura and E. Iwase. Hybrid hinge structure with elastic hinge on self-folding of 4d printing using a fused deposition modeling 3d printer. 2021.

[31] S. Akbari, A. Sakhaei, B. Yang, A. Serjouei, Z. Yuanfang, and Q Ge. Enhanced multimaterial 4d printing with active hinges. 2018.

[32] M. Ashir, A. Nocke, and C. Cherif. Adaptive hinged fiber reinforced plastics with tailored shapememory alloy hybrid yarn. 2019.

[33] O. Testoni, T. Lumpe, J. Huang, M. Wagner, S. Bodkhe, R. Spolenak, J. Paik, P. Ermanni, L. Muñoz, and K. Shea. A 4d printed active compliant hinge for potential space applications using shape memory alloys and polymers. 2021.

[34] S. Akbari, A. Sakhaei, B. Yang, A. Serjouei, Z. Yuanfang, and Q Ge. Shape-reversible 4d printing aided by shape memory alloys. 2022.

[35] S. Akbari, A. Sakhaei, S. Panjwani, A. Serjouei, and Q Ge. Multimaterial 3d printed soft actuators powered by shape memory alloy wires. 2019.

[36] M. Lalegani Dezaki, M. Bodaghi, A. Serjouei, S. Afazov, and A. Zolfagharian. Adaptive reversible composite-based shape memory alloy soft actuators. 2022.

Designing an interactive hinge using shape memory polymers and alloys

Wessel Marcelis, Jovana Jovanova, Sepideh Ghodrat

September 21, 2023

Abstract

This research aims to design and simulate a hinge consisting of shape-memory alloys and polymers, which can be actuated along two axes. The hinge consists of a shape-memory body that is actuated externally by shape-memory alloy springs. To achieve maximum deformation, two small single hinges are made, of which the body has the shape of a plate and which are actuated externally by two springs. The two hinges are then stacked, where the second hinge is twisted 90°, so it can move in two directions. Tensile tests of Nitinol wires were carried out to investigate the behavior. Shape-memory springs were manufactured with this Nitinol wire. Then, the springs were deformed, the temperature of the springs was increased in steps of 10 °C, and the force was measured at each temperature step. Simulations were also carried out and compared to the force tests. The best type of Nitinol was chosen for the shape of memory wires. A prototype of the hinge was built and tested. First, the small single hinges were tested, where the displacement was documented. The hinge was not deemed energy efficient. Finally, simulations were carried out for the single and stacked hinges, which showed that the results were similar to reality. Hereafter, the range of motion of the stacked hinge is determined.

1 Introduction

Due to technological advancement, the use of smart systems has increased. Smart systems usually require multiple sensors and actuators—the increase in components increases weight, volume, and cost. An increase in weight and volume increases energy consumption. Therefore, systems need to be designed efficiently, not only for economic reasons but also for environmental gains. The use of smart materials can be a way to achieve these goals. Smart materials can sense and react to environmental stimuli (1). Shape-memory material is an example of a smart material.

A shape-memory material is a smart material that can remember its original shape when deformed. When an external stimulus is applied, the material can return to its original shape. Several external stimuli can trigger the shape-memory effect, but the most common one is an increase in temperature. The shape-memory effect occurs when the temperature of the material exceeds a certain threshold. Because of this, shape-memory materials have an excellent potential to make systems smart. Because it returns to its original shape, it can be used as an actuator and as a sensor as it deforms when the temperature exceeds its threshold (2). Two essential classes of shape-memory materials can be distinguished: shape-memory alloys and shape-memory polymers.

Phase transformation is the driving force behind the shape-memory effect of shape-memory alloys. Shape-memory alloys may assume two phases: martensite and austenite. Each phase has a different crystal structure and associated properties. The martensite has a lower Young's modulus than the austenite phase. Shape-memory alloys have a permanent shape and a temporary shape. When the alloy is at a low temperature in the permanent shape, it is in the martensite phase with a twinned structure. When the alloy is deformed to its temporary shape, it changes to a detwinned structure but is still in the martensite phase. When the deformed alloy is heated, it transforms into the austenite phase. When the temperature decreases, the alloy will return to the twinned martensite phase. The phase transformation results from shear lattice distortion

Shape-memory polymers generally exhibit a higher capacity for elastic deformation than shape-memory alloys but have, on the other hand, lower strength. A shape-memory polymeric network consists of permanent netpoints connected by chain segments. These chain seg-

ments can form switches. Permanent netpoints are not affected by deformation, and that is why a shape-memory polymer can remember its original shape. The switches are sensitive to an external stimulus, which triggers the shape recovery effect (3)(4). The permanent phase has a higher entropy than the temporary phase, and the shape-memory effect is caused by entropic elastic behavior. The interest in shape-memory polymer has recently increased due to the development of 3D printing.

Shape-memory material can be used in numerous fields of engineering. One of these fields is soft robotics. Because shape-memory polymers are flexible and lightweight, it is safe to use around humans (5). An application prospect for shape-memory material is to use it as a hinge actuator. This actuator type will set a system in motion by rotating it. A potential prospect of shape-memory hinges is that they can be used in transport engineering. Shape-memory hinges may push objects from one conveyor belt to another, lift objects, or serve as a gripper.

Much research has been conducted concerning shape-memory material hinges. Two major classes of shape-memory hinges are one-way and two-way shape-memory material hinges. One-way shape-memory hinges can return to their permanent shape from a programmed temporary shape. The shape-memory effect is not reversible, only when the hinge is programmed again. Examples of one-way shape memory hinges are designs of Liu et al.(6)(7), who designed different shape memory polymer composite hinges that are used in space.

On the other hand, two-way shape-memory material hinges can alter between two or more different shapes. The most common way to achieve this is by using two shape-memory materials. One shape-memory material actuates the hinge from the starting position to the actuated position. The other shape-memory material actuates the hinge back to the start position. An example of a two-way shape memory hinge is the design of Akbari et al. (8), which consists of a shape memory body with embedded Nitinol wires. This hinge was used as a gripper Another example of a two-way shape memory hinge is the design of Testoni et al. (9), which also consists of a shape-memory body, but has Nitinol springs attached externally. This design was used to rotate solar panels in a satellite.

In most research about shape-memory hinges, the hinge can be actuated in the 2D plane like an elbow joint. Very little research was conducted concerning hinges that work in the 3D space. For some purposes, it can be useful for a hinge to be able to actuate along more axes to increase mobility. For example, when using an interactive hinge for a soft robotic arm, multi-axe actuation allows a robot to be actuated in horizontal and vertical actuation. *This paper investigates how to design an interactive hinge with shape memory alloys and polymers that can be actuated along two axes.*

2 Design methodology

To design an interactive hinge, some steps need to be completed to get to the most optimal design. These steps are visualized in a flowchart, seen in Figure 1. Literature study showed what the research gap is, from which a problem definition can be drawn up. A conceptual design is made, using the basic design cycle described in the Delft Design Guide (10). This design cycle consists of 5 stages: analyze, synthesize, simulate, evaluation, and decision.

In the analyze stage, aspects related to the design problem are analyzed. In this stage, the design criteria are drawn up. In the synthesize stage, possible solutions are generated. This is done by sketching some solutions to solve the problem. These sketches can be seen in Figure 2. Designs A and B had embedded shape memory alloy wires in an SMP body with soft material, while C, D, E, and F had externally applied shape memory springs with an SMP body. In all designs, the SMA was used to bend the hinge from permanent to temporary position, while the SMP was used for shape recovery. In the simulate stage, the designs are simulated to determine the expected behavior. The geometry of the designs is implemented in the finite element analysis software (FEA) Comsol, and a force is applied at the tip to simulate the actuation of the SMA. The tip displacement is evaluated for each design. In the evaluation stage, the designs are evaluated using the design criteria. Finally, in the decision stage, a decision for a concept is made. The concept of the stacked plate hinge in Figure 2f had the most satisfactory results because the displacement at the tip was the largest compared to the other sketches, which is why this concept is developed further.

After the conceptual design, the materials of the hinge are selected. The SMP body consists of polylactic acid (PLA). This material has a transition temperature of 65 °C (11). The material used for the shape memory springs is Nitinol. To get to the final design, in which the dimensions of the hinge are specified, the characteristics of the Nitinol springs need to be determined first.

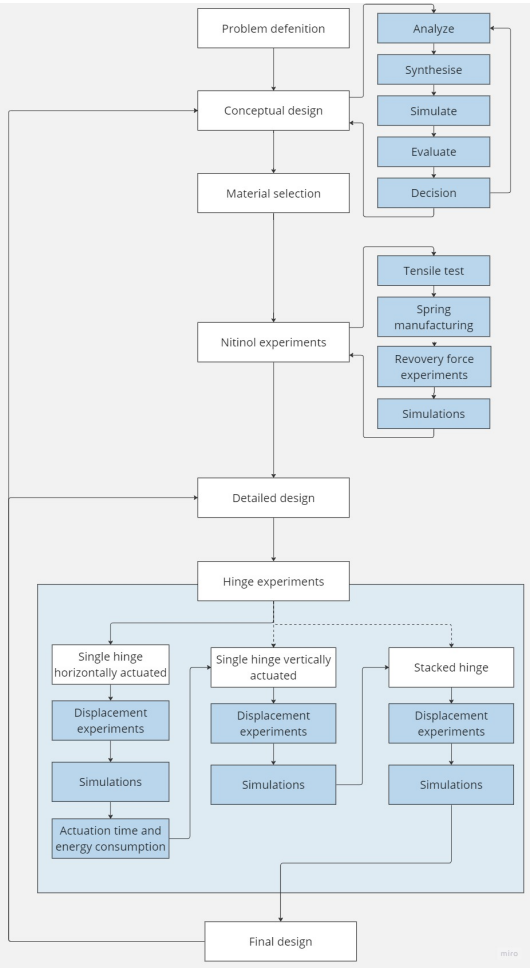

Figure 1: Flow chart which shows the design steps for designing the interactive hinge

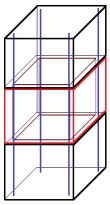

(a) Square-shaped embedded wire hinge

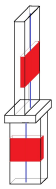

(b) Stacked embedded wire hinge

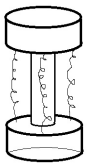

(c) Round body hinge with externally applied SMA springs

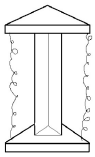

(d) Triangle body hinge with externally applied SMA springs

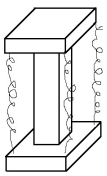

(e) Square body hinge with externally applied SMA springs

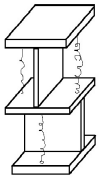

(f) Stacked plate hinge with externally applied SMA springs

Figure 2: Sketches of ideas for multi-axial actuated hinge that were made for the conceptual design process

3 Nitinol springs

Tensile test

The hinge is actuated using shape-memory springs, and the material used for the springs is Nitinol, a nickel-titanium alloy. It is important to know how Nitinol behaves because it influences how much the hinge can bend. Important information can be retrieved from tensile tests, like the Young's modulus and if and when the superelastic effect takes place.

Tensile tests are carried out to see the stress-strain curve of Nitinol with different material compositions. It was found that the Nitinol with 50% Nickel and 50% Titanium has the best properties to be used for the hinge because of the superelastic effect at low stress. The tensile test behavior of this wire can be seen in Figure 3. These tests were displacement-controlled with a test speed of 2 mm/min and carried out at room temperature.

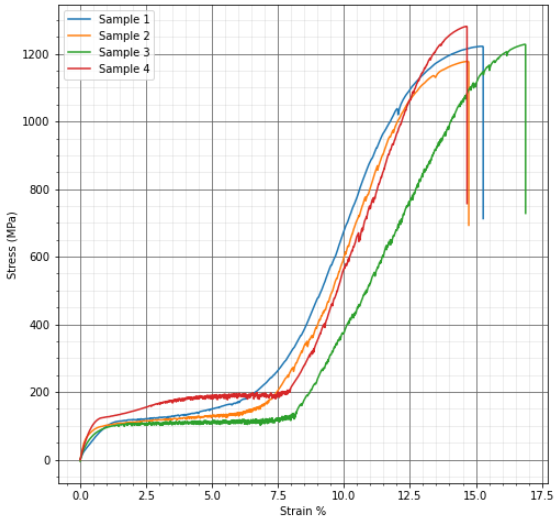

Figure 3: Tensile test of wire with 50% Nickel and 50% Titanium and diameter of 0.5 mm

Manufacturing of springs

With the previously mentioned wire, springs were made. This is done by twisting the wire on a screw thread, and clamping the ends between nuts so it stays in its shape. Then, the samples are put in the oven for 30 minutes, followed by rapidly cooling the spring. Table 1 shows the properties of the manufactured springs.

Recovery force experiment

The actuation force of the springs' recovery force must be determined. This is done by connecting one end of the spring to a spring scale and fixing the other end to a

Wire diameter	Material composition	Inner diameter spring	Spring length	Pitch	Wire length
0.5 mm	50%Ni 50%Ti	4 mm	30 mm	0.7 mm	573 mm

Table 1: Table which shows the properties of the manufactured spring

specified place, which causes the spring to deform. The force needed to deform the spring can be read on the spring scale. This is the spring force when it is not actuated. The springs are heated via joule heating by a programmable DC power supply. One end of the spring is connected to the plus side of the power supply, and the other to the minus side. The temperature of the spring is measured with a K-type thermocouple.

Multiple tests were carried out with the 0.5 mm NiTi spring. Nine samples were manufactured of this spring type. Three springs were deformed using the experimental setup to a state where the total spring length was 60 mm, three to a length of 100 mm, and three to a length of 140 mm. The springs are then heated using joules heating to 80 °C in steps of 10 °C.

Figure 4 shows the force-temperature graph for the NiTi springs. They all have similar behavior. At what temperature the force increases is the austenite start temperature, and at what temperature the force stops to increase is the austenite finish temperature. At what temperature the force increases and stops to increase differs for each graph. This is expected because the start and finish temperatures increase with an increase in stress (12).

For the hinge to be actuated multiple times, it is useful to see how the actuation force of the spring degrades over time. This can be seen in Figure 5. When the spring is deformed to a length of 60 mm, there is a dip in reaction force after actuation number 1, but after that, the reaction force is relatively stable. When the springs are deformed to 100 mm and 140 mm, the reaction force decreases after the first few actuations. After about six actuations, the reaction force stabilizes, as it barely does not change anymore after this point.

Spring simulations

FEA simulations are carried out with the simulation software Comsol Multiphysics to simulate the behavior of the spring. It is determined if the recovery force of the spring in the simulations and the experiments are alike. The geometry of the spring is modeled as a helix, with the corresponding radius, thickness, axial pitch, and the number of turns. Material properties are also important parameters for performing accurate simulations. Some are found online, while others are determined based on the experiments.

The temperature when austenite starts to form and when the material is entirely austenite is determined from Figure 4. The Young's modulus in the martensite phase is determined based on Figure 3. The value of the E-modulus is the gradient of the linear part of the stress-strain graph. For the NiTi wire, this results in an E-modulus of 16.25 GPa. Since the machine for tensile testing when the wire is heated was unavailable, the austenite Young's modulus was guessed based on the recovery force measurement results. The austenite E-modulus was set as 40 GPa for the NiTi wire. Solid mechanics physics is used in this simulation. One end of the helix is selected as a fixed constraint, while the other is displaced. The shape-memory alloy material model is applied. The reaction force of the helix at the end is determined when the temperature of the helix is between 20°C and 80 °C, with intervals of 10 °C.

The results can be seen in Figure 6. The simulations and experiments follow a similar trend when looking at these results. You can see that the simulations have lower values for the 60 mm deformation than the experiments. Still, when the deformation becomes larger, the simulations shift more to the top until the simulations have higher values than the experiments.

4 Final design

From the conceptual design, a final design is made. The CAD model of the final design of a single hinge, which can actuate along one axis, can be seen in Figure 7a, and the dimensions of that single hinge can be seen in Figure 7b. The stacked hinge that can be actuated along multiple axes can be seen in Figure 7c. These are two single hinges, but bolts and nuts connect them at the corners of the ABS part. As can be seen, the hinges consist of multiple parts. The gray helix is the shape-memory alloy spring made with 0.5 mm NiTi wire with an initial length of 30 mm and deformed to 62 mm. The white part is the shape-memory polymer body made with a 3D printer. It consists of PLA with a 100 % filament. Heating films are glued on both sides of the PLA part, which heats the PLA

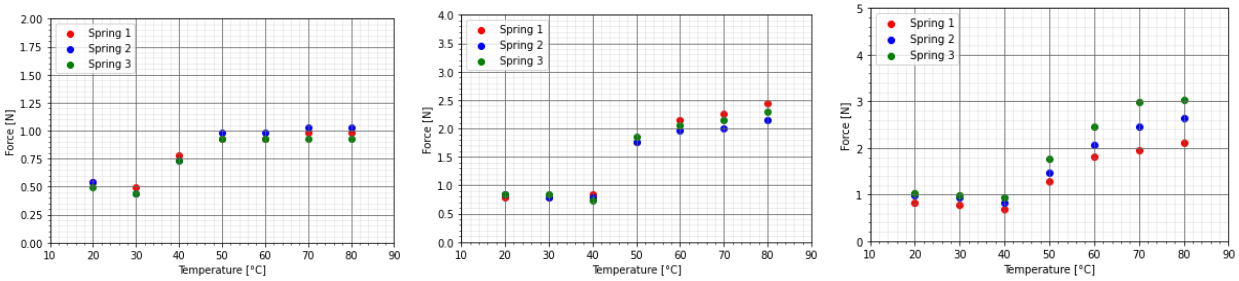

(a) Deformation NiTi spring to a length of 60 mm **(b)** Deformation NiTi spring to a length of 100 mm **(c)** Deformation NiTi spring to a length of 140 mm

Figure 4: Force-Temperature graph for the 0.5 mm diameter wire NiTi springs when deformed to 3 different lengths

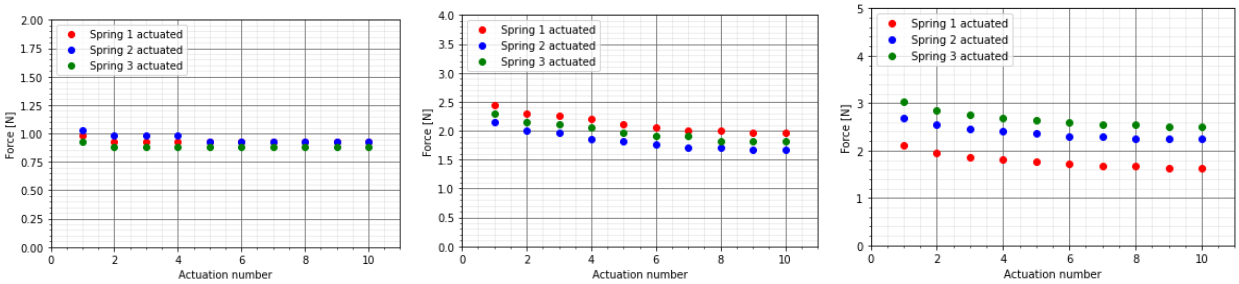

(a) Deformation NiTi spring to a length of 60 mm **(b)** Deformation NiTi spring to a length of 100 mm **(c)** Deformation NiTi spring to a length of 140 mm

Figure 5: The recovery force development when the NiTi springs are actuated multiple times when deformed to 3 different lengths

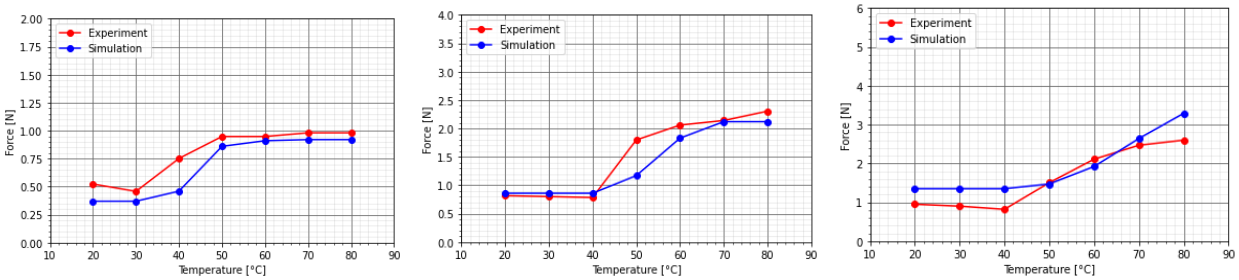

(a) Deformation NiTi spring to a length of 60 mm **(b)** Deformation NiTi spring to a length of 100 mm **(c)** Deformation NiTi spring to a length of 140 mm

Figure 6: Force-Temperature graph Comparing the simulation values to the experiments

above its transition temperature. Because the Nitinol can reach temperatures of up to 80 °C, the springs would cut through the SMP body, which is why an intermediate part is used. The black rectangles on the edges are the intermediate parts made out of Acrylonitrile Butadiene Styrene (ABS). The Nitinol springs are connected to the intermediate parts with bolts and nuts.

5 Hinge experiments

5.1 Horizontally actuated single hinge

Displacement experiments

First, the hinge's working range is determined. The hinge is actuated as follows: first, the heating films are heated till about 65 °C, so the PLA is above the transition temperature. When this temperature is reached, one of the springs is actuated by increasing power to the spring in small steps until the maximum recovery force is reached. For each step, the distance is measured from the outer end of one of the ABS plates to the outer end of the other ABS plate. Then, the power to the spring is stopped, and the hinge will recover its shape. This is done multiple times.

The results of the tests can be seen in Figure 8. This figure shows the distance when fully actuated. As can be seen, the distance of the first actuation is smaller, but when actuated multiple times, the distance stabalizes to about 60 mm.

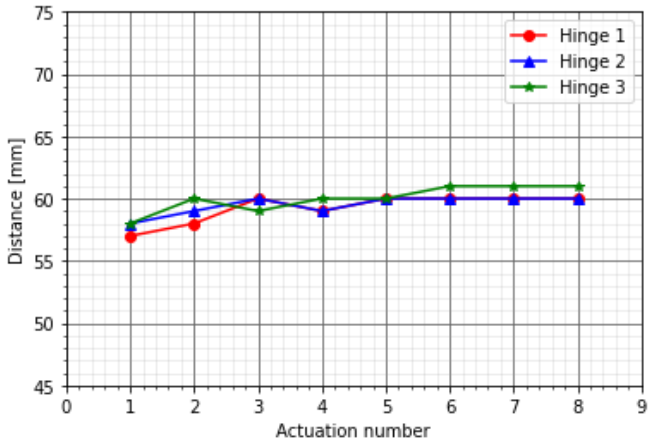

Figure 8: The ABS-to-ABS distances of the horizontal hinge when fully actuated where each spring is actuated alternately

Simulations

After the working range experiments, the hinge is simulated. The hinge was designed in Solidworks, as seen in Figure 7. The geometry was imported into Comsol. The materials were created with the right material properties. The density of the materials was obtained by weighing the parts and dividing the volume of the parts by the weight. For Nitinol, the same E-moduli were used as in the simulations in section 3, while the ABS E-modulus was found online. Two materials were created for Nitinol: one with the martensite E-modulus and one with the austenite E-modulus. As mentioned before, the PLA part is 3D printed. Several printing parameters can affect the E-modulus of 3D printed PLA (13). That is why the E-modulus is obtained from the simulations.

Solid mechanics physics is used in the simulations. One outer end of the ABS part is fixed. Gravity is applied, and gravity acts accordingly depending on whether the horizontal or vertical actuation is simulated. The actuation of the springs is simplified. An initial strain is applied to the springs. The low E-modulus martensite material is applied when the spring is not actuated. When the spring is actuated, the higher E-modulus austenite material is applied. The unknown material property is the PLA E-modulus. The heating film is glued to the PLA in the experiments. This increases the E-modulus. The E-modulus of the PLA in the simulations will be the combination of the PLA itself and the heating film. To determine the E-modulus of the PLA, it is checked at what E-modulus the experiments and simulation behave the same way. This is done by evaluating the displacement of a point on the ABS plate in Comsol.

The E-moduli of the PLA were determined using the horizontal actuation of a single hinge. When one of the springs is actuated when the PLA is not heated, it was found that the distance from ABS-to-ABS was 66 mm. It was found that when the E-modulus was set to 620 MPa, the simulations had an ABS-to-ABS distance at the end corner of about 66 mm. When the PLA is heated to 65 °C, the ABS-to-ABS distance is about 58 mm. This corresponds to an E-modulus of 28 MPa. The results of the simulations can be seen in Figure 9.

Energy consumption and actuation time

To determine the energy efficiency of the hinge, it is determined how long it takes for the PLA body and the Nitinol springs to be heated. This is done by applying power to both heating films and measuring the temperature of the

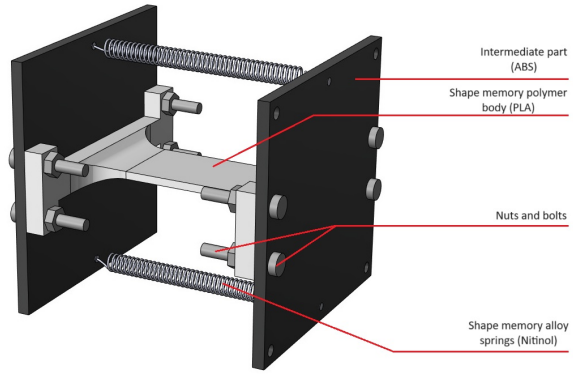

(a) Impression single hinge

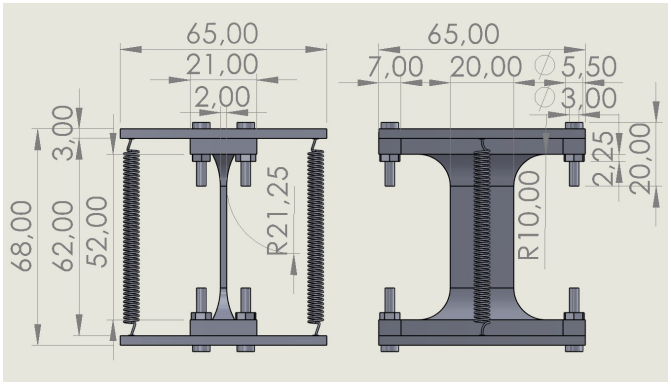

(b) Drawing single hinge with dimensions

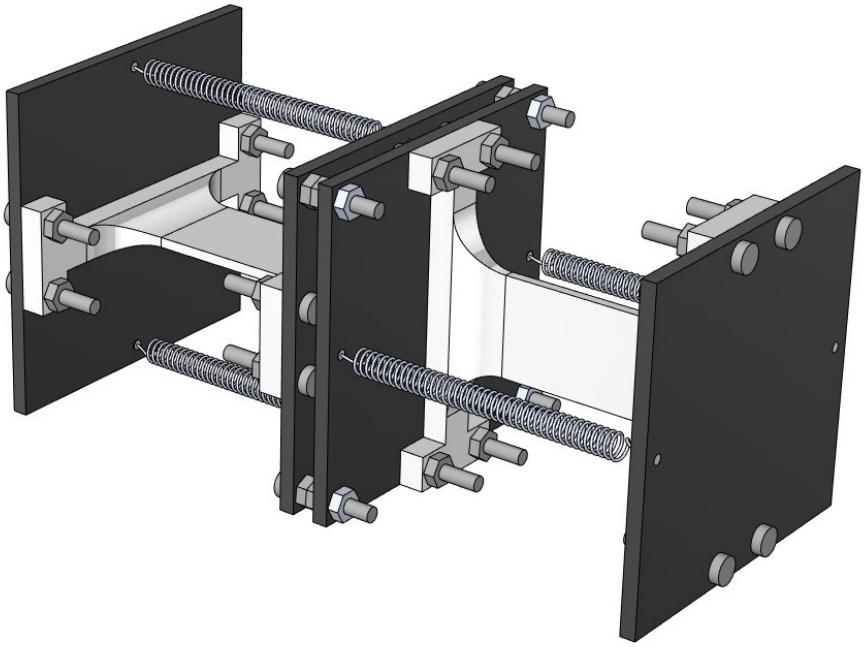

(c) Impression stacked hinge

Figure 7: CAD-models of the hinges

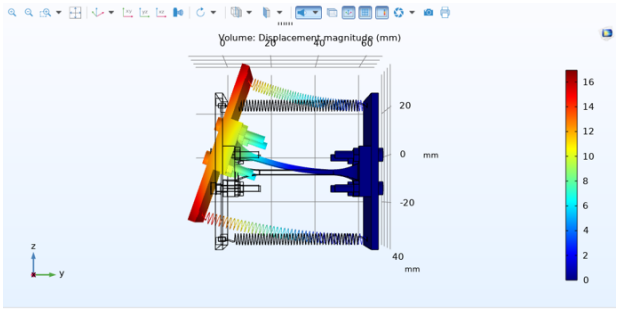

(a) Actuation spring 1

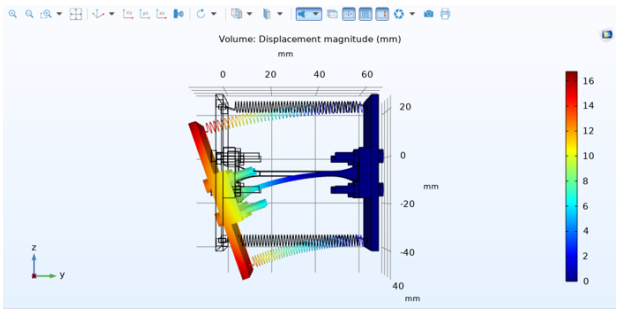

(b) Actuation spring 2

Figure 9: Top view simulations of horizontal actuated hinge

PLA with the k-type thermocouple. This is done when two different powers are supplied to the heating films. The results can be seen in Figure 10.

It is also determined how fast a spring is heated. The austenite finish temperature is 50 °C when the spring is deformed to 60 mm. This is the temperature at which the

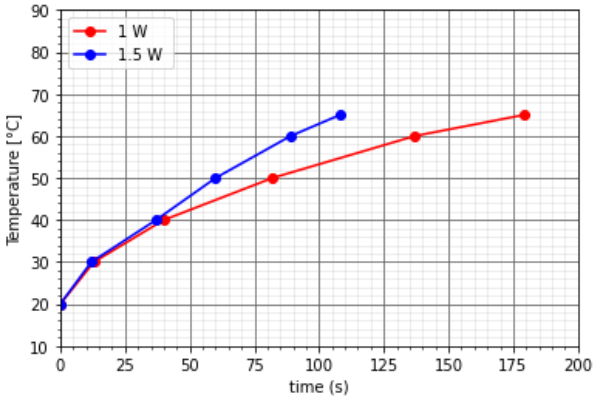

Figure 10: Time versus temperature relation of the PLA when two different powers are supplied to each heating film

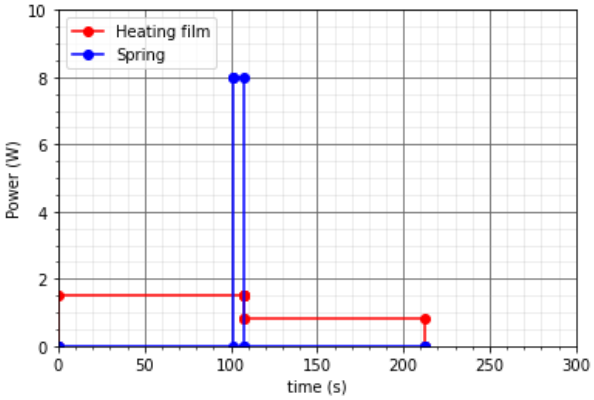

Figure 11: Power supply over time for one actuation cycle

spring needs to be heated to give the maximum force with the lowest temperature. It is checked how fast the spring heats when different powers are supplied to the spring. It is found that the spring is heated to 50 °C in 33 seconds when a power of 4 W is supplied, 10 seconds when 6 W is supplied, and 7 seconds when 8 W is supplied.

Using the formula $E = P \times t$, it is found that the heating films were the most energy efficient when 1.5 W was supplied, while the springs were the most energy efficient when 8 W was supplied. Figure 11 shows the energy supply to the heating films and the spring. As can be seen, when the hinge is fully actuated, the film's power is dropped to 0.8 W, so the PLA stays at 65 °C, while the power to the spring is cut off. At this point, the shape recovery takes place and lasts 104 seconds. The integral of this graph has to be determined to determine the amount of energy that has to be supplied for the actuation of a single hinge. This results in an energy use of 546.4 J, when each heating film is powered with 1.5 W and the spring is powered with 8 W.

Much energy is needed to heat the PLA when it is still at room temperature to be able to actuate it. If the hinge is already at 65 °C, the actuation cycle now only consists of heating the spring and, subsequently, shape recovery. The actuation cycle now takes 111 seconds with an energy consumption of 248 J.

5.2 Vertically actuated single hinge

Displacement experiments

The same experiment was conducted as in section 5.1. The results can be seen in Figure 12. First, the top spring is actuated, which is the uneven actuation numbers, followed by the bottom spring, which is the even actuation numbers. The difference in distance is because the top spring must overcome the gravity of the hinge, which results in a larger distance compared to the bottom spring actuation. It can be seen that after a few actuations, the top spring actuation distance stabalizes to about 65 mm while the bottom spring actuation stabalizes to about 53 mm.

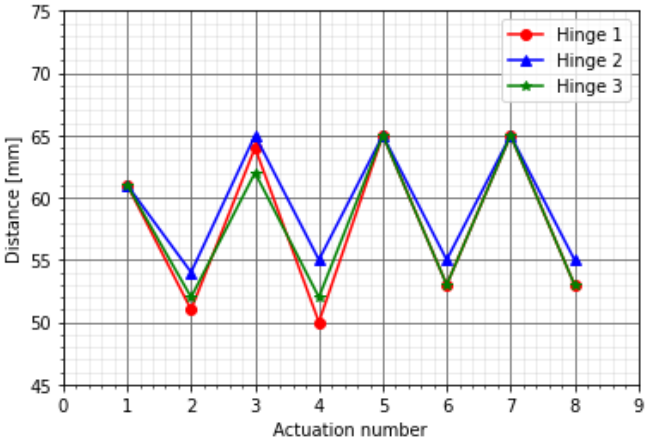

Figure 12: The ABS-to-ABS distances of the vertically actuated hinge when fully actuated where each spring is actuated alternately

Simulations

It is now determined if the E-moduli for the PLA at 65 °C, obtained from the horizontal simulation, can be used in the vertical simulation and still have similar results. When looking at Figure 12, it can be seen that the top spring actuation distance is about 61 mm. The simulation values using an E-modulus of 28 MPa result in a distance of 60.9 mm. The simulations can be seen in Figure 13.

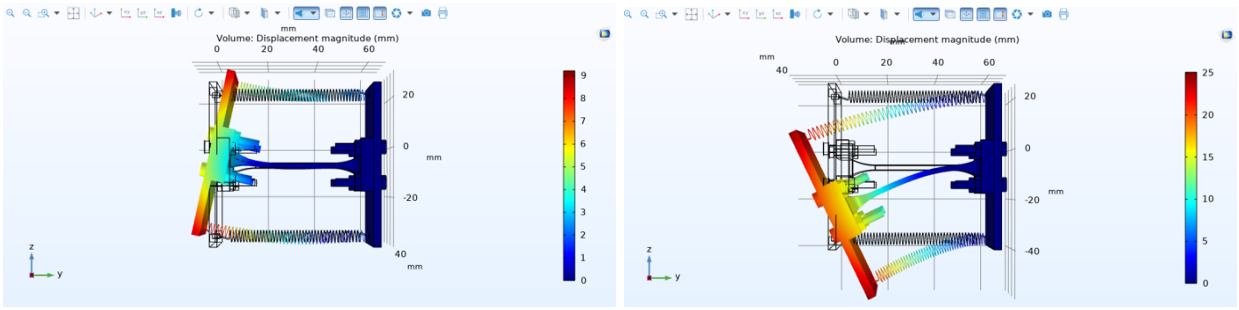

(a) Top spring Actuation

(b) Bottom spring actuation

Figure 13: Side view vertical simulations

5.3 Stacked hinge

Displacement experiments

Finally, the stacked hinge is tested. The test hinge consists of 2 single hinges in series. The first hinge acts horizontally, while the second hinge is connected to the first hinge and acts vertically. It is now mainly interesting how the first hinge behaves because the conditions of the second hinge are similar to the hinge in subsection 5.2.

Figure 14 shows the result of the stacked hinge when the first hinge is actuated. The distance also stabalizes after a few actuations. One problem was that when the first hinge was heated, the hinge sagged a little bit. The weight of hinge 2 caused this. Furthermore, the hinge was also twisted. The twist direction depended on which side was actuated.

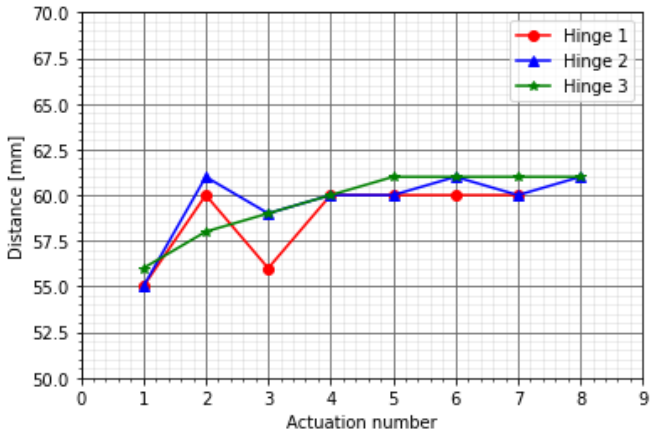

Figure 14: The ABS-to-ABS distances of the stacked hinge where each spring is alternated actuated

Simulations

Finally, it is checked what the results would be if the stacked hinge is simulated when the E-modulus of the PLA is 28 MPa. The results can be seen in Figure 15. The ABS-to-ABS distance of the first hinge was about 56 mm in the experiments. When the hinge was simulated, the distance was 56 mm. The simulation can be seen in Figure 15.

It is determined what the range of motion is for the stacked hinge. This is done by adding a point at the tip of the hinge in the middle of the ABS plate. The hinge is actuated to 8 different positions by actuating different springs. It is determined how the added point moves when actuated in different positions. The stacked hinge can be moved much more in the x-direction than in the y-direction, resulting from the second hinge enlarging the deformation at the tip. The tip of the stacked hinge can be displaced from unactuated position 39 mm to both sides horizontally. Vertically, the hinge can be moved 0.3 mm to the top and 24.6 mm to the bottom. Due to gravity, the range in the positive y-direction is much lower than in the negative y-direction.

6 Discussion

This research has shown that an interactive hinge with a simple design that could be actuated along two axes is relatively easy to manufacture. The hinge was able to be actuated multiple times without requiring manual reprogramming. The distance, when actuated, stabalizes after a few actuations. As was mentioned before, the first hinge of the stacked hinge sagged a bit, and the tip of the hinge twisted. These problems could be solved in numerous ways. One way to tackle this is to make the PLA part of the first hinge thicker or wider or use a shape-memory polymer with a higher E-modulus. However, this will affect the range of motion. To increase the displacement when actuated, shorter wires can be used, resulting in a larger recovery force. Also, a thicker wire can be used to increase the recovery force. The deformation of the hinge is measured by measuring the ABS-to-ABS distance. Using software that tracks the deformation using a camera

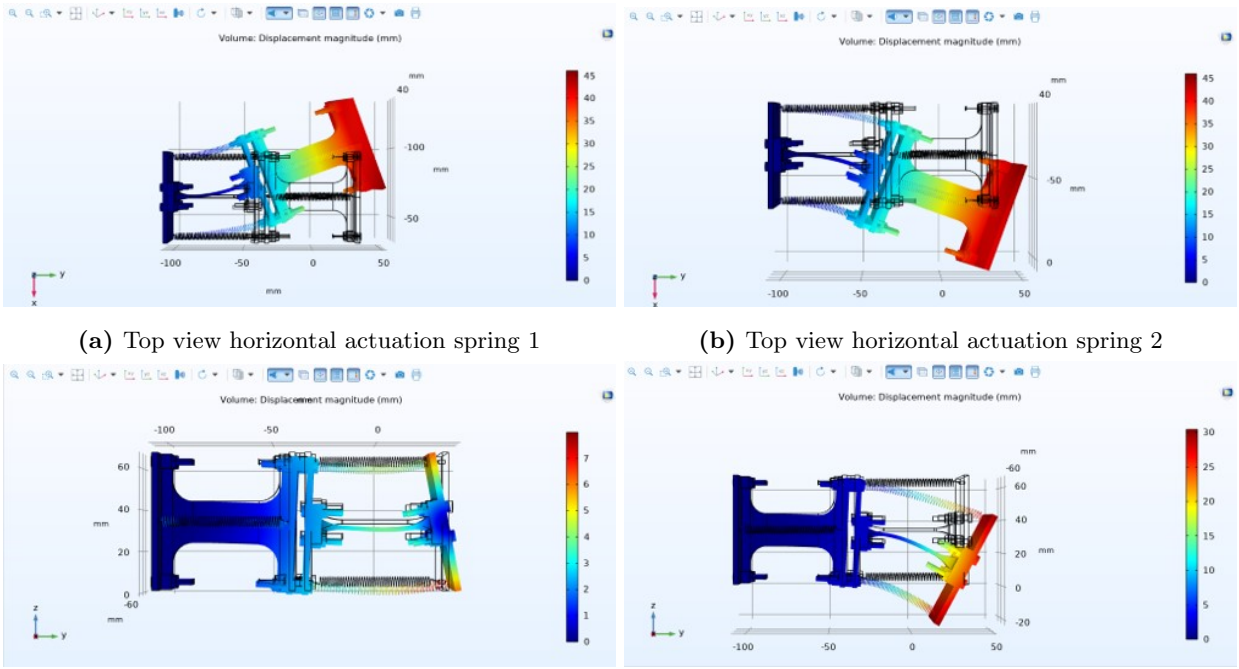

(a) Top view horizontal actuation spring 1

(b) Top view horizontal actuation spring 2

(c) Side view vertical actuation top spring

(d) Side view vertical actuation bottom spring

Figure 15: Stacked hinge simulations

might be a better way to see how the hinge deforms. The simulation of the hinge was carried out linearly. Since there are large displacements, non-linear simulations will probably be more accurate. It can be concluded that the hinge is very inefficient. It takes some time for the PLA of the hinge to heat up for the hinge to be actuated. The energy efficiency can be improved by embedding the heating films in the PLA plate and by using heating films with more power. Embedding the heating films in the PLA will also increase the range of motion because attaching the heating films on the PLA's outer ends increases the PLA's stiffness.

7 Conclusion

Different designs for an interactive hinge were made using the basic design cycle. The chosen working principle of the design was a 3D printed shape-memory polymer body that is actuated externally by shape-memory springs. To maximize the range of motion, the body of the hinge has the shape of a plate, and to obtain motion along two axes, a second hinge is stacked at the end of the first part. The springs were made of Nitinol, and the body was made of PolyLactic Acid (PLA).

The actuation force that the Nitinol springs can deliver was determined. Springs were elongated to three different lengths, and the temperature was increased in steps of 10 °C to see how the recovery force changed. The springs were also actuated multiple times to see if the recovery force changed. For each spring and deformation, the recovery force eventually stabilizes. The simulation of the springs followed a similar trend when compared to the experiments.

Three different tests are carried out: a single hinge actuated horizontally, a single hinge vertically, and a stacked hinge. When actuated from an undeformed configuration, the horizontal hinge had an ABS-to-ABS distance of about 58 mm, the vertical actuated hinge had a distance of 61 mm, and the stacked hinge had a distance of about 56 mm. For each test, the hinge had a smaller ABS-to-ABS distance when actuated from an undeformed configuration than when actuated multiple times. The distance of the hinges stabalizes after a few actuations. The energy consumption of the hinge was determined. When the PLA was still at room temperature, it took 108 seconds to heat the PLA to 65 °C when the heating films were powered by 1.5 W. The heating of the springs took 7 seconds when powered by 8 W. From undeformed to actuated position took 108 seconds. Shape recovery took 104 seconds, resulting in a total actuation cycle of 212 seconds. The energy consumption of this actuation cycle was 546.4 J. If the hinge is already at 65 °C, the actuation cycle takes 111 seconds with an energy consumption of 248 J.

Finally, the hinges were simulated. The E-modulus of PLA at room temperature was determined by adjusting the E-modulus of the simulation so it resembles the ex-

periments for the horizontal actuated single hinge. The E-modulus was found to be 620 MPa at 65 °C and 28 MPA at 20 °C. These values were also applied to the simulations of the vertical actuated hinge and stacked hinge tests. The maximum difference in distance between the simulations and the tests was 0.1 mm. The range of motion of the stacked hinge was determined. The tip of the hinge could be actuated 39 mm horizontally in both directions, 0.3 mm in the top direction, and 24.6 mm in the bottom direction.

Future research should focus on increasing the range of motion and the hoist capacity of the hinge. The hinge is not energy efficient, which can also be improved. The shape-memory effect's contribution of the PLA to shape recovery could be investigated. Also, the degradation of the shape-memory effect and the fatigue behavior of the PLA is an interesting topic to investigate. Research can be conducted that scales the hinge to see how the behavior of the hinge changes and if the simulations will still be accurate in that case. Also, other physics can be added in Comsol that simulates the heating of the hinge because heat affects material properties.

References

[1] R.E. Meirowitz. Coating processes and techniques for smart textiles. 2016.

[2] J. Kunzelman, T. Chung, P.T. Mather, and C. Weder. 2008.

[3] H. Xie, C. Cheng, X. Deng, C. Fan, L. Du, K. Yang, and Y. Wang. Creating poly(tetramethylene oxide) glycol-based networks with tunable two-way shape memory effects via temperature-switched netpoints. 2017.

[4] A. Melocchi, M. Uboldi, M. Cerea, A. Foppoli, A. Maroni, L. Palugan S. Moutaharrik, L. Zema, and A. Gazzaniga. Shape memory materials and 4d printing in pharmaceutics. 2021.

[5] G. Scalet. Two-way and multiple-way shape memory polymers for soft robotics: An overview. 2020.

[6] T Liu, L. Liu, Q. Li, C. Zeng, X. Lan, and J. Leng. Integrative hinge based on shape memory polymer composites: Material, design, properties and application. 2019.

[7] Z. Liu, X. Lan, L. Liu, Q. Li, Y. Liu, and J. Leng. Design, material properties and performances of a smart hinge based on shape memory polymer composites. 2020.

[8] S. Akbari, A. Sakhaei, S. Panjwani, A. Serjouei, and Q Ge. Multimaterial 3d printed soft actuators powered by shape memory alloy wires. 2019.

[9] O. Testoni, T. Lumpe, J. Huang, M. Wagner, S. Bodkhe, R. Spolenak, J. Paik, P. Ermanni, L. Muñoz, and K. Shea. A 4d printed active compliant hinge for potential space applications using shape memory alloys and polymers. 2021.

[10] A. van Boeijen, J. Daalhuizen, J. Zijlstra, and R. van der Schoor. *Delft Design Guide*, chapter 2. BIS, 2013.

[11] J.S. Bergstrom and D. Hayman. An overview of mechanical properties and material modeling of polylactide (pla) for medical applications. 2016.

[12] D.C. Lagoudas. *Shape memory alloys: modeling and engineering applications*, chapter 1.3. Springer, 2008.

[13] T.J. Suteja and A. Soesanti. 2020.